PASSIVE NONCOOPERATIVE RF EMITTER LOCALIZATION VIA MOVING SENSORS

PhD Dissertation

Seçkin ULUSKAN

Eskişehir 2018

PASSIVE NONCOOPERATIVE RF EMITTER LOCALIZATION VIA MOVING SENSORS

Seçkin ULUSKAN

DOCTOR OF PHILOSOPHY DISSERTATION

Electrical and Electronics Engineering

Supervisor: Assoc. Prof. Tansu FİLİK

Eskişehir

Anadolu University

Graduate School of Sciences

March 2018

This study was funded under the project number 1606F559 which was accepted by the BAP (Scientific Research Projects) Commission.

FINAL APPROVAL FOR THESIS

This thesis titled “Passive Noncooperative RF Emitter Localization via Moving Sensors” has been prepared and submitted by Seçkin ULUSKAN in partial fullfillment of the requirements in “Anadolu University Directive on Graduate Education and Examination” for the Degree of Doctor of Philosophy (PhD) in Electrical and Electronics Engineering Department has been examined and approved on 23/03/2018.

Committee Members	**Title Name Surname**	**Signature**
Member (Supervisor)	: Assoc. Prof. Dr. Tansu FİLİK	.....
Member	: Prof. Dr. Ömer Nezih GEREK	.....
Member	: Prof. Dr. T. Engin TUNCER	.....
Member	: Prof. Dr. Rıfat EDİZKAN	.....
Member	: Assist. Prof. Dr. Mehmet FİDAN	.....

Prof. Dr. Ersin YÜCEL

Director of Graduate School of Sciences

ÖZET

HAREKETLİ SENSÖRLERLE PASİF İŞBİRLİKSİZ
YAYICI KONUMLANDIRMA

Seçkin ULUSKAN

Elektrik-Elektronik Mühendisliği Anabilim Dalı
Anadolu Üniversitesi, Fen Bilimleri Enstitüsü, Mart 2018
Danışman: Doç. Dr. Tansu FİLİK

Hareketli sensörlerle radyo frekansı (RF) yayıcı konumlandırma; rota planlaması, sağlam tahmin sistemleri ve verimli konumlandırma algoritmaları vb. konularını içeren çok boyutlu bir sorundur. Bu çalışma, hareketli sensörlerle başarılı bir konumlandırma sistemi elde etmek için eksiksiz bir yapı sunmaktadır. Rota planlamasına yönelik olarak bu çalışmada, sürekli rotalar boyunca sürekli ölçümler alındığını varsayan Fisher sürekli bilgi matrisi (FCIM) adı verilen yeni bir kavram oluşturmuştur. FCIM'ler kullanılarak, sınırlı uzunlukta doğrusal bir rota için en iyi doğrultunun, yalnızca toplam hareket uzunluğunun yayıcıya başlangıç uzaklığına oranın bir fonksiyonu olduğu kanıtlanmıştır. Dahası, alınan sinyal gücü (RSS) tabanlı konumlandırma için, hareket eden sensör yayıcıya ulaşabiliyorsa, en iyi rotanın yayıcıya doğru hareket etmek olduğu tespit edilmiştir. Sonraki aşamada, RSS tabanlı konumlandırma için yol kayıp katsayısının (PLE) ve yayıcının gücünün bilinmediği durumlarda, Üstel Bilinmezlik Doğrultusu (DEU) olarak adlandırılan yeni güçlü bir geometrik çözüm önerildi. DEU, yayıcının konumunu tahmin etmeden ona doğru hareket etmek için temel oluşturmaktadır. Bu nedenle DEU, hareketli sensörler için etkili bir rota planlama aracı ve dahası Cramer Rao Alt Sınırını (CRLB) yakalayan ve hesaplama verimliliğini artıran etkin bir konumlandırma sistemi olarak önerilmektedir. Yayıcı konumlandırmada hareket eden sensörlerden yararlanılması, kaçınılmaz olarak sensör konumlarına yönelik bilginin hatalı olmasına neden olur. Bunun için bu çalışma, yayıcıyı özel bir çember boyunca arayarak Maksimum Olabilirlik tahmininin (MLE) genel minimumunu güvenli bir şekilde bulan Dairesel Belirsizlik adı verilen yeni bir konum belirleme stratejisi önermektedir. Diğer yöntemler kısmen başarısız olurken, Dairesel Belirsizlik yöntemi her durum için CRLB'yi yakalayabilmektedir.

Anahtar Sözcükler: Konumlandırma, İnsansız Hava Aracı (İHA), Rota Planlaması, Alınan Sinyal Kuvveti (RSS), Belirsiz Sensör Konumu.

ABSTRACT

PASSIVE NONCOOPERATIVE RF EMITTER LOCALIZATION
VIA MOVING SENSORS

Seçkin ULUSKAN

Department of Electrical and Electronics Engineering
Anadolu University, Graduate School of Sciences, March 2018

Supervisor: Assoc. Prof. Tansu FİLİK

Localization of radio frequency (RF) emitters with moving sensors is a multidimensional problem which requires trajectory planning, robust estimation systems and efficient localization algorithms etc. This study provides a complete framework to achieve a successful localization system with moving sensors. For trajectory planning, this study introduces a new concept called Fisher continuous information matrix (FCIM) which assumes continuous observations through continuous trajectories. Using FCIMs, this study proves that the best direction of a limited linear trajectory is only a function of the ratio between the total travel length and the initial distance to the emitter. Moreover, for received signal strength (RSS) based localization, the best trajectory is found to move towards the emitter, if the moving sensor is able to reach it. Next, a new powerful geometrical solution called Direction of Exponent Uncertainty (DEU) is proposed for RSS based localization when path loss exponent (PLE) and transmit power are both unknown. DEU is a basis to move towards the emitter without estimating the emitter location. Therefore, DEU is proposed as an efficient route planning tool for moving sensors and an effective localization scheme which attains Cramer Rao Lower Bound (CRLB) with increased computational efficiency. Exploiting moving sensors in emitter localization inevitably results in imprecise sensor positions. Therefore, this study proposes a new search strategy, namely Circular Uncertainty which safely finds the global minimum of Maximum Likelihood estimation (MLE) by searching for the emitter along a special circle. Circular Uncertainty attains CRLB, where other competing methods partly fail.

Keywords: Localization, Unmanned Aerial Vehicle (UAV), Trajectory Planning, Received Signal Strength (RSS), Imprecise sensor position.

ACKNOWLEDGEMENT

I would like to thank my advisor, Assoc. Prof. Dr. Tansu Filik, for his continuous support and guidance during my Ph.D. studies. I am also grateful to Prof. Dr. Ömer Nezih Gerek and Assist. Prof. Mehmet Fidan for their support and guidance throughout my studies. Finally, I would like to thank my family for their endless support.

Seçkin ULUSKAN

March 2018

23/03/2018

STATEMENT OF COMPLIANCE WITH ETHICAL PRINCIPLES AND RULES

I hereby truthfully declare that this thesis is an original work prepared by me; that I have behaved in accordance with the scientific ethical principles and rules throughout the stages of preparation, data collection, analysis and presentation of my work; that I have cited the sources of all the data and information that could be obtained within the scope of this study, and included these sources in the references section; and that this study has been scanned for plagiarism with "scientific plagiarism detection program" used by Anadolu University, and that "it does not have any plagiarism" whatsoever. I also declare that, if a case contrary to my declaration is detected in my work at any time, I hereby express my consent to all the ethical and legal consequences that are involved.

Seçkin Uluskan

TABLE OF CONTENTS

LIST OF TABLES

LIST OF FIGURES

LIST OF SYMBOLS AND ABBREVIATIONS

α	: Alpha
β	: Beta
δ	: Delta (Lower Case)
Δ	: Delta (Upper Case)
θ	: Theta
λ	: Lambda
π	: Pi
σ	: Sigma (Lower Case)
Σ	: Sigma (Upper Case)
AOA	: Angle of Arrival
CRLB	: Cramer Rao Lower Bound
CU	: Circular Uncertainty
dB	: Decibel
DEU	: Direction of Exponent Uncertainty
DRSS	: Differential Received Signal Strength
FCIM	: Fisher Continuous Information Matrix
FDOA	: Frequency Difference of Arrival
FIM	: Fisher Information Matrix
GPS	: Global Positioning System
LLS	: Linear Least Squares
LS	: Least Squares
MLE	: Maximum Likelihood Estimation
MSE	: Mean Squared Error
NLS	: Nonlinear Least Squares
PLE	: Path Loss Exponent
RF	: Radio Frequency
RMSE	: Root Mean Squared Error
RSS	: Received Signal Strength
RSSD	: Received Signal Strength Difference
SC	: Scan Based
TDOA	: Time Difference of Arrival

TFO : Time of Flight

TOA : Time of Arrival

UAV : Unmanned Aerial Vehicle

WLS : Weighted Least Squares

1. INTRODUCTION

Mobile communication devices that communicate in the radio frequency (RF) band are getting extensively widespread throughout the world because of the ease of use and implementation of wireless communication systems. Localization of these and other similar devices is an important requirement in both civil and military areas and has a wide range of applications. For several different applications, accurate localization systems are created to meet a broad range of needs including smart transportation systems to mobile user tracking, rescue activities to defense systems and so on. For this reason, positioning different types of RF emitters with various different techniques is an important problem which is vigorously studied in the literature of signal processing and wireless communications.

The localization system should be able to cover many different types of emitters and a wide range frequency spectrum to able to achieve various tasks. Several issues (such as the signals of target RF emitters are weak, the duration of the broadcast is short, the signal is distorted due to rural or urban terrain and weather conditions, the target RF emitter are moving and so on) make it necessary to mount the localization systems on moving platforms (mostly on aerial vehicles). The localization system should be able to move towards the coverage area of the target RF emitter and scan the relevant area in a short time to effectively localize the target RF emitter. Therefore, all these requirements make it inevitable to exploit moving sensors in localization systems.

The previous studies in this area can be divided into two parts according to the use of single or multiple platforms in the localization systems. In multi-platform systems, organizing the coordination or synchronization between the platforms and compensating time delays between measurements if necessary are complicating the localization system. For this reason, it is necessary to develop systems with single or limited number of platforms that are less costly than multi-platform systems. Previous studies in this area have been carried out with the capabilities of unmanned aerial vehicles (UAVs) in military standards (in terms of flight time, altitude, power, equipment etc.). However, increasing popularity of wireless devices in civil area requires the use of mini UAVs in RF emitter localization systems. Mini UAVs are small, inexpensive, and easily accessible mini-sized aerial vehicles which are mostly used for civilian purposes, and they have significant restrictions on the amount of useful load they may carry and flight time. Therefore, the use of these mini UAVs requires the existing localization

algorithms to be made feasible under very important constraints and lower components, so it requires new research.

Wireless localization is the estimation of the location of the emitters (or sometimes the receivers) within the frameworks of various receiver-emitter scenarios using radio frequency waves. These studies are divided into two main categories in terms of the localization scenario: cooperative/collaborative and non-cooperative scenarios. In cooperative scenarios, there is a cooperation between the receivers and the emitter to achieve determination of the emitter location. On the other hand, when there is no co-operation between receivers and emitter, then it is called non-cooperative scenario. In these scenarios, the receivers have to accomplish the positioning task by themselves.

The most commonly used parameters in RF source localization are received signal strength (RSS), angle of arrival (AOA), time of arrival (TOA), time difference of arrival (TDOA) and finally hybrid parameters. TDOA and AOA based systems have been attributed to yield more accurate localization systems compared to RSS. While RSS based localization systems are criticized not to able to result in robust solutions, undoubtedly they are the most affordable solutions among other RF localization parameters. Because of their physical constraints, moving platforms bear the necessity to use the most efficient hardware and software combination. Therefore, there exists a growing attention on RSS based localization systems to take the advantage of their affordable and simple structures.

In Figure 1.1, a moving platform which is designed as a moving sensor is illustrated. The UAV shown in Figure 1.1 basically includes a GPS, an RSS sensor (or any different type of sensor) and a processing unit. The RSS sensor measures the RSS values regarding to the signal incoming from the emitter. The GPS is engaged in order to locate the UAV itself, so each RSS measurements can be matched with the measurement location. The processing unit can be utilized to make the necessary computation to estimate the location of the emitter or to dynamically determine the route of the UAV. If such a processing unit is missing, then each RSS value and measurement location must be transmitted to a central station which estimates the emitter location and controls the movement of the UAV. In this study, advanced algorithms for these moving platforms are created in order to allow these platforms to estimate the emitter location more effectively.

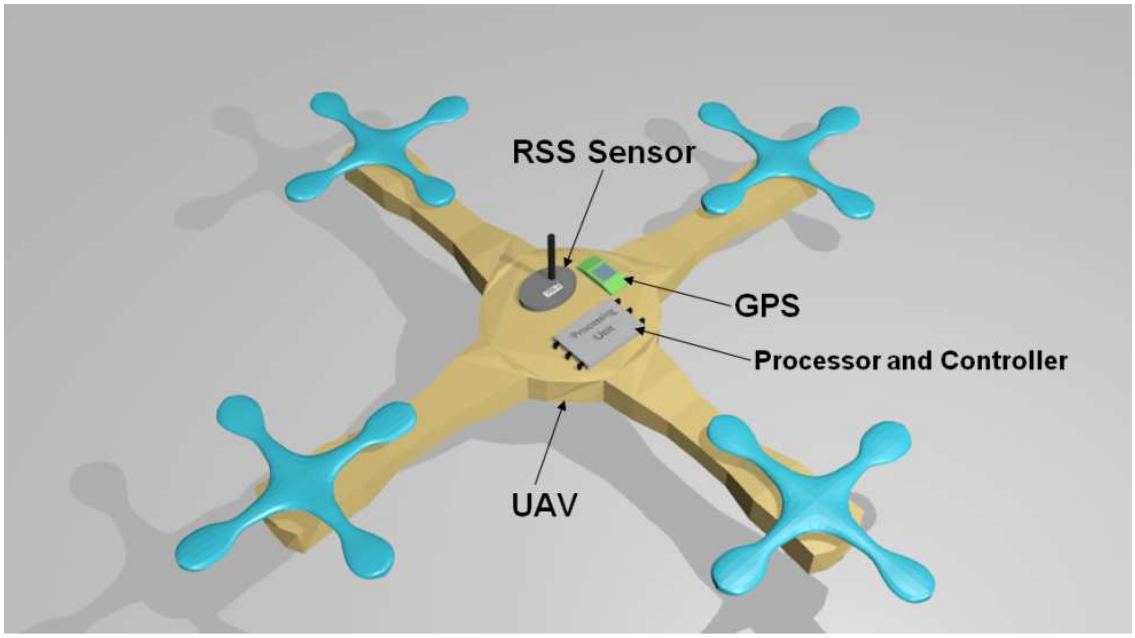

Figure 1.1. *Unmanned Aerial Vehicle (UAV) with RSS sensor designed as a moving sensor.*

Section 2 provides a literature review which first illustrates the basics of RSS and range-only localization. Second, current research areas in RSS based localization are discussed and then a broad literature review on Differential RSS (DRSS) is presented. Next, the previous studies about joint estimation of path loss exponent and emitter's location, and RSS based Localization via UAVs are provided. Then, trajectory optimization for emitter localization are discussed and finally, a comprehensive literature review on sensor position uncertainty is presented. When a moving sensor travels with the aim of estimation the location of the emitter, the first goal must be to create an effective route planning strategy which statistically guarantees the best possible estimation capability at the end of the travel of the moving sensor. Section 3 deals with trajectories of the moving sensors and describes the essence of trajectory planning with new understandings. It explores the best angular direction given a limited length travel for both RSS and range-only based localization.

After trajectory planning, an effective and efficient localization framework is necessary to be able to successfully achieve the main goal i.e. localization of the emitter. Path loss model which describes RSS as a function of the distance to the emitter is a useful building block for creating RSS based localization systems, however, it is possible that most of the parameters in path loss model can be unknown. Therefore, Section 4 provides a new localization as well as a route planning strategy called

Direction of Exponent Uncertainty [1] in order to deal with the harsh localization conditions where both path loss exponent and emitter's signal power are unknown. The proposed solution is an efficient geometrical solution which attains Cramer Rao Lower Bound (CRLB) i.e. the statistical lower bound given the noise level.

Finally, when dealing with moving sensors, it is very likely that the measurement positions are also uncertain in some extent due to the movement of the platform. Therefore, Section 5 creates an advanced localization scheme called Circular Uncertainty [2] in which measurement position errors are handled in a smart way to achieve the statistically best solution. Section 6 presents the discussions about each section and finally Section 7 provides the conclusion of the study.

2. LITERATURE REVIEW

In this section, a comprehensive literature review is provided. First, basics of RSS and range-only localization are discussed with illustrative flow diagrams depicting the localization process. Second, current research areas in RSS based localization are discussed and then a broad literature review on Differential RSS (DRSS) is presented. Next, the previous studies about joint estimation of path loss exponent and emitter's location, and RSS based Localization via UAVs are provided. Then, trajectory optimization for emitter localization are discussed and finally, a comprehensive literature review on sensor position uncertainty is presented.

2.1. Basics of Received Signal Strength (RSS)

Received signal strength can be regarded as the average power of an incoming signal received by a sensor. Path loss model formulates the received signal strength (RSS) in dB (or dBm) as the following way [3]:

$$P = p_0 - 10\, n\, \log_{10}(d/d_0) + W \tag{1}$$

where p_0 is the emitter's power in dB (namely the RSS value at a reference distance d_0), d is the distance between the sensor and the emitter, and n is the path loss exponent. An additive zero mean Gaussian error W with standard deviation σ are included within the model to represent the measurement error. Because W is a random variable, P is also a random variable. Therefore, the mean value of P is a function of p_0, n and finally d.

In some of the studies in literature, the power of emitter p_0 and the path loss exponent n can be assumed to be known if the characteristics of the emitter and the terrain are known. Basically, an RSS value provides a cue for the distance between the sensor and the emitter, therefore by means of the knowledge of the distances between the multiple measurement points and the emitter, the localization algorithms are trying to find the best possible position of the emitter. It is also possible that p_0 is not a known parameter in advance if the characteristics of the emitter can not be guessed. In this case, the difference between two RSS values from two different positions is providing a cue about the ratio of the distances of the emitter to these two distinct positions. Therefore, localization process becomes more complicated and a new feature called Differential RSS (DRSS) has been introduced to deal with these situations.

Moreover, path loss exponent can be also unknown prior to the localization of the emitter. Path loss exponent is a parameter which depends on the medium or the environment that the signal is propagating. In the literature for outdoor environments, it is recorded that this value can range between 2 and 4. On the other hand for indoor environments, it is possible that path loss exponent can even be as high as 5 or 6. It is also possible that path loss exponent can be lower than 2, if a corridor of the buildings creates a tunnel effect which results in a sustained signal along this corridor. While there exists very important uncertainty in path loss exponent in applications, in the literature there are only a few studies which take path loss exponent as an unknown parameter. This situation reveals an important gap in the literature that needs to be filled by advanced studies.

2.2. Fundamentals of RSS Based and Range-Only Localization

In this section, RSS based and range-only localization are mathematically presented and also visually depicted by means of flow charts. One of most important schemes of RSS based localization is depicted in Figure 2.1. As illustrated, RSS measurements depend basically on the positions of the sensors and the emitter. RSS measurements are also influenced by the level of measurement error which is sometimes referred to as "Log-Normal Shadowing". As seen in Figure 2.1, these RSS measurements are converted to the information of the distances between the emitter and each sensors. Now, the issue is that because of measurement errors, it is not possible to find a position for the emitter which satisfies all the distance conditions declared by RSS measurements. Therefore, the aim of the localization is to find such an estimation for the position of emitter that the mismatch between the measured and the estimated distances will be minimum. One of the way of achieving this task is to employ Nonlinear Least Squares (NLS) method to find a point which minimizes the mean of squared distance error as shown in (2) where (x_i, y_i) is the location of the ith sensor, and D_i is the measured distance by ith sensor (or measurement) and N is the total number of sensors (or measurements):

$$(\hat{x}, \hat{y}) = \underset{(x,y)}{\operatorname{argmin}} \sum_{i=1}^{N} \left(\sqrt{(x_i - x)^2 + (y_i - y)^2} - D_i \right)^2 \tag{2}$$

This way of localization is called "lateration". Lateration (or sometimes tri-lateration) is a general name for the processes which accomplish localization using distance (or range) information when distance information are obtained through many different ways such as RSS, time of arrival (TOA) and time of flight (TOF) and so on. Lateration can be the statistically best solution as long as the error in distance-to-emitter measurements is assumed to be Gaussian. As mentioned above for RSS based localization, the error is modelled as log-normal shadowing, yet NLS solution can still effectively approximate Cramer Rao Lower Bound (CRLB).

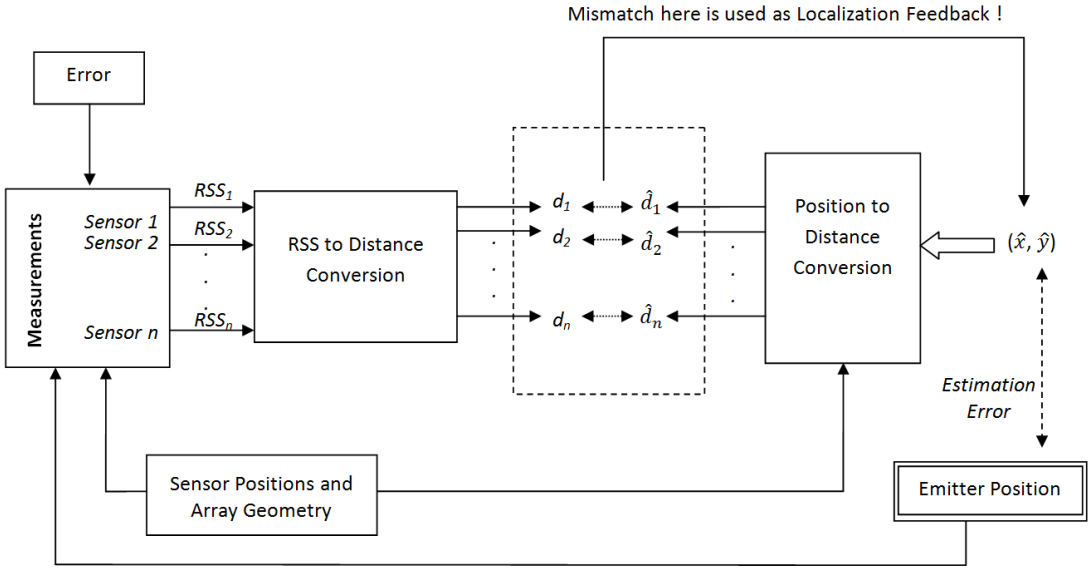

Figure 2.1. *NLS solution of RSS based localization: RSS based lateration*

In Figure 2.2, another RSS based localization scheme is provided again by means of a flow diagram. In this figure, the measured RSS values are not converted to distance values. On the other hand, by setting a prospective point for the emitter, the distances between the emitter and each sensors are determined, and then converted to RSS values. In this scheme, the aim of the localization is to find such an estimation for the position of the emitter that the mismatch between the measured and estimated RSS values will be minimum. This task is achieved by finding a point which minimizes the mean of squared RSS error as shown in (3):

$$(\hat{x},\hat{y}) = \underset{(x,y)}{\operatorname{argmin}} \sum_{i=1}^{N} \left(P_i - p_0 + 10.n.\log_{10}\left(\frac{\Delta_i(x,y)}{d_0}\right)\right)^2 \qquad (3)$$

where P_i is the RSS value measured at ith sensor and $\Delta_i(x, y)$ is the distance of ith sensor to any (x, y) location as the following:

$$\Delta_i(x, y) = \sqrt{(x_i - x)^2 + (y_i - y)^2} \tag{4}$$

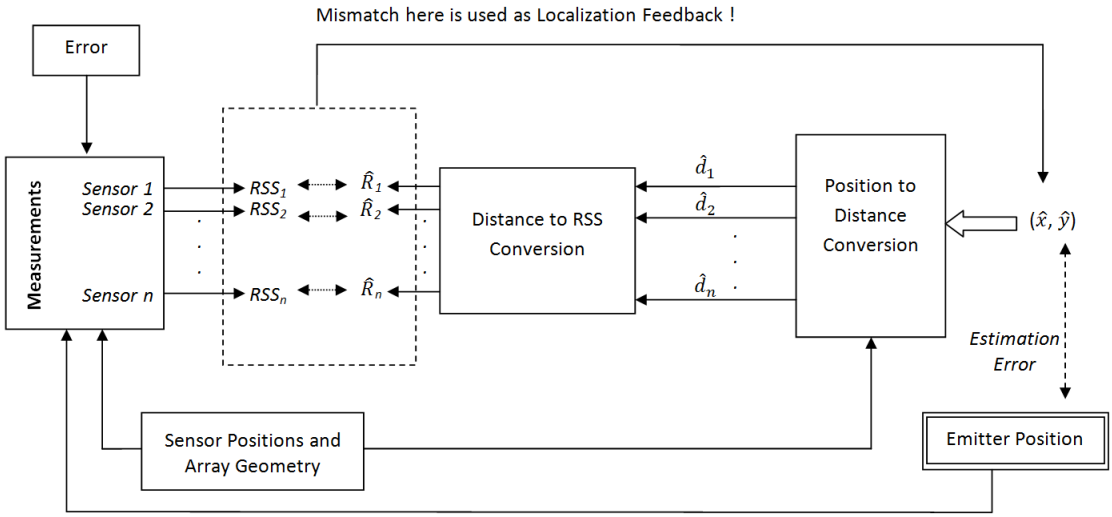

Figure 2.2. *An important RSS localization scheme: RSS based MLE*

Under the assumption of Log-Normal shadowing which proposes normally distributed errors in RSS values, this localization scheme corresponds to Maximum Likelihood Estimation (MLE). Now, let us define an RSS error vector whose ith element is the ith RSS error for the estimation of the emitter location:

$$\vec{P}_{err}(i) = P_i - p_0 + 10.n.\log_{10}(\Delta_i/d_0) \tag{5}$$

The joint probability density function of $\vec{P}_{err}$ can be written as in (6):

$$p(\vec{P}_{err}|x, y) = \frac{1}{\sqrt{(2\pi)^N|C|}} \exp\left(-\frac{1}{2}(\vec{P}_{err})^T C^{-1}(\vec{P}_{err})\right) \tag{6}$$

where C is the covariance matrix of $\vec{P}_{err}$. Because $\vec{P}_{err}(i)$'s are independent, C becomes a diagonal matrices whose diagonal elements are σ^2 i.e. the standard deviation of error. Therefore, (6) can be rewritten as the multiplication of each ith term as shown in (7):

$$p(\vec{P}_{err} \mid x,y) = \prod_{i=1}^{N} \frac{1}{\sqrt{2\pi\,\sigma^2}} \exp\left(-\frac{1}{2\sigma^2}\left(P_i - P_0 + 10.n.\log_{10}\left(\frac{\Delta_i(x,y)}{d_0}\right)\right)^2\right) \quad (7)$$

If the natural logarithm of (7) is taken, then the following equation is obtained:

$$\ln\left(p(\vec{P}_{err} \mid x,y)\right) = -N\,\ln\left(\sqrt{2\,\pi\,\sigma^2}\right) - \frac{1}{2\sigma^2}\sum_{i=1}^{N}\left(P_i - p_0 + 10.n.\log_{10}\left(\frac{\Delta_i(x,y)}{d_0}\right)\right)^2 \quad (8)$$

It can be observed that maximizing (8) corresponds to minimization of (3). Because of this reason, (3) can be directly called as MLE solution of RSS based localization. To sum up, in this section two important schemes of RSS localization have been discussed. Figure 2.1 and Figure 2.2 are important pictures of RSS localization, so the next sections will mention these pictures again. Therefore, these important pictures can be called as "RSS-Localization Flow Charts".

2.3. Current Research Areas in RSS Based Localization

This section briefly lists and illustrates the trends in current research related to RSS based localization. Even though there exists a wide variety of studies, majority of the studies falls into one of these topics listed below [3]:

- **Source of Location Error** (Shadow Fading, systemic bias etc.)
- **New Statistical Models for RSS** (i.e. new path loss models)
- **Statistical modeling of DRSS**
- **Geometrical interpretation and solutions**: for RSS and DRSS based lateration
- **Least Squares optimization** (linearization of NLS i.e. NLS to linear least squares (LLS) conversion)
- **Probabilistic approaches:** Assuming that RSS has a log-normal probability density distribution, the position of the emitter is estimated as the most likely location.
- **Statistical supervised learning:** The sample distribution of the location estimations are obtained through statistical learning.
- **Sensor Array Geometry and Positioning:** In this field, the aim is to find the optimum sensor array geometry to minimize the overall localization estimation error in the area of interest. Path or trajectory planning can be listed in this field.
- **Kernel Based Algorithms:** A kernel function is a nonlinear and parameterized function of input variables. Model-based algorithms use standard statistical models to

provide a relationship between distance and RSS, therefore these algorithms require a prior knowledge, and they are not able encapsulate the complex relation with the distance and RSS for indoor environments. Oppositely, RSS fingerprinting includes a training phase to learn the relation between RSS and distance. Kernel Based Algorithms is to mix both model-based and RSS fingerprinting algorithms.

- **RSS fingerprinting:** In these methods, machine learning tools are employed to map RSS values to the certain locations in x-y domain through a training data. These methods are useful especially for indoor localization when the relation between distance and RSS is not straightforward due to the complicated structures of building.

2.4. Literature Review on Differential RSS

The literature of RSS based localization is so spread that different expressions are being used for the same concepts by different authors. For this reason, this section is providing a rigorous literature review which exhaustively includes all related previous studies by unifying the related concepts. RSS difference, differential RSS or RSS ratio are all same concepts which refers to RSS difference in dB (or equivalently RSS ratio in magnitude) between any two sensors located at different positions. This concept has been built to remove the necessity to know the emitter's transmit power within RSS based localization algorithms. In one of early studies on this subject, [4] has built a method which is primarily based on comparison of relative strength of RSS values on different sensors instead of using directly RSS values on each sensor. In [5], authors discuss that emitter's transmit power can be considered as an unknown parameter, therefore they mention about only considering the differences between RSS values measured at pairs of receivers. They emphasize that RSS difference is analogous to TDOA, because it removes the necessity to know the actual transmit power. Then, they explain that they are utilizing RSS differences between directional antennas within a sensor node to be able determine angle of arrival (AOA).

In [6], in order to discard the dependency on transmit power, magnitude RSS values at two sensors are divided each other and then Taylor expansion are applied both to nominator and denominator to simplify the equation. They called the ratio of magnitude RSS values as energy ratio. In [7], it is first time that the term differential received signal strength (DRSS) is used to refer to taking difference between RSS values in dB at two sensors. They mentioned that DRSS curves can be represented by

circles, just as TDOAs can be represented by hyperbolic functions. By referring to [8], they explain that DRSS circle is a different notion than the circles of RSS-based lateration. After explaining some geometrical aspects of DRSS, they created a least squares estimation method based on DRSS. In [9], they used the term "RSS difference (RSSD)" (in decibels) to refer to the same concept. After explaining that this feature is suitable for uncooperative scenarios, they explicitly mentioned that a RSSD is defining a specific circle, and they formulated the center and the radius of this circle as a function of the RSSD value and the locations of two sensors. They also created non-linear and linear least square solutions to estimate the location of the emitter. In [10], they clearly matched the term RSS difference with uncooperative scenarios. In their studies [10], they gave a couple of RSSD algorithms for non-cooperative emitters. In [11], the ideas related to DRSS in [7] are represented in more detail. In [12], this time the authors called DRSS circle as DRSS based lateration.

In [13], by using one of sensors as the reference, they convert all their RSS values to DRSS and then applied Weighted Least Squares (WLS) method for localization. In [14], performance of maximum likelihood (ML) location estimators for both received signal strength (RSS) and received signal strength difference (RSSD) are shown to be equivalent to each other as opposed to the common perception that the RSS-based ML location would perform better. In [15], a brief literature review specifically about DRSS is provided. [16] and [17] preferred to use "RSS ratio" to refer to DRSS, while [18] used both the terms DRSS and RSS ratio in their paper. In [19] as a recent study, Taylor series expansion approximations and semidefinite relaxation (similar to [6]) based on DRSS are applied. More recently, [20] renamed the concept of DRSS as power difference of arrival.

As can be seen, the terms DRSS, RSSD, RSS ratio and power difference of arrival are used interchangeably each other in the previous studies. The authors are also sometimes publishing their studies independently, which is also mentioned by [15]. Hence, by collecting all these terms, this study removes the barriers of ambiguity in terminology and the difficulties to access all these related studies in this area. In order to maintain consistency, the term "DRSS" is used in the remaining of this study.

Even though there exist many different related studies as mentioned above, there is an important gap in the literature regarding to the geometrical or analytical details of DRSS. Even though some geometrical explanations to DRSS are present, the common

point of all of the previous studies on this subject is to create a cost function by means of DRSS and try to solve non-convex cost functions or to find linear approximations. Although it was explicitly explained that DRSS curves are circles with certain parameters, this information has not been utilized in localization problems. On the other hand, geometrical properties of DRSS can be effectively exploited to create a very efficient algorithm in RF localizations. More recently, intersection of DRSS circles are studied in [20]. However, the key point is that DRSS circles are Apollonius circles, therefore all of the properties of Apollonius circles also apply to DRSS circles. Consequently, this study carefully investigated the analytical and geometrical aspects of DRSS circles from a broad perspective to build a geometrical closed form solution based on DRSS.

2.5. Joint Estimation of Path Loss Exponent and Emitter's Location

In Section 2.1, it has been mentioned that path loss exponent can take several different values regarding to the environmental factors. Therefore, in some applications, it is necessary to jointly estimate both the location of the emitter and the path loss exponent. In [21], it is mentioned that if path loss exponent (PLE) is assumed to be known a priori for RSS based localization, then it is a significant oversimplification for many application scenarios. They illustrated the effect of unknown PLE on the localization performance. In [22], they argue that in actual environments, path loss exponent for each link between emitter and receivers can be quite unpredictable. They obtain a higher localization accuracy via joint estimation of path loss exponent and the location compared to the conventional localization method using the same path loss exponent for all the links. Below, some other studies on this subject are listed:

- Mao et al. (2007) "Path loss exponent estimation for wireless sensor network localization" [23]

- Chan et al. (2011) "Received signal strength localization with an unknown path loss exponent" [24]

- Wang et al. (2012) "On received-signal-strength based localization with unknown transmit power and path loss exponent" [25]

- Salman et al. (2012) "On the joint estimation of the RSS-based location and path-loss exponent" [26]

- Chan et al. (2012) "Estimation of emitter power, location, and path loss exponent" [27]

- Gholami et al. (2013) "RSS-based sensor localization in the presence of unknown channel parameters" [28]

These studies all deal with localization in the case of unknown PLE. However unlike these ones, in this study, the problem of unknown PLE will be solved effectively by means of new powerful geometrical definitions.

2.6. RSS Based Localization via UAVs

Passive RF localization with unmanned aerial vehicles (UAV) is one of the emerging topic within academic and industrial environments. There exist previous studies which created RSS based localization systems with multiple UAVs (e.g. [29]). Recently, there are new studies which are building systems specifically based on DRSS (rather than RSS) for localization by UAVs. In [30] and [31], to obtain optimal trajectories for multiple UAVs during localization of multiple sources, the authors directly exploited the concept of DRSS. They built their study based on Kalman filters. In [32], a GPS jammer localization system with a single UAV is created by means of a DRSS geolocation approach. Below, some other studies which are related to RSS based or range-only localization via UAVs are listed:

- Uluskan, S. et al. (2017) "RSS based localization of an emitter using a single mini UAV" [33]

- Wagle & Frew et al. (2010) "A particle filter approach to wifi target localization" [34]

- Carvalho (2014) "Unmanned Air Vehicle Based Localization and Range Estimation of Wi-Fi Nodes" [35]

- Ibrahim & Sharawi (2014) "Real Time RSS Based Adaptive Beam Steering Algorithm for Autonomous Vehicles" [36]

- Ullah et al. (2013) "An Experimental Study on the Behavior of Received Signal Strength in Indoor Environment (Small UAV)" [37]

- Cheng et al. (2012) "An indoor localization strategy for a mini-UAV in the presence of obstacles" [38]

- Walter et al. (2012) "Localization of RF emitters using compressed sensing with multiple cooperative sensors (Small UAV)" [39]

In this study, by means of a geometrical approach, a building block (i.e. DEU) is proposed which is a significant contribution for DRSS based localization and target tracking with moving sensors.

2.7. Trajectory Optimization for Emitter Localization

Radio frequency (RF) source localization with moving platforms is a challenging research area which deals with both trajectory optimization and target localization at the same time. While authors previously used to use the terms such as observer trajectory or receiver trajectory optimization to name their studies [40], with the dramatic increase in the availability of small UAVs, the authors shifted from these terms directly to UAV trajectory optimization [41]. Even though RF localization with UAVs has a great potential for many applications such as search and rescue activities etc., because of the physical constraints of UAVs, the need for very efficient solutions has emerged in terms of both hardware and software [29].

Many different UAV path planning systems have been discussed which are based on different sensors such as angle of arrival (AOA), time difference of arrival (TDOA), scan-based (SC) and finally received signal strength (RSS) [42]. Among these, RSS based systems have a special place because they require less complex hardware and software combinations [29]. Because of this reason, since the earlier studies about UAV based RF localization [43], RSS sensors are frequently included in UAV trajectory planning. RSS or differential RSS based UAV trajectory planning recently obtained significant attention by the researchers [30, 31, 44, 45].

The common point of the previous studies is to model the motion of the UAVs as a set of discrete waypoints. Moreover, to decrease the computational complexity, the space of movement of the UAVs is also quantized [44]. In order to optimize the trajectories of UAVs, the waypoints are updated dynamically throughout the motion of the UAVs. Trajectory planning (or namely trajectory optimization) problem can be viewed as a special extension of sensor placement problem. Fisher information matrix (FIM) is a significant basis to obtain a trajectory control objective function. For optimal trajectories, there are many criteria which are based on FIM. In D-optimality criterion, the determinant of FIM is maximized to minimize the area of error ellipse [41].

However, motions of UAVs are more than just discrete measurement states. First, UAVs can continue to take measurements between two waypoints. Therefore, assuming

that measurements are only taken at specific points can lead to loss of some important portion of data. Previously in [46], continuous measurements along continuous trajectories are discussed within the context of weather forecasting. Therefore, building a model for continuous measurements along the trajectories of UAVs can be an inspiring solution for the systems in which the measurements can be taken so frequently (such as RSS based trajectory planning). Second, instead of discrete waypoints, modeling UAV trajectories as continuous paths can bring a stronger basis for trajectory optimization. Finally, modeling continuous trajectories together with continuous measurements can create a new understanding which results in significant convenience for optimal trajectory planning.

2.8. Literature Review on Sensor Position Uncertainty

This study provides an effective new method to solve the localization problem with distance-to-target measurements in the presence of sensor positions errors. Source localization with imprecise sensor positions is an old research area which has been subject of many different applications since the late 1970s. The uncertainty in sensor positions first discussed for the large towed array of hydrophones in the field of underwater acoustic research. The distortion in the shape of the array of hydrophones due to the movement of the tow ship was mentioned as a reason of positional uncertainty in the receiving hydrophones [47, 48, 49]. This type of arrays are then regarded as randomly perturbed arrays and the initial Cramer Rao lower bound (CLRB) derivations are obtained for range and bearing estimation [50]. In [51], it is mentioned that overall localization accuracy can be dominated by the uncertainty in the sensor positions. Therefore, they mentioned about calibrations of sensor array geometries for better localization of a single far-field source. In [52], the issue of uncertainty in the sensor positions is listed under additional topics of the sensor array processing.

In [53], it is mentioned that error in sensor locations can emerge when the sensors are randomly deployed in an ad hoc network or when sensors move to different positions in time. In [54], it has been discussed that in modern localization applications, the receivers can be airplanes or unmanned aerial vehicles (UAVs) therefore their positions as well as velocities can not be precisely known. Therefore, they explicitly mentioned that deployment of UAVs as moving receivers brings the issue of uncertainty in receiver position. As a result, the new trend of using UAVs as moving sensors has

increased the importance of localization with imprecise sensor positions. Therefore, localization with imprecise sensor positions via time difference of arrival (TDOA) or frequency difference of arrival (FDOA) have remained as an interesting research area until today. In [55], for TDOA based localization, a calibration emitter is proposed to calibrate the location of the sensors to compensate sensor position errors. In [56, 57], they give a significant emphasis to TDOA based source localization with random sensor position errors by dividing their study into two parts for specifically static sensors and then mobile sensors with imprecise positions. In [58], the authors deal with TDOA and FDOA based localization and in [59], a TDOA based localization with inaccurate sensor positions is discussed and so on.

Imprecise sensor positions are also specifically discussed for source localization with distance-to-target (or range-only) measurements. In [60] and [61], they introduced distance based localization schemes in wireless sensor networks when both the locations of the nodes and the anchors are unknown or imprecise. They built semi-definite and second order cone programming to address this issue. In [62], the focus is directly on source localization by means of time of arrival (TOA) in the presence of sensor position errors. They build CRLB for range based localization of a source with imprecise sensor positions. They emphasized that the source localization is highly sensitive to the inaccuracy in sensor positions. Finally, they built a Weighted Least Square (WLS) solution for sensor position errors which are quite small. In [63], TOA and TDOA based localization with sensor position errors were discussed in terms of again WLS solutions but this time for larger sensor position error levels compared to [62]. Maximum likelihood estimation (MLE) solution is also mentioned to attain CRLB without explicitly presenting MLE solution in their paper. In [64], TOA based localization with sensor position errors is solved by a two-stage algorithm where an initial estimate for the location of source at the first stage is further improved at the second stage.

3. PATH PLANING: BEST DIRECTION GIVEN A LIMITED TRAJECTORY

When a moving sensor travels with the aim of estimating the location of the emitter, the first goal must be to create an effective route planning strategy which statistically guarantees the best possible estimation capability at the end of the travel of the moving sensor. This section deals with trajectories of the moving sensors and describes the essence of trajectory planning through a new perspective namely Fisher Continuous Information Matrix. It explores the best angular direction given a limited length of travel for both RSS and range-only based localization.

3.1. Fisher Information Matrix and D-Optimality Criterion

Range only measurements are the measurements which give us cues about the distance between the source (or target) and the sensor. Therefore, a range only measurement R_i can be modeled as the following:

$$R_i = \sqrt{(x - x_i)^2 + (y - y_i)^2} + W \sim N(0, \sigma) \tag{9}$$

where (x_i, y_i) is the position of the ith sensor, (x, y) is the position of the target and W is a zero mean Gaussian noise with a standard deviation σ. Fisher information matrix (FIM) for estimating the parameters (x, y) given the range only measurements from N spatially distinct points can be written as the following [65]:

$$I_{range}(x, y) = \frac{1}{\sigma^2} \begin{bmatrix} \sum_{i=1}^{N} \frac{(x - x_i)^2}{(x - x_i)^2 + (y - y_i)^2} & \sum_{i=1}^{N} \frac{(x - x_i)(y - y_i)}{(x - x_i)^2 + (y - y_i)^2} \\ \sum_{i=1}^{N} \frac{(x - x_i)(y - y_i)}{(x - x_i)^2 + (y - y_i)^2} & \sum_{i=1}^{N} \frac{(y - y_i)^2}{(x - x_i)^2 + (y - y_i)^2} \end{bmatrix} \tag{10}$$

Received signal strength (RSS) is a function of the distance between the target and the measurement point, so each RSS measurement indirectly provides us with a range information. In accordance with path loss model, an RSS measurement provides us with the information of logarithm of distance between the sensor and the source. When the RSS sensor measurement errors are assumed to be zero-mean Gaussian, each RSS measurement can be expressed as the following:

$$S_i = P_0 - 10.n \log_{10} \left[\left(\sqrt{(x - x_i)^2 + (y - y_i)^2} \right) / d_0 \right] + W \sim N(0, \sigma) \tag{11}$$

where P_0 is the emitter's power in dB (at a reference distance d_0), n is the path loss exponent. With this measurement model, Fisher information matrix for the RSS measurements from N spatially distinct points can be expressed as the following [66]:

$$I_{RSS}(x,y) = K\begin{bmatrix} \sum_{i=1}^{N} \frac{(x-x_i)^2}{[(x-x_i)^2+(y-y_i)^2]^2} & \sum_{i=1}^{N} \frac{(x-x_i).(y-y_i)}{[(x-x_i)^2+(y-y_i)^2]^2} \\ \sum_{i=1}^{N} \frac{(x-x_i).(y-y_i)}{[(x-x_i)^2+(y-y_i)^2]^2} & \sum_{i=1}^{N} \frac{(y-y_i)^2}{[(x-x_i)^2+(y-y_i)^2]^2} \end{bmatrix} \quad (12)$$

where K is a constant such that:

$$K = \frac{1}{\sigma^2}\left(\frac{10\,.n}{\ln(10)}\right)^2 \quad (13)$$

Because of RSS measurements are related to the logarithm of the distance, the accuracy of the range information reduces as the distance between the source and the target increases. This is the main distinction between the range-only and RSS based localization.

For the vector $[\hat{x},\hat{y}]^T$ which contains unbiased estimators for the x and y positions of the target, the inverse of the Fisher Information Matrix is the lower bound for the covariance matrix of this estimation vector [67]:

$$Cov(\hat{x},\hat{y}) \geq I(x,y)^{-1} = \sum(x,y) \quad (14)$$

In accordance with the principle component analysis, the orientations of two dimensional error distribution for the estimation are the eigenvectors (i.e. $\vec{u}_1$ and $\vec{u}_2$) of $I^{-1}(x,y)$. Moreover, the variances along these orientations are eigenvalues (i.e. λ_1 and λ_2) of $I^{-1}(x,y)$ [68]. The error distribution of estimation can be represented by means of an ellipse within two dimensional space. As the number measurement increases, the error ellipse is supposed to diminish around the exact target location as illustrated in Figure 3.1.a and Figure 3.1.b.

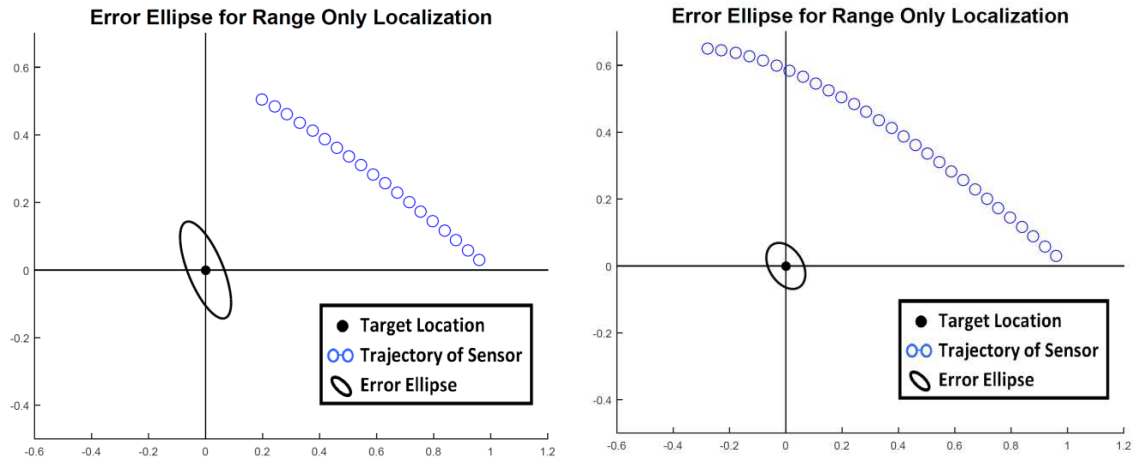

(a) (b)

Figure 3.1. *The size of error ellipse decreases as the number of measurements increases while moving sensor moves along its path*

The size of error ellipse can be considered to be proportional to the determinant of $I^{-1}(x, y)$ which is equal to the product of the eigenvalues λ_1 and λ_2.

$$Size\ of\ Error\ Ellipse\ \sim \det(I^{-1}) = \lambda_1 \cdot \lambda_2 \tag{15}$$

Trajectory optimization which is a special version of optimal sensor placement is to manage the motion of moving sensor in order to obtain the highest possible estimation capability in the vicinity of the target. In order to minimize the error ellipse, the determinant of inverse FIM matrix must be minimized, or oppositely the determinant of FIM must be maximized. This criterion which is commonly used in trajectory optimization is called D-optimality criterion [41].

3.2. Optimal Sensor Placement

In the last section, it has been mentioned that trajectory optimization is a special case of optimal sensor placement, therefore it is necessary to first understand the basics of optimal sensor placement. In order to simplify the overall task, in the studies about optimal sensor placement, the target is assumed to be located at the origin (i.e. $x = 0$ and $y = 0$), so the FIM in (10) for range only localization can be rewritten as the following:

$$I_d^R = \frac{1}{\sigma^2}\begin{bmatrix} \sum_{i=1}^{N} \frac{x_i^2}{x_i^2+y_i^2} & \sum_{i=1}^{N} \frac{x_i\, y_i}{x_i^2+y_i^2} \\ \sum_{i=1}^{N} \frac{x_i\, y_i}{x_i^2+y_i^2} & \sum_{i=1}^{N} \frac{(y-y_i)^2}{x_i^2+y_i^2} \end{bmatrix} \tag{16}$$

Moreover, if the location of the ith measurement point is expressed as polar coordinates (r_i, θ_i), then FIM can be written as:

$$I_d^R = \frac{1}{\sigma^2}\begin{bmatrix} \sum_{i=1}^{N} \cos^2(\theta_i) & \sum_{i=1}^{N} \sin(\theta_i)\cos(\theta_i) \\ \sum_{i=1}^{N} \sin(\theta_i)\ \cos(\theta_i) & \sum_{i=1}^{N} \sin^2(\theta_i) \end{bmatrix} \tag{17}$$

The interesting point in (17) is that the radial coordinates (i.e. r_i's) of measurement points do not appear within FIM. In other words, only the angular coordinates are important, so the radial coordinates can be simply neglected during optimal sensor placement. Therefore, not the exact points of the sensors but their radial projections onto the unit circle can be taken into account in order to emphasize the importance of the angular position during optimization of sensor positions for range-only localization.

When x and y coordinates of the radial projections of the N measurements points onto the unit circle are expressed as separate vectors i.e. $\vec{X}$ and $\vec{Y}$ as shown below,

$$\vec{X} = [\cos(\theta_1)\ , \cos(\theta_2)\ , \cos(\theta_3) \ldots\ \cos(\theta_N)\ ] \tag{18}$$

$$\vec{Y} = [\sin(\theta_1)\ , \sin(\theta_2)\ , \sin(\theta_3) \ldots\ \sin(\theta_N)\ ] \tag{19}$$

then FIM in (17) can be expressed as the following:

$$I_d^R = \frac{1}{\sigma^2}\begin{bmatrix} \vec{X}\cdot\vec{X} & \vec{X}\cdot\vec{Y} \\ \vec{X}\cdot\vec{Y} & \vec{Y}\cdot\vec{Y} \end{bmatrix} = \frac{1}{\sigma^2}\begin{bmatrix} \left|\vec{X}\right|^2 & \left|\vec{X}\right|\ \left|\vec{Y}\right|\cos(\varphi) \\ \left|\vec{X}\right|\ \left|\vec{Y}\right|\cos(\varphi) & \left|\vec{Y}\right|^2 \end{bmatrix} \tag{20}$$

where φ is angle between $\vec{X}$ and $\vec{Y}$ within N dimensional space. In accordance with the D-optimality criterion, the vectors $\vec{X}$ and $\vec{Y}$ must be specifically chosen so that $\det(I_d^R)$ given below is maximized:

$$\det\left(I_d^R\right) = \frac{1}{\sigma^4}\left|\vec{X}\right|^2\left|\vec{Y}\right|^2\left[1-\cos(\varphi)^2\right] \tag{21}$$

given the constraint [65]:

$$\left|\vec{X}\right|^2 + \left|\vec{Y}\right|^2 = N \tag{22}$$

Consequently, this maximization process declares that the vectors $\vec{X}$ and $\vec{Y}$ must be in same size and perpendicular to each other within N dimensional space [65]. In x-y domain, this corresponds that sensors must be placed as apart as possible to each other. If it is assumed that sensors are only allowed to be placed along the unit circle, then they must be equally separated to obtain the highest estimation capability around the origin. Figure 3.2.a illustrates an optimal sensor placement around the origin for three sensors, and Figure 3.2.b shows the corresponding $\vec{X}$ and $\vec{Y}$ vectors within N dimensional space. As seen, $\vec{X}$ and $\vec{Y}$ are perpendicular to each other and in the same size (i.e. on the same sphere) for this optimal sensor placement.

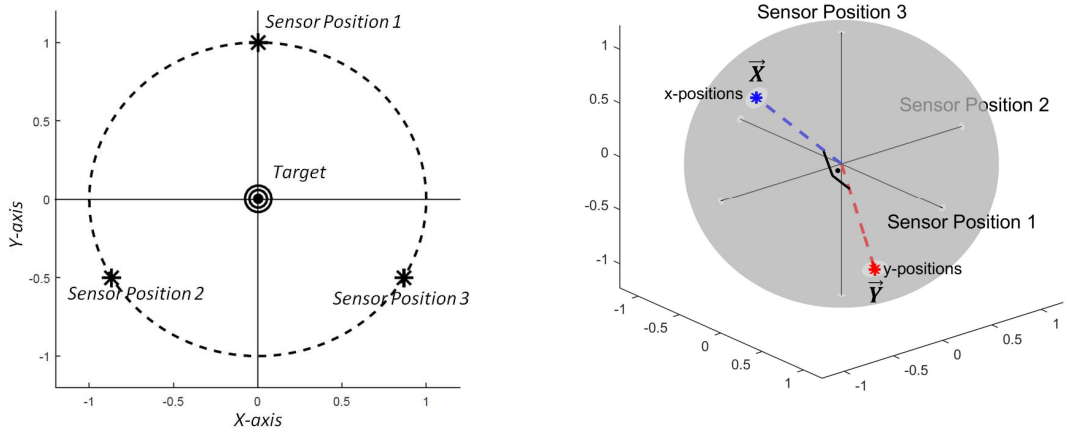

(a) (b)

Figure 3.2. *(a) An optimal sensor placement around the origin for three sensors, (b) $\vec{X}$ and $\vec{Y}$ (i.e. the vectors of x and y positions of the sensors respectively) must be perpendicular to each other and in the same size (i.e. on the same sphere) for optimal sensor placement.*

To sum up, for optimal sensor placement, the radial projections of measurement points must be uniformly distributed along the unit circle. Therefore for the optimal trajectories, it can be intuitively argued that the projection of the trajectory (i.e. the projection of the measurement points along the trajectory) must correspond to the largest arc along the unit circle. Moreover, the projections of measurement points along the unit circle must be aligned as uniformly as possible.

When the target is located at the origin and the location of the ith measurement point is expressed as polar coordinates (r_i, θ_i), then FIM in (12) can be rewritten as:

$$I_d^S = K \begin{bmatrix} \sum_{i=1}^{N} \frac{\cos^2(\theta_i)}{{r_i}^2} & \sum_{i=1}^{N} \frac{\sin(\theta_i)\ .\cos(\theta_i)}{{r_i}^2} \\ \sum_{i=1}^{N} \frac{\sin(\theta_i)\ .\cos(\theta_i)}{{r_i}^2} & \sum_{i=1}^{N} \frac{\sin^2(\theta_i)}{{r_i}^2} \end{bmatrix} \tag{23}$$

Please note a difference exists between this FIM with the one in (17). Unlike (17), the radial coordinates of the measurement points are also important in Fisher Information Matrix and consequently in sensor placement or trajectory optimization. The measurement points which are close to the target are more valuable because they provide us with a more accurate range information because of log-normal shadowing. Therefore, in addition to the objectives mentioned above (i.e. the longest projected arc on unit the circle and the most possible uniform distribution of the projected sensor positions), the moving sensor must also try get closer to target while planning its trajectory in RSS based localization.

3.3. Continuous Trajectories: Fisher Continuous Information Matrix

The common point of trajectory optimization studies is to model the motion of the sensor as a set of discrete waypoints together with discrete measurements. However, the motion of moving sensors is in fact a continuous path, therefore when measurements are frequent enough, they can be regarded as continuous time stochastic processes. The summation operators within FIM can be appropriately converted to line integrals [69]. To provide a detailed insight into trajectory optimization for range-only and RSS-based localization, this study shifts the scope of Fisher Information Matrix (FIM) from discrete measurement geometries to continuous measurement curves.

In order to differentiate continuous curve FIMs from usual FIMs, the FIMs associated with continuous trajectories will be called as Fisher Continuous Information Matrices (FCIM) in the remaining of this study. Now, FCIMs for continuous curves of range-only and RSS measurements will be defined. For a continuous curve *L*, the summation operators within the FIM matrices in (17) and in (23) are converted to line integrals as in the following:

$$I_c^R = \frac{1}{\sigma^2}\begin{bmatrix} \int_L cos^2(\theta)\ ds & \int_L sin(\theta).cos(\theta)\ ds \\ \int_L sin(\theta).cos(\theta)\ ds & \int_L sin^2(\theta)\ ds \end{bmatrix} = \frac{1}{\sigma^2}\begin{bmatrix} a_{11}^R & a_{12}^R \\ a_{21}^R & a_{22}^R \end{bmatrix} \quad (24)$$

$$I_c^S = K\begin{bmatrix} \int_L \frac{\cos^2(\theta)}{r^2}\ ds & \int_L \frac{\sin(\theta).\cos(\theta)}{r^2}\ ds \\ \int_L \frac{\sin(\theta).\cos(\theta)}{r^2}\ ds & \int_L \frac{\sin^2(\theta)}{r^2}\ ds \end{bmatrix} = K\begin{bmatrix} a_{11}^S & a_{12}^S \\ a_{21}^S & a_{22}^S \end{bmatrix} \quad (25)$$

FCIM can be regarded as an overall FIM which is characteristically related to the continuous curve L. Therefore, FCIM is a measure of the capability of the overall curve L to estimate the location of the emitter. FCIM is independent of measurement frequency along the curve. FIMs of the discrete measurements which are frequently taken throughout the curve L can be approximated as the following:

$$I_d^R \cong f.\ I_c^R \quad (26)$$

$$I_d^S \cong f.\ I_c^S \quad (27)$$

where f is the rate of the measurement per unit length. As f increases, I_d^R and I_d^S can be better approximated by the right sides of (26) and (27) respectively. Figure 3.3 illustrates the new proposed definition namely FCIM for a continuous curve of measurement. FCIM shifts the scope of FIM from discrete measurement geometries to continuous curves.

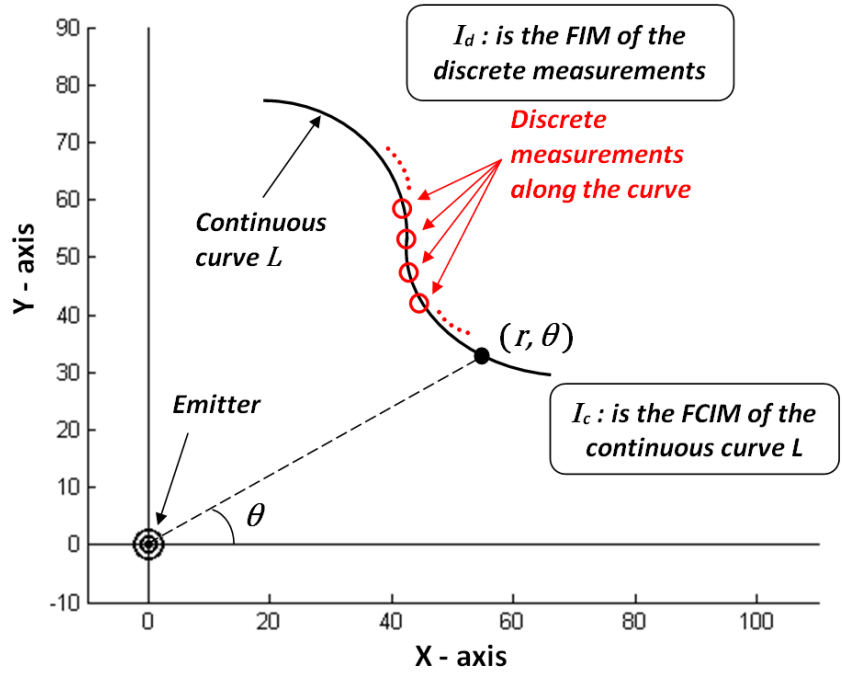

Figure 3.3. *Fisher continuous information matrix of a continuous curve of measurement.*

3.4. Calculation of Line Integrals for Linear Trajectories

In this section, calculation of line integrals in FCIMs for linear trajectories will be discussed. In order to calculate the line integrals in FCIMs, lines must be represented in terms of polar coordinates as shown in Figure 3.4.

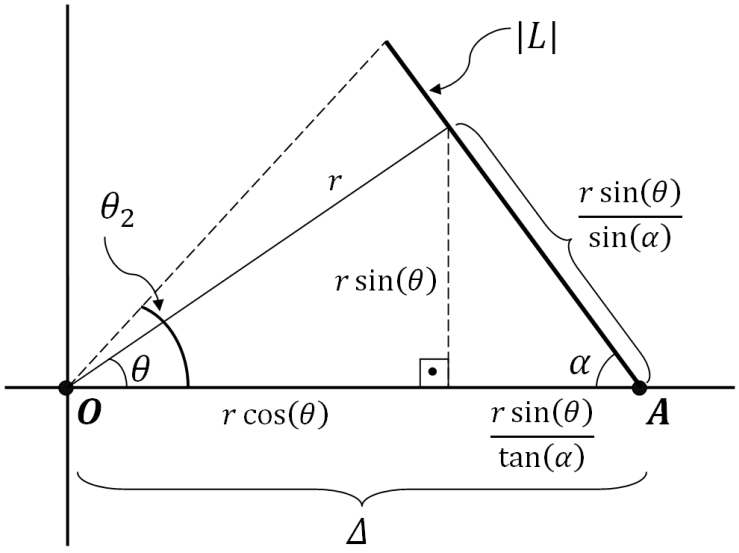

Figure 3.4. *The geometry of the linear trajectory and its parameters.*

The equation of the line passing from the initial point of movement (i.e. the point A in Figure 3.4) can be written in terms of polar coordinates as the following:

$$r(\theta) = \Delta / \left(\cos(\theta) + \frac{\sin(\theta)}{\tan(\alpha)} \right) = \frac{\Delta \sin(\alpha)}{\sin(\alpha + \theta)} \tag{28}$$

where Δ is the distance between the point A and the emitter, and the α is the angle between the curve L and x-axis. In this equation, the radial coordinate r is expressed as a function angular coordinate θ. The upper limit θ_2 for the angular coordinate which makes the length of the curve be equal to $|L|$ can be written as:

$$\theta_2 = arccot\left(\frac{\Delta}{|L|} \frac{1}{sin(\alpha)} - \cot(\alpha) \right) \tag{29}$$

The line element ds can be calculated as the following [70]:

$$ds = \sqrt{r^2 + \left(\frac{dr}{d\theta} \right)^2}\, d\theta = \frac{r}{\sin(\theta + \alpha)}\, d\theta \tag{30}$$

After these calculations, the integrals in (24) and (25) can be calculated with respect to θ. Let us reorganize the integrals within the elements of I_c^R:

$$a_{11}^R = \int_0^{\theta_2} \cos^2(\theta)\ ds = \int_0^{\theta_2} \frac{\cos^2(\theta)\ r(\theta)}{\sin(\theta + \alpha)}\, d\theta = \Delta \sin(\alpha) \int_0^{\theta_2} \frac{\cos^2(\theta)}{\sin^2(\theta + \alpha)}\, d\theta \tag{31}$$

$$a_{22}^R = \int_0^{\theta_2} \sin^2(\theta)\ ds = \int_0^{\theta_2} \frac{\sin^2(\theta)\ r(\theta)}{\sin(\theta + \alpha)}\, d\theta = \Delta \sin(\alpha) \int_0^{\theta_2} \frac{\sin^2(\theta)}{\sin^2(\theta + \alpha)}\, d\theta \tag{32}$$

$$a_{12}^R = a_{21}^R = \int_0^{\theta_2} \sin(\theta)\ \cos(\theta)\ ds = \Delta \sin(\alpha) \int_0^{\theta_2} \frac{\sin(\theta)\ \cos(\theta)}{\sin^2(\theta + \alpha)}\, d\theta \tag{33}$$

Similarly, the integrals within the elements of I_c^S can be rewritten as:

$$a_{11}^S = \int_0^{\theta_2} \frac{\cos^2(\theta)}{r^2(\theta)}\, ds = \int_0^{\theta_2} \frac{\cos^2(\theta)}{r(\theta) \sin(\theta + \alpha)}\, d\theta = \frac{1}{\Delta \sin(\alpha)} \int_0^{\theta_2} \cos^2(\theta)\ d\theta \tag{34}$$

$$a_{22}^{S} = \int_{0}^{\theta_2} \frac{\sin^2(\theta)}{r^2(\theta)}\, ds = \int_{0}^{\theta_2} \frac{\sin^2(\theta)}{r(\theta)\sin(\theta+\alpha)}\, d\theta = \frac{1}{\Delta \sin(\alpha)} \int_{0}^{\theta_2} \sin^2(\theta)\; d\theta \tag{35}$$

$$a_{12}^{S} = a_{21}^{R} = \int_{0}^{\theta_2} \frac{\sin(\theta)\;\cos(\theta)}{r^2(\theta)}\, ds = \frac{1}{\Delta \sin(\alpha)} \int_{0}^{\theta_2} \sin(\theta)\;\cos(\theta)\; d\theta \tag{36}$$

As seen, the indefinite integrals of I_c^S can be easily obtained in order to calculate determinant of the matrix in the closed form. However, the indefinite integrals of I_c^R are not too straightforward, so numerical calculation of integrals can be utilized for I_c^R for the next sections.

3.5. Best Orientation is only a function of $|L|/\Delta$

In this section, it will be proved that the best orientation for a linear trajectory in terms of estimation capability is only a function of the ratio between total length of travel and the initial distance to target (i.e. $|L|/\Delta$). Based on (31-33) and (34-36), determinants of I_c^R and I_c^S can be expressed as:

$$\det(I_c^R) = \frac{\Delta^2 \sin^2(\alpha)}{\sigma^4}\; g(\alpha, \theta_2) \tag{37}$$

$$\det(I_c^S) = \frac{K^2}{\Delta^2 \sin^2(\alpha)}\; h(\alpha, \theta_2) \tag{38}$$

where $g(\alpha, \theta_2)$ and $h(\alpha, \theta_2)$ are the functions which can be determined after calculating the integrals in (31-33) and (34-36). If the ratio $|L|/\Delta$ is designated as ρ, then θ_2 which has been defined in (29) is a function of only α and ρ. Therefore determinant of I_c^R and I_c^S can be rewritten as:

$$\det(I_c^R) = \frac{\Delta^2}{\sigma^4}\; g'(\alpha, \rho) \tag{39}$$

$$\det(I_c^S) = \frac{K^2}{\Delta^2}\; h'(\alpha, \rho) \tag{40}$$

where $g'(\alpha, \rho)$ and $h'(\alpha, \rho)$ are the functions which represent the parts of the determinants which depend on α and ρ. To find the best directions i.e. $\alpha_B{}'s$ which

maximize the determinants, the partial derivative of determinants with respect to α must be taken and then the roots of these equations must be found:

$$\frac{\partial\ (\det(I_c^R\ ))}{\partial\ \alpha} = 0 \tag{41}$$

$$\frac{\partial\ (\det(I_c^S\ ))}{\partial\ \alpha} = 0 \tag{42}$$

The terms Δ^2/σ^4 and K^2/Δ^2 disappear while taking partial derivative, so the best directions i.e. $\alpha_B{}'s$ which maximize the determinants I_c^R and I_c^S are found to be functions of only ρ i.e. $|L|/\Delta$. Next section, the relation between ρ and α_B will be explored for both range-only and RSS-based localization.

3.6. Best Possible Orientation given a limited length of travel

Moving sensors can be carried by many different moving platforms such unmanned aerial vehicles etc. Mini UAVs can have a couple of physical constraints including maximum flight time, maximum weight of useful load etc. All these constraints can lead to a limited range of travel for small UAVs. Moreover, the emergency of the localization mission may imply time constraints which also result in limited total lengths of travel. Therefore, the best possible estimation capability can be desired given a limited length of travel which is shorter than initial distance to emitter. In this section, the best orientations of the linear trajectories will be discussed by the means of FCIMs.

In Figure 3.5.a, the determinants of the FIMs for linear discrete measurements are illustrated for various possible orientations of the trajectory. To obtain the best capability of estimation, this study sets three distinct criteria: (1) the radial projection of the trajectory onto unit circle must correspond to the longest possible arc, (2) the projections of the measurements along trajectory must be uniformly distributed as much as possible, and for RSS based localization (3) the measurements must be as close as possible to the target. In some extent, all these three criteria contradict each other. Considering the RSS based localization, based on the first criterion, moving along the x-axis appears as the best way because it yields the closest measurements to the target. However, this trajectory strictly violates first and second criteria because the radial projection of it has no arc length. It will be also shown that first and second criteria also

contradict each other. Therefore, best orientation must take all the tradeoffs between these criteria into account. Consequently, the direction marked with the ellipse in Figure 3.5.a is the best orientation which maximizes the determinant of FIM under a certain constraint on the total length of travel. Figure 3.5.b depicts the continuous trajectory version of this maximization process. As seen, the best directions correspond to each to other for discrete and continuous trajectories. In this section, the best direction will be demonstrated with respect to $|L|/\Delta$ by means of FCIMs.

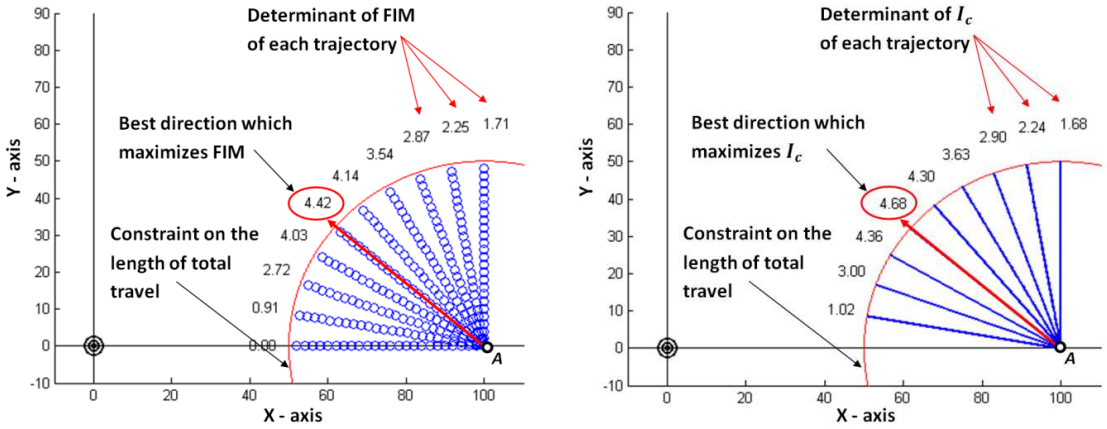

(a) (b)

Figure 3.5. *The best direction for best estimation capability around the origin given a constraint on the length of total travel: (a) maximizing the determinant of the FIM for linear discrete measurements, (b) maximizing the determinant of the FCIM for linear continuous trajectories.*

Figure 3.6 shows a trajectory and its radial projection on unit circle. For simplicity, Δ is assigned to be 1, so the initial point of movement of moving sensor is set to be (1,0). The constraint on the total length is represented by means of circle centered at (1,0) with radius is $|L|$. As seen, the first criterion (i.e. obtaining longest projected arc length) can be achieved when α is equal to $arccos(|L|/\Delta)$. It has been mentioned the third criterion is only for RSS based localization, so it is not relevant to range only localization. Therefore, it can be assumed that the best direction for range only localization can be simply formulated as $arccos(|L|/\Delta)$ in accordance with the first criterion. However, first and second criteria also contradict each other, which causes the best direction deviate from $arccos(|L|/\Delta)$.

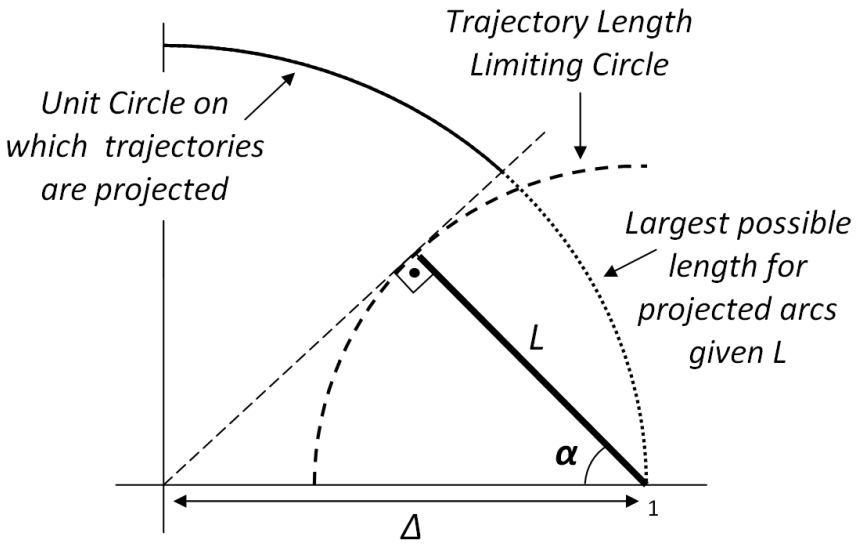

Figure 3.6. *The first criterion (i.e. obtaining longest projected arc length) can be achieved when α is equal to* $arccos(|L|/\Delta)$

Figure 3.7.a shows the case that α is set to $arccos(|L|/\Delta)$, therefore trajectory has the longest projected arc length. In this case, it can be observed that the radial projections of the measurement points close to the initial point are positioned near to each other compared to those in the end of trajectory. This structure violates the second criteria which requires radial projections to be uniformly distributed as much as possible. Figure 3.7.b shows the case in which the radial projections of measurements are uniformly distributed as much as possible along the unit circle.

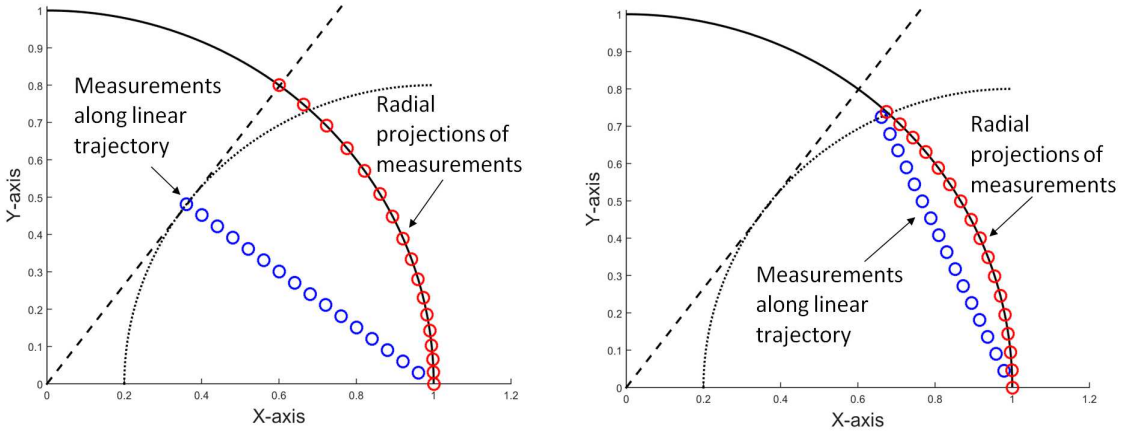

(a) (b)

Figure 3.7. *(a) The first criterion contradicts the second criterion (i.e. the radial projections of measurements must be uniformly distributed as much as possible), (b) one of the best case for second criterion.*

Figure 3.8 shows the plots of the best angular orientation for range only and RSS based localization with respect to $|L|/\Delta$. As can be seen, for range only localization, the best angular orientation mostly matches the arccosine function for small values of $|L|/\Delta$. However, for large values $|L|/\Delta$, the best angular orientation deviates from the arccosine function because the second criterion (i.e. the need for uniform distribution of projected measurements along unit circle) starts to be important compared to first criterion (i.e. the need for longest projected arc). For RSS based localization, the best angular orientation always stays below arccosine because third criterion is now valid for RSS based localization. The important point regarding to RSS based localization is that the best angular direction is 0 degree when $|L|/\Delta$ is 1. In other words, if the moving sensor is able to reach to target, than it must be directed towards the target for the best possible estimation capability. In the next section, a new method called Direction of Exponent Uncertainty is introduced which aims to create a direction towards the emitter for any time of the travel.

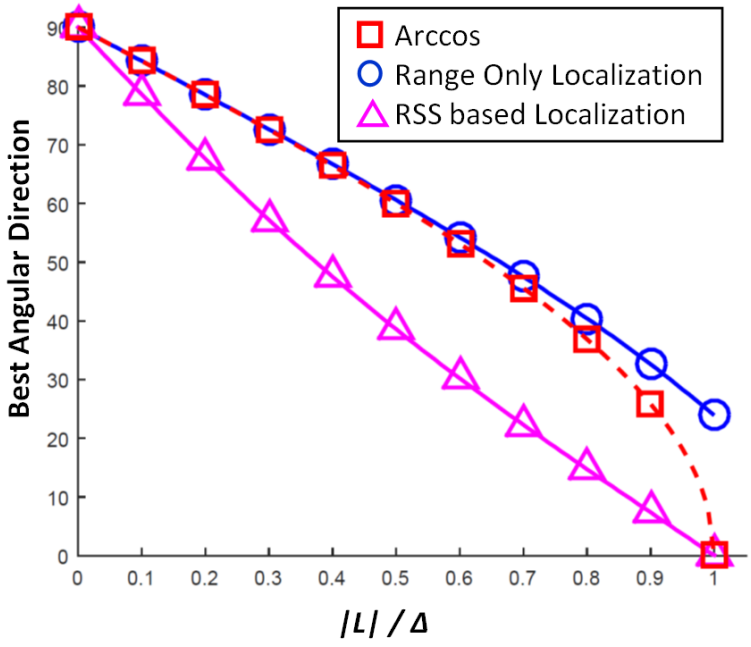

Figure 3.8. *The best angular orientation for range only and RSS based localization with respect to* $|L|/\Delta$

4. A NEW ROUTE PLANNING AND LOCALIZATION METHOD: DIRECTION OF EXPONENT UNCERTAINTY

In Section 3.6, it has been shown that if the moving sensor is able to reach to target, than it must be directed towards the target for the best possible estimation capability. In this study, a new powerful geometrical closed-form solution called as Direction of Exponent Uncertainty (DEU) [1] is proposed for received signal strength (RSS) based far-field localization when path loss exponent (PLE) and transmit power are both unknown. The uncertainty in the PLE due to environmental factors is a significant challenge for RSS based localization. DEU is built after careful investigation of geometrical behaviors of differential received signal strength (DRSS) circles, i.e. the locus of possible location of the emitter when transmit power is unknown. It is shown that the uncertainty in the PLE corresponds to a linear uncertainty for the location of the emitter in two dimensional space. This critical observation creates a basis for the sensor to move towards the emitter without estimating the emitter location after only three measurements. Furthermore, with only four different measurements, it is possible to effectively estimate the location of the emitter as well as the PLE by means of intersection of DEUs. Intersection of DEUs attains Cramer Rao Lower Bound (CRLB) with a dramatically reduced execution time compared to nonlinear least squares (NLS) estimator. DEU is also proposed as an efficient route planning tool for moving sensors such as unmanned aerial vehicles (UAVs).

4.1. Feedback Domains of RSS Based Localization

In Section 2.2, two important schemes of RSS based localization was introduced. Now, in this chapter, the advantages and disadvantages of these schemes will be discussed to come up with new ideas of solution for localization. Figure 4.1 shows the flow chart of the information-flow during RSS based localization. This flow chart is distinctively divided into three domains, namely RSS domain, distance domain and (x, y) domain. In Section 2.2, it was discussed that in RSS-MLE solution, the feedback for the goodness of the estimation of the emitter location is provided from RSS domain. The mismatch between measured and the estimated RSS values are used to evaluate the goodness of the estimation. On the other hand, in RSS based lateration, the feedback for the goodness of the estimation of the emitter location is provided from distance domain. As depicted in Figure 4.1, as the feedback domain approaches to left, the statistical

meaning of the localization becomes higher. Oppositely, as the feedback domain shifts to right, the localization process obtains a higher level of geometrical meaning.

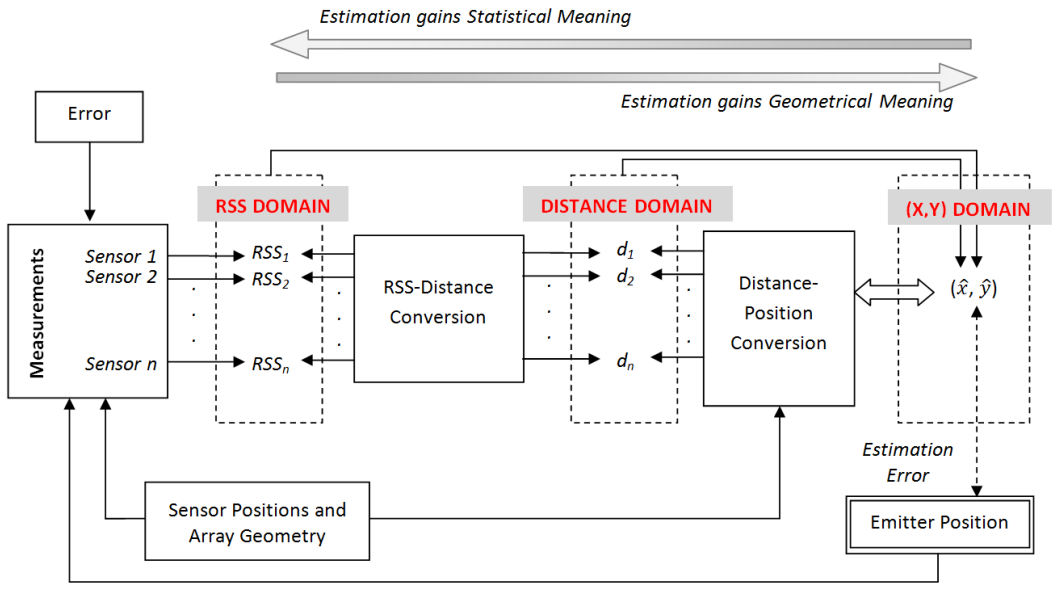

Figure 4.1. *Flowchart of RSS based Localization*

As discussed in Section 2.2, when RSS domain is used as the feedback domain, the localization scheme corresponds to MLE solution. Therefore, RSS domain based localization schemes have a high level of statistical meaning. It is easy to statistically explain the validity of this estimation structure. On the other hand, this localization schemes lacks geometrical point of view. Furthermore, the localization feedback is relatively far from the (x, y) domain. In other words, the mismatch in RSS domain provides a difficult cue about how to adjust the estimation of emitter position. This situation results in a complicated cost function to be minimized:

$$(\hat{x}, \hat{y}) = \underset{(x,y)}{\operatorname{argmin}} \sum_{i=1}^{k} \left(P_i - p_0 + 10.n.\log_{10}\left(\frac{\sqrt{(x_i - x)^2 + (y_i - y)^2}}{d_0} \right) \right)^2 \qquad (43)$$

Figure 4.2.a and Figure 4.2.b show respectively the surface of the cost functions when the emitter is located somewhere at the middle of the sensors and when the emitter is located far from the sensors. In both cases, there exist irregularities, saddle points and local minima which may trick the minimum point search algorithm. Furthermore, especially at Figure 4.2.b, the minimum point is not located at the bottom of a good convex structure. In other words, the minimum point is visually not apparent.

This situation will yield a more difficult task including large number of iterations during search for the minimum point.

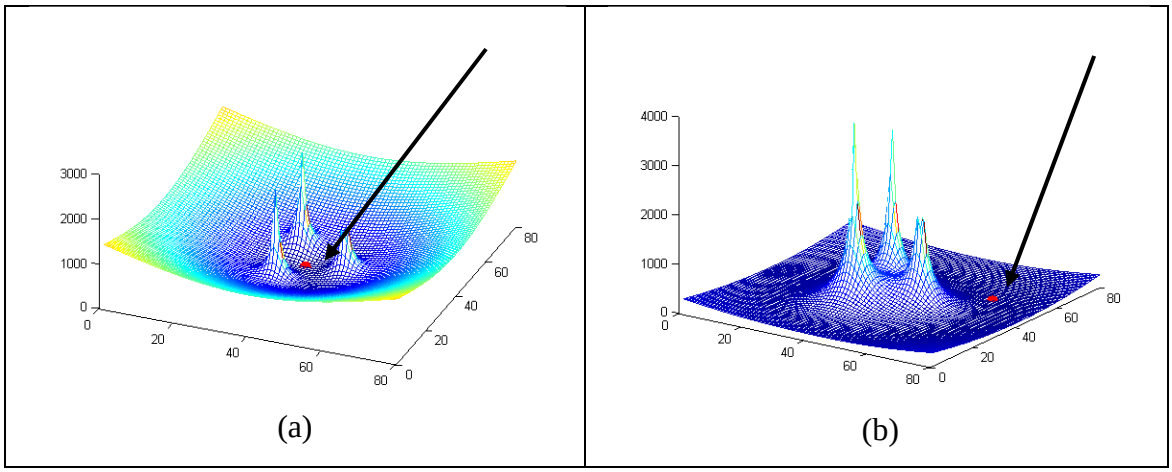

Figure 4.2. *Example Structures of Cost Functions of MLE (RSS domain feedback)*

To sum up, when RSS-domain used as the feedback domain, the following situations are arising [71]:

- NLS equation corresponds to MLE solution
- It is easy to statistically explain the validity of the estimation
- The estimation lacks geometrical meaning
- Feedback is relatively far from the (x, y) domain (i.e. complicated cost function)

When distance domain used as the feedback domain, the localization scheme do not have a high level of statistical meaning. It is not very easy to statistically explain the validity of this estimation structure. Minimizing the squared error in distance can be only regarded as an approximation of MLE function. On the other hand, this localization schemes has a geometrical point of view so that this localization schemes are called as lateration. Some of the resources (e.g. [8]) have directly classified lateration based localization under geometrical solutions. Furthermore, the localization feedback is relatively closer to the (x, y) domain, in other words, the mismatch in RSS domain provides a simpler cue about how to adjust the estimation of emitter position. This situation results in an efficient cost function to be minimized:

$$(\hat{x}, \hat{y}) = \underset{(x,y)}{\operatorname{argmin}} \sum_{i=1}^{k} \left(\sqrt{(x_i - x)^2 + (y_i - y)^2} - d_i \right)^2 \tag{44}$$

Figure 4.3.a and Figure 4.3.b show respectively the surface of the cost functions when the emitter is located somewhere at the middle of the sensors and when the

emitter is located far from the sensors. In both cases, there exist smooth regular surfaces which may help the global minimum searching algorithm. Furthermore, the minimum points are located at the bottom of good convex structures. The minimum points are even visually apparent. This situation will yield simpler tasks including smaller number of iterations during search for the minimum point.

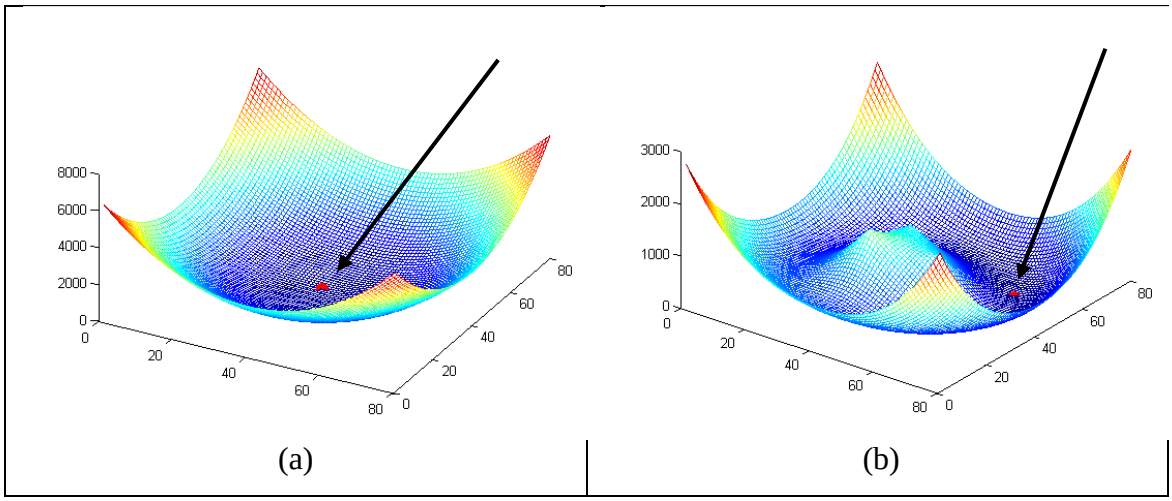

Figure 4.3. *Example Structures of Cost Functions of RSS based lateration (Distance domain feedback)*

To sum up, when distance-domain used as the feedback domain, the following situations are arising [71]:

- NLS equation corresponds to RSS-based lateration
- It is not easy to statistically explain the validity of the estimation
- The estimation has a geometrical point of view
- Feedback is relatively closer to the (x, y) domain (i.e. simple cost function)

4.2. A New Geometrical Solution: Direction of Exponent Uncertainty

Based on the following sections, a new discussion can be initiated about performing localization directly within (x, y) domain. As it has been discussed in previous sections, as the path of feedback for localization error becomes longer, it is difficult to handle with the localization algorithm. Therefore, this study will focus on localization systems directly operating in (x, y) domain as shown in Figure 4.4. In order to achieve this task, RSS measurements must be first converted to some geometrical definitions within (x, y) domain. Next sections will introduce Direction of Exponent Uncertainty which is a powerful geometrical tool for trajectory planning and localization.

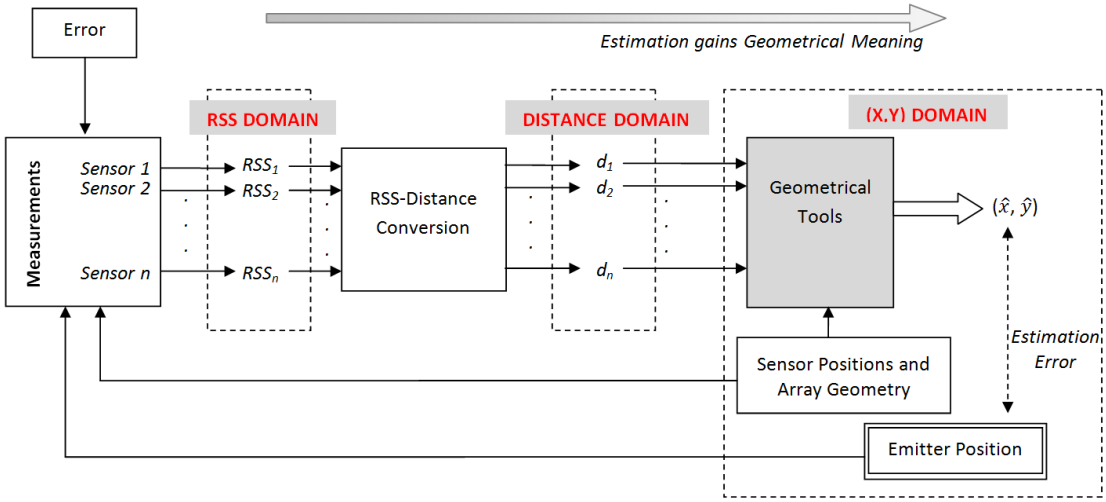

Figure 4.4. *Localization directly within* (x, y) *domain: geometrical tools*

By using RSS parameters, some major techniques are employed to obtain solutions to localization problem [3]: mapping (fingerprinting) which is based on building a learner which maps the specific RSS values to the related locations, statistical techniques which are providing theoretical frameworks to overcome difficulties in the presence of noise, range-based solutions such as trilateration and finally geometrical solutions. RSS fingerprinting is criticized for requiring a large initial data to train the system, but it is found useful for indoor localization when the relation between distance and RSS values are complicated. Based on a predefined model, statistical methods are criticized for not being able encapsulate the complex relations between the distance and RSS values [72]. Even though geometrical solutions provide very simple approaches, it is not always possible to explain the optimum solution in case of noisy or imperfect environments by means of geometrical concepts.

Recently new applications have gain importance which mount sensor systems on moving platforms such as unmanned aerial vehicles (UAV). Because of the physical constraints of moving platforms, these applications bear the necessity to use the most efficient hardware and software combination. With this motivation, RSS based systems emerge as significant tools for affordable solutions. Moreover, building a geometrical solution for RSS based localization will provide a very efficient localization system which also exploits the simplicity of geometrical approaches. In this study, a new powerful geometrical solution called as Direction of Exponent Uncertainty (DEU) is introduced which shows that the uncertainty in the location of the emitter can be

modeled as a special line when path loss exponent is unknown. It is shown that intersection of DEUs attains Cramer Rao Lower Bound (CRLB) with a dramatically reduced execution time compared to nonlinear least squares (NLS) estimator. Furthermore, since DEU proposes a closed-form solution, the algorithm does not have a divergence issue. The new method is constituted of only mathematical and trigonometric equations. On the other hand, NLS solution requires a difficult nonconvex optimization and the localization algorithm can fail. DEU is also proposed as an efficient route planning tool for moving sensors such as unmanned aerial vehicles (UAVs), because it helps the sensor move efficiently towards the target.

4.3. Problem Formulation

This part carefully sheds a light to the geometrical behaviors of DRSS circles with an emphasis how they can be exploited in RF localization. As proved by many previous studies [12], path loss model can be formulated as a log-distance equation as described in (1). The path loss exponent n in (1) determines the rate of change in RSS values with respect to log-distance. Path loss exponent n can vary due to different environmental conditions. It can take a value between the range 2 and 4 for outside, while it can also drop below 2 or exceed 4 for some special situations [27] as described in Section 2.1. Therefore, uncertainties in path loss exponent create a significant challenge in RSS based localization.

4.3.1. DRSS Problem Formulation

In accordance with the path loss model, it can be shown that DRSS locus of two different measurements must satisfy the following equation:

$$\frac{d_1}{d_2} = \sqrt[n/2]{\frac{RSS_2[mag]}{RSS_1[mag]}} \tag{45}$$

where d_1 and d_2 are distances of RF emitter to the first and second sensors, and $RSS_1[mag]$ and $RSS_2[mag]$ are RSS values in magnitude in first and second sensors respectively. Geometrically, the set of all points satisfying (45) can be shown to be a circle called DRSS circle [7]. In essence, DRSS circle is an Apollonius Circle [73] defined as the points with constant ratio of distances to two fixed points. Even though

previous studies did not explain DRSS circle through Apollonius circle, they successfully defined the center of the DRSS as the following [9],

$$x_{center} = \frac{(x_1 - K_{12}.x_2)}{(1 - K_{12})} \quad , \quad y_{center} = \frac{(y_1 - K_{12}.y_2)}{(1 - K_{12})} \tag{46}$$

where (x_1, y_1) and (x_2, y_2) are the location of the first and second sensor and K_{12} is defined as,

$$K_{12} = \sqrt[n/2]{\frac{RSS_2[mag]}{RSS_1[mag]}} \tag{47}$$

It can be also shown that the radius of DRSS circles is [20]:

$$Radius = \sqrt{\frac{K_{12}.(x_2^2 + y_2^2) - x_1^2 - y_1^2 + \frac{(x_1 - K_{12}.x_2)^2}{(1 - K_{12})} + \frac{(y_1 - K_{12}.y_2)^2}{(1 - K_{12})}}{(1 - K_{12})}} \tag{48}$$

As an Apollonius circle, DRSS circle has two important properties. First, the center of DRSS circle must be located along the line which passes through the sensors' locations. Second, DRSS circles must pass between two sensors. Figure 4.5 illustrates the structure of an DRSS circle.

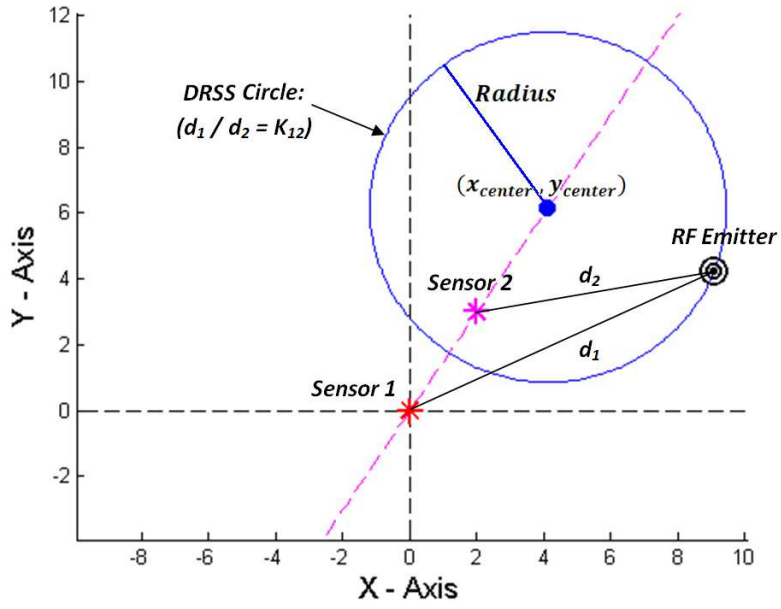

Figure 4.5. *Illustration of DRSS circle which is a special type of Apollonius Circle*

4.3.2. DRSS based Cost Function and Localization

The DRSS based cost function for location estimation is defined as [9],

$$Q(x,y,n) = \sum_{k<l} \left[DRSS_{kl}[dB] - 5.n \,.\log_{10} \left[\frac{(x-x_l)^2 + (y-y_l)^2}{(x-x_k)^2 + (y-y_k)^2} \right] \right]^2 \tag{49}$$

where $DRSS_{kl}[dB]$ is the difference of RSS values in dB between k^{th} and l^{th} sensors, (x_k, y_k) and (x_l, y_l) is the location of k^{th} and l^{th} sensors respectively, and finally (x, y) is the possible location of the emitter. To obtain a nonlinear least squares (NLS) solution, the estimator needs to jointly find the (x, y) location and the n value which will minimize the cost function $Q(x, y, n)$. This study finds a very effective geometrical closed form solution which perfectly approximates NLS solution and attains CRLB with very low computational requirements compared to the NLS solution.

4.3.3. Circle-Circle Intersection

It is possible to estimate the location of the emitter by intersecting the DRSS circles [9]. In Figure 4.6, intersection of two circles are depicted. Let us designate the center points of the circles as (x_1,y_1) and (x_2,y_2) and the radii of the circles as r_1 and r_2 respectively for first and second circles. There will be two intersection points namely P_1 and P_2. Let us call the line which passes through the circles' centers as l_1, the distance between the centers of two circles as d, the angle between the l_1 and x-axis as β and finally the angle between l_1 and the line which connects (x_1,y_1) and P_1 as α, then the location of P_1 and P_2 can be formulated as the following,

$$d = \sqrt{(x_2 - x_1)^2 + (y_2 - y_1)^2} \tag{50}$$

$$\beta = \arctan\left(\frac{(y_2 - y_1)}{(x_2 - x_1)} \right) \tag{51}$$

$$\alpha = \arccos\left(-\frac{r_2^2 - r_1^2 - d^2}{2.r_1.d} \right) \tag{52}$$

$$\theta_1 = \beta + \alpha \quad and \quad \theta_2 = \beta - \alpha \tag{53}$$

$$P_1 = (x_1 + r_1.\cos(\theta_1) \;,\; y_1 + r_1.\sin(\theta_1)) \tag{54}$$

$$P_2 = (\ x_1 + r_1.\cos(\theta_2)\ ,\ y_1 + r_1.\sin(\theta_2))\tag{55}$$

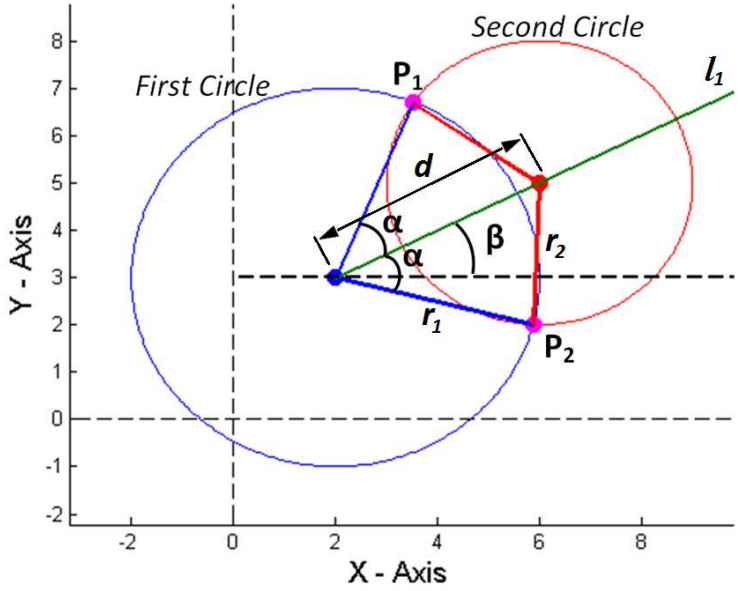

Figure 4.6. *Illustration of circle-circle intersection*

4.3.4. Intersection of DRSS circles

In Figure 4.7, three RSS measurements are taken from three different positions in order to estimate the location of the emitter. It has been discussed that two measurements from two different locations enables us to draw a DRSS circle. Therefore, taking three measurements provides us with three distinct DRSS circles for each of three pairs of measurements. Here, it is important to emphasize that these three circles are confined to intersect always at only two points (even under noise) [73]. While any three circles can normally intersect at six distinct points, three Apollonius circles of three fixed points can only intersect at two points [73]. Because any two of these circles are enough for localization, one of these circles can be discarded. Furthermore, because DRSS circles must pass between the associated measurement points as mentioned in Section 4.3.1, one of the intersection points must stay close to measurement points and the other one is located at a distant position. This study assumes that the emitter is located far from the measurement locations (or the starting point where the sensor begins its motion), therefore the intersection point which is close to the measurement points will be neglected. Consequently, for the scope of this study, three measurements are enough to detect the location of the emitter when the path loss exponent is known.

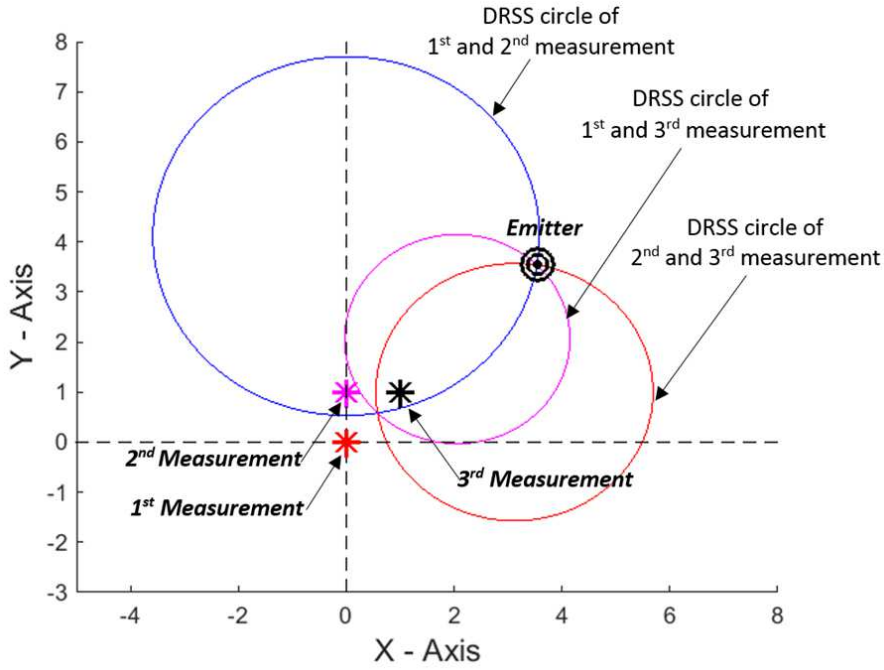

Figure 4.7. *Intersection of DRSS circles*

4.4. Direction of Exponent Uncertainty: A New Localization Method

In Section 4.3.4, it has been discussed that taking three measurements is enough to locate the RF emitter when path loss exponent (n) is known. However, as it has been discussed in Section 2.1, it is very common that n can be unpredictable due to environmental or some other factors. Therefore, detection of the exact location of the emitter by means of three measurements is not possible. However, in this study, it will be proved that having no knowledge about the value of n is not an obstacle for the moving sensor to be directed towards the emitter. It will be shown that with three measurements, a direction which passes through the emitter can be determined which yields an effective localization system.

4.4.1. Direction of Exponent Uncertainty: Definition

Figure 4.8 shows the intersections of DRSS circles when path loss exponent values are accepted as 2, 3 and 4 where the real n value is 3. As shown, when the accepted values of path loss exponent (denoted as n_{Guess}) increases, DRSS circles grow and the intersection point of the circles (possible location of the emitter) changes. It can be observed that only when n_{Guess} is equal to exact n, the guess point coincides with the correct location of the emitter.

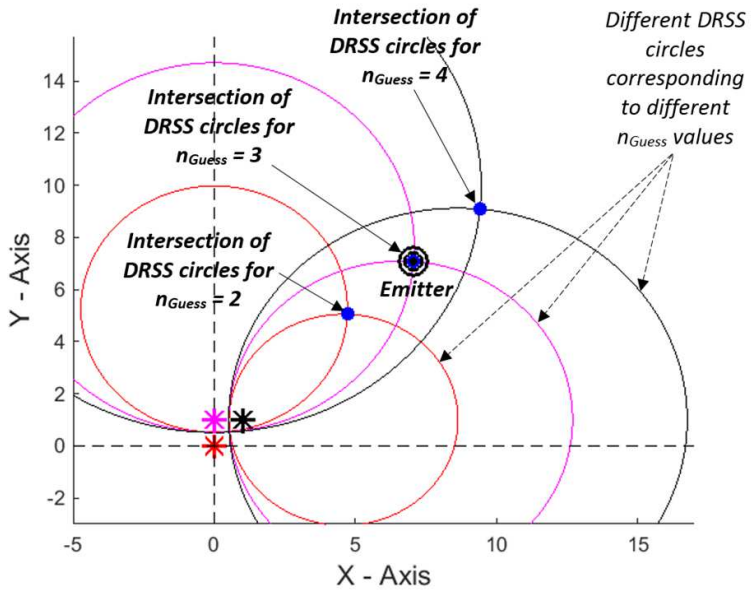

Figure 4.8. *Intersection of DRSS circles for different n_{Guess} values*

The main idea of this study is that the possible locations of the emitter corresponding to different values of n constitute a line in two dimensional space. Furthermore, the coordinates of these points can be modeled as a linear function of the values of path loss exponent. This phenomenon can be better observed in Figure 4.9. The guess points for different n_{guess} values have a perfect tendency to align linearly (even for values of n which are not physically meaningful). The uncertainty in the n values creates a linear uncertainty in the location of emitter. This study calls this phenomenon as Direction of Exponent Uncertainty (DEU).

Consequently, when there are three measurements as shown in Figure 4.9, the localization system can determine a line which passes through the location of the emitter. It is also possible to use this important observation to move to the location of the emitter with a moving sensor at the smallest possible duration when the value of n is unknown. After three measurements, if the moving sensor settles its motion along the DEU, then it catches a linear path which goes to the emitter.

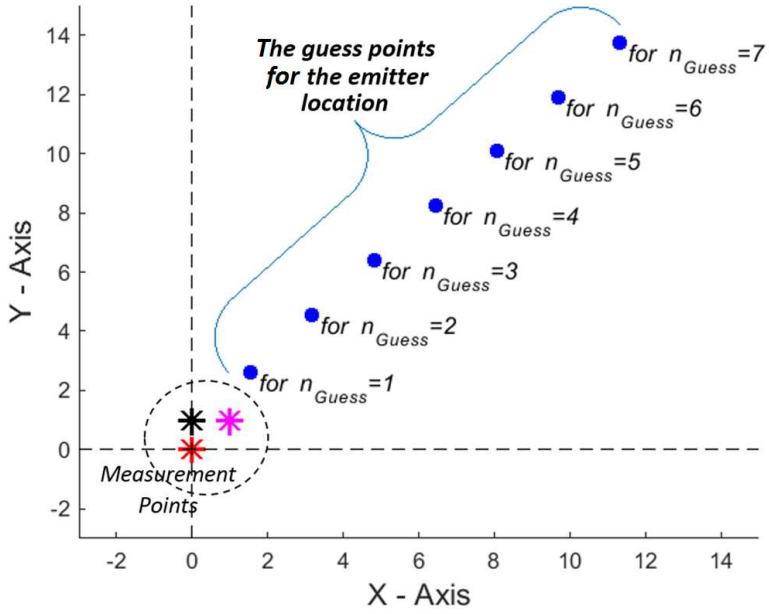

Figure 4.9. *Illustration of the new phenomenon: Direction of Exponent Uncertainty (DEU)*

The linear structure of DEU is valid when there exists a non-linear measurement geometry. Section 4.5.3 presents the case when there are three linear measurements.

4.4.2. Proof of DEU

Now, the existence of DEU (i.e. linearity of guess points with respect to different n values) will be proved. In Figure 4.10, the DRSS circle based on the first and second measurements is labeled as DRSS Circle-12 and the DRSS circle based on the second and three measurements is labeled as DRSS Circle-23. As explained in the Section 4.3.4, the x component of the guess point of the emitter can be expressed as in the following equation:

$$x_{guess}(n) = x_{12}(n) + r_{12}(n) \cdot \cos(\theta(n)) \tag{56}$$

where $r_{12}(n)$ and $x_{12}(n)$ are respectively the radius and the x component of the center of DRSS Circle-12, and $\theta(n)$ is the angle between x axis and the line which passes through the center of DRSS Circle-12 and the intersection of the DRSS circles. x_{12} and r_{12} both depend on the n value and the RSS values of first and second measurements. In addition to these parameters, $\theta(n)$ also depends on the RSS value of third measurement. Now, if it is proved that the derivative of $x_{guess}(n)$ with respect to n is a constant term, or at least converges to a constant term very quickly even for very

small values of n, then the proof will be complete. The derivative of $x_{guess}(n)$ with respect to n can be expressed as the following:

$$\frac{d\, x_{guess}(n)}{d\, n} = \frac{d\, x_{12}(n)}{d\, n} + \frac{d\, r_{12}(n)}{d\, n}\,.\cos(\theta(n)) + \, r_{12}(n)\,.\frac{d\, \cos(\theta(n))}{d\, n} \tag{57}$$

In accordance with (47), let us drop the label $[mag]$ and define $K_{12}(n)$ such that:

$$K_{12}(n) = \sqrt[n/2]{RSS_2 \,/\, RSS_1} \tag{58}$$

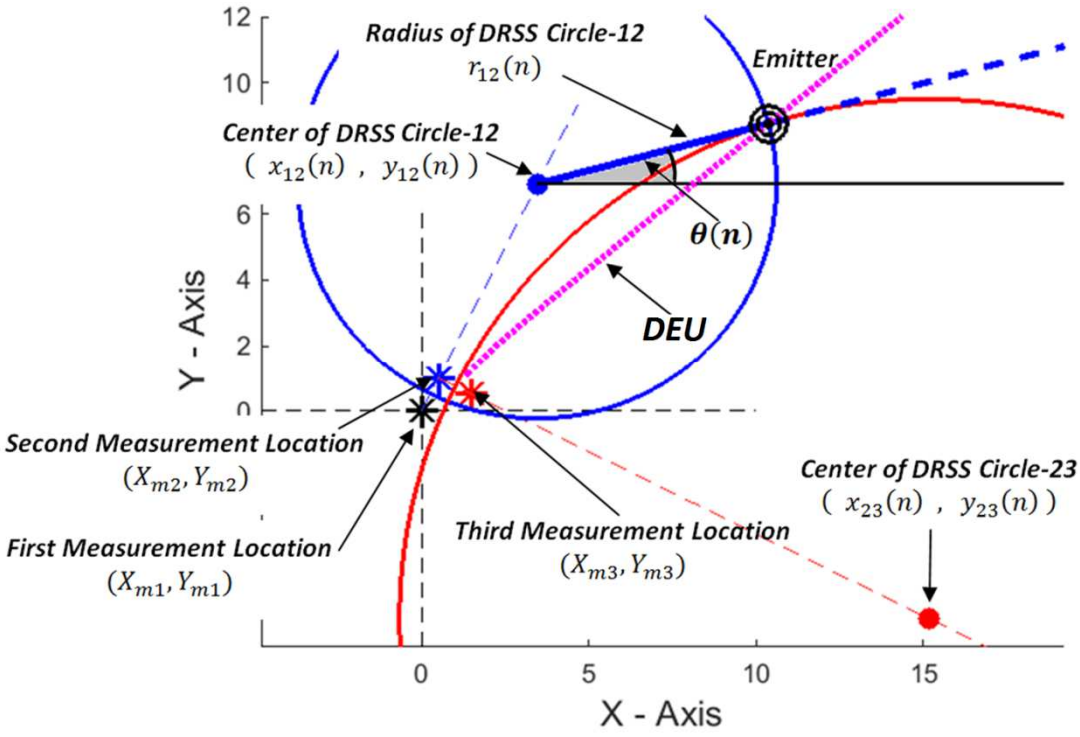

Figure 4.10. *Formulation of the guess point with respect to n*

Now, after inserting $K_{12}(n)$ into (46) and (48), the following the derivatives with respect to n can be obtained:

$$\frac{d\, x_{12}(n)}{d\, n} = (X_{m2} - X_{m1})\,.\,\ln\left(\frac{RSS_2}{RSS_1}\right)\frac{2\,.K_{12}(n)}{n^2(\,K_{12}(n) - \,1)^2} \tag{59}$$

$$\frac{d\, r_{12}(n)}{d\, n} = \, d_{m12}\,.\,\ln\left(\frac{RSS_2}{RSS_1}\right)\frac{\sqrt{K_{12}(n)}(K_{12}(n) \,+\, 1)}{n^2(\,K_{12}(n) - \,1)^2} \tag{60}$$

where X_{m1} and X_{m2} are respectively the x components of the first and second measurement points, and d_{m12} is the distance between these two points. After these, the limit values of these functions as n approaches to infinity can be found as,

$$\lim_{n\to\infty} \frac{d\, x_{12}(n)}{d\, n} = \frac{(X_{m2} - X_{m1})/2}{\ln\left(\frac{RSS_2}{RSS_1}\right)} \tag{61}$$

$$\lim_{n\to\infty} \frac{d\, r_{12}(n)}{d\, n} = \frac{d_{m12}/2}{\ln\left(\frac{RSS_2}{RSS_1}\right)} \tag{62}$$

Taking limit of $\theta(n)$ as n approaches to infinity is not straightforward, however, it can be numerically shown that $\theta(n)$ also converges a limit value θ_{lim}. Now, it will be investigated how quickly these functions reach their limit values. In Figure 4.11, it can be observed that all three functions demonstrate very short transition periods and reach their limit values very quickly. After the n value that DRSS Circle-12 and DRSS Circle-23 start to intersect (the vertical dashed lines at the left in Figure 4.11), all three functions have great tendency to catch their limit values. When n is equal to 2 (physically the lower bound for path loss exponent for most of the environments), they are almost settled to their limit values.

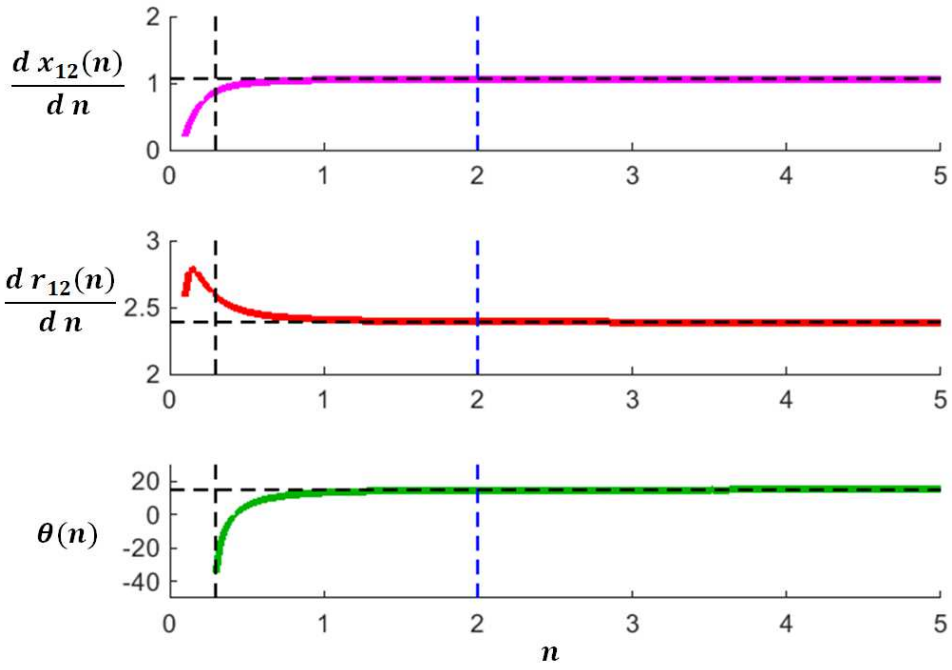

Figure 4.11. *The plots of $\theta(n)$ and the derivative of $x_{12}(n)$ and $r_{12}(n)$ with respect to n*

Finally, the derivative of $x_{guess}(n)$ in (56) can be rewritten as the following,

$$\frac{d\, x_{guess}(n)}{d\, n} = \frac{(X_{m2} - X_{m1})/2}{\ln\left(\frac{RSS_2}{RSS_1}\right)} + \frac{d_{m12}/2}{\ln\left(\frac{RSS_2}{RSS_1}\right)} .\ \cos(\theta_{lim}) + r_{12}(n) \,.0 \tag{63}$$

Therefore, taking the integral of the above function yields the following equation:

$$x_{guess}(n) = \frac{(X_{m2} - X_{m1}) + d_{m12}.\cos(\theta_{lim})}{2\ \ln\left(\frac{RSS_2}{RSS_1}\right)}\, n + C_1 = A\, n + C_1 \tag{64}$$

A similar equation regarding to the y component of the guess point of the emitter can be written as in the following,

$$y_{guess}(n) = \frac{(Y_{m2} - Y_{m1}) + d_{m12}.\sin(\theta_{lim})}{2\ \ln\left(\frac{RSS_2}{RSS_1}\right)}\, n + C_2 = B\, n + C_2 \tag{65}$$

which finalizes the proof of DEU.

4.4.3. Parameters of DEU

To speak roughly, the parameters of DEU depends strictly on the measurement geometry. As an example, when the measurement geometry is a right triangle whose legs are aligned with x and y axes (as shown in Figure 4.9), the slope of the DEU can be written as:

$$m_{DEU} = \frac{d_{m23}}{d_{m12}}\, \frac{\ln\left(\frac{RSS_2}{RSS_1}\right)}{\ln\left(\frac{RSS_3}{RSS_2}\right)} = \frac{d_{m23}}{d_{m12}}\, \frac{\ln(RSS_2) - \ln(RSS_1)}{\ln(RSS_3) - \ln(RSS_2)} \tag{66}$$

where RSS_i denotes RSS values in magnitude of the ith measurement, d_{m12} is the distance between first and second measurement locations and d_{m23} is the distance between second and third measurement locations. If the measurement geometry is further isosceles right triangle, the slope can be written as:

$$m_{DEU} = \frac{\ln\left(\frac{RSS_2}{RSS_1}\right)}{\ln\left(\frac{RSS_3}{RSS_2}\right)} = \frac{\ln(RSS_2) - \ln(RSS_1)}{\ln(RSS_3) - \ln(RSS_2)} \tag{67}$$

Another important parameter regarding to DEU is the ratio of the emitter distance to n, namely $\Delta_{emitter}$. This parameter represents the distance between two successive

guess points when the guess value of n is incremented by 1. The equation of the $\Delta_{emitter}$ for isosceles right triangle is as the following,

$$\Delta_{emitter} = 1/\left(ln\left(\frac{RSS2}{RSS1}\right) . ln\left(\frac{RSS3}{RSS2}\right) . \sqrt{\frac{ln\left(\frac{RSS2}{RSS1}\right)^2 + ln\left(\frac{RSS3}{RSS2}\right)^2}{ln\left(\frac{RSS2}{RSS1}\right)^2 . ln\left(\frac{RSS3}{RSS2}\right)^2}} \right) \quad (68)$$

This parameter allows us to quickly estimate the value of n after the location of the emitter is determined. Finally, at least a point is required through which the DEU passes to be able to completely define the DEU. With this motivation, it is investigated if there exists a common point through which all possible DEUs for all different bearings pass. Figure 4.12 shows that one third of the all DEUs shares a common point, while other one third of them shares another common point etc. Therefore, there are three common points corresponding to three different groups of all possible DEUs. The observations suggest that these common points constitute a equilateral triangle, however the size and the location of this equilateral triangle strictly depends on measurement geometry.

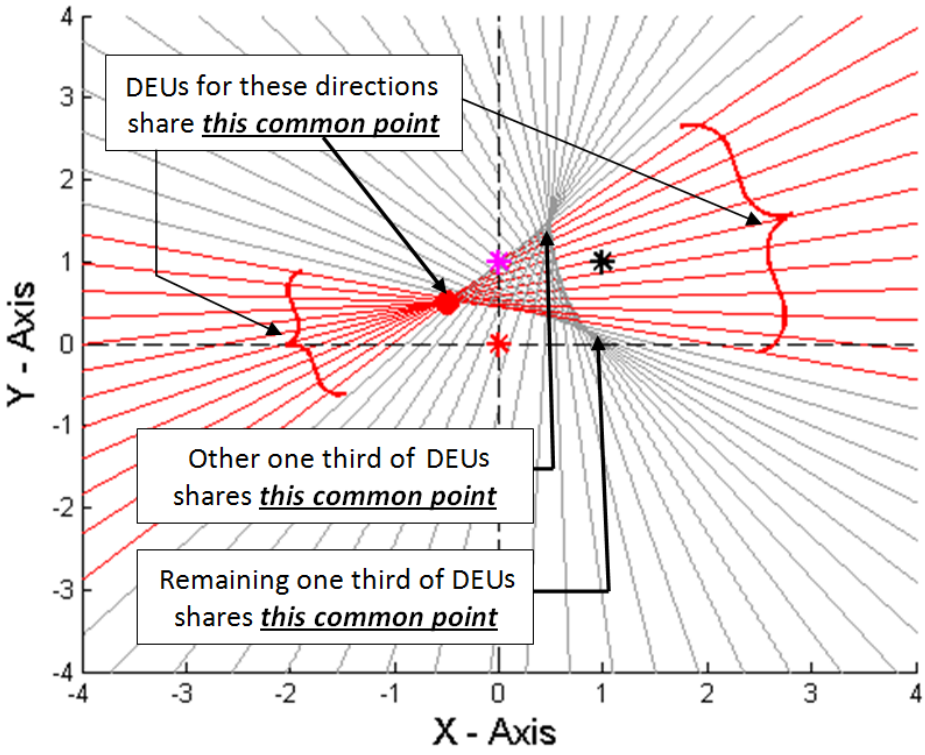

Figure 4.12. *Common points for DEUs for different directions*

Consequently, in order to avoid complex formulation, a simple way to obtain parameters of DEU for all measurement geometries is established: use the analytic equations in Section 4.3.3 only twice to obtain intersection points for n_1 = 2 and n_2 = 4 as shown in Figure 4.8. The line which passes through both of these two intersection points corresponds to DEU. The value of $\Delta_{emitter}$ can be also calculated by dividing the distance between these intersection points to the value of $(n_2 - n_1)$.

4.5. Simulations and Results

In this section, the performance of DEU which is a powerful geometrical tool for RSS based localization is presented for the scenarios when both the path loss exponent and the source signal power are unknown.

4.5.1. Intersection of DEUs

In Section 4.3.2, the DRSS based NLS cost function which is a nonconvex optimization problem was provided. When path loss exponent is known and there are only three measurements in 2-D space, the intersections of DRSS circles are the NLS solution for the location of the emitter,

$$(\hat{x}, \hat{y}) = \underset{(x,y)}{\operatorname{argmin}}\ Q(x, y\,; RSS_1, RSS_2, RSS_3) \tag{69}$$

Furthermore, the intersection points of DRSS circles are the points where not only the cost function is minimized but also the cost function is equal to zero,

$$Q(\hat{x}, \hat{y}) = 0 \tag{70}$$

Similarly, in the case that path loss exponent is unknown, the intersection points of DRSS circles are the points where the cost function is minimized for a certain n_{guess} value,

$$(\hat{x}, \hat{y}) = \underset{(x,y)}{\operatorname{argmin}}\ Q\big(x, y\,; RSS_1, RSS_2, RSS_3, n_{guess}\big) \tag{71}$$

Therefore, DEU can be defined as the collection of NLS estimation points for different guess values of n. In other words, for three RSS measurements case, two statements below which relate y to x are equivalent to each other:

$$Q\big(x, y\,; RSS_1, RSS_2, RSS_3, n_{guess}\big) = 0 \quad \Leftrightarrow \quad y = m_{DEU}\,.\,x + l_{DEU} \tag{72}$$

where m_{DEU} and l_{DEU} are the parameters of the associated DEU. When there are more than three measurements denoted as the vector $\overrightarrow{RSS}$, different DEUs can be derived for each different nonlinear triple combinations of measurement locations. For example, in case of four measurements, there are four different DEUs. The intersection of these DEUs is an effective approximation for the NLS solution:

$$(x, y, n)_{DEU} \cong \underset{(x,y,n)}{\operatorname{argmin}}\ Q\left(x, y, n\,;\, \overrightarrow{RSS}\right) \tag{73}$$

Intersection of DEUs can be handled by the best intersection point of the lines [74]. In Figure 4.13, in a noisy environment, both NLS and intersection of DEUs make an erroneous guess for the location of the emitter. However, the important thing is that they point exactly the same wrong location. This is because intersection of DEUs is an effective approximation of NLS solution. To keep in mind, even though the guess is wrong, this can be considered as the best guess under noise.

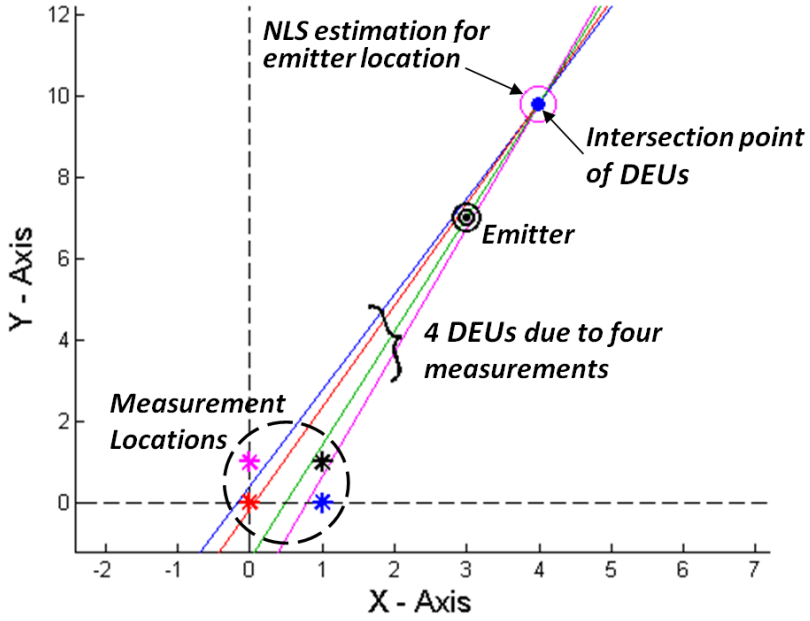

Figure 4.13. *Illustration of intersection of DEUs*

Figure 4.14 shows the results of Monte Carlo Simulations to compare the performance of NLS with the intersection of DEUs method for different additive error levels in dB. Monte Carlo simulation is designed such that four sensors are located around origin at (1,1), (-1,1), (1,-1) and (-1,-1) where the emitter location is allowed to randomly be anywhere within the range of [-10,10] along both x and y axis. However, because of the assumption that emitter is located at a distant position which is already

mentioned in Section 4.3.4, the emitter is not allowed to stay close to the origin less than 4 units. For each noise level, Monte Carlo simulation is conducted by 1000 iterations. Consequently, the new method, namely intersection of DEUs, achieved equivalent or even superior performance compared to DRSS based NLS by also performing very close to Cramer Rao Lower Bound (CRLB) [75, 76, 27] for different noise levels. As shown in Figure 4.15, similar results are obtained with 8 sensors which are circularly located around origin.

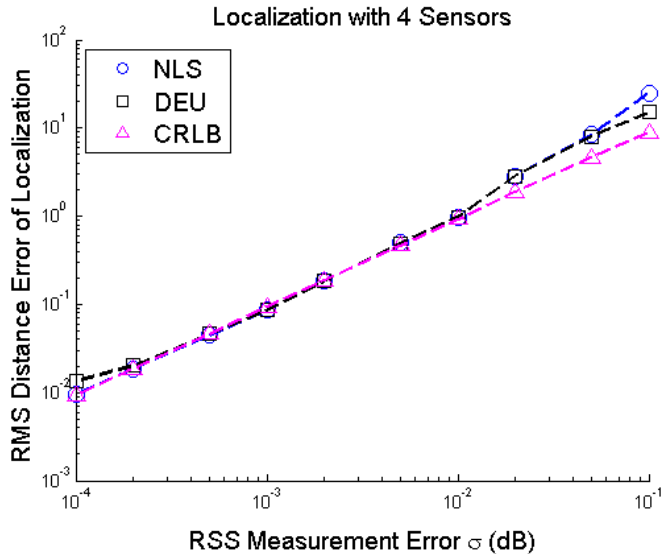

Figure 4.14. *Comparison of the performance of NLS and intersection of DEUs via Monte Carlo Simulation (4 sensors)*

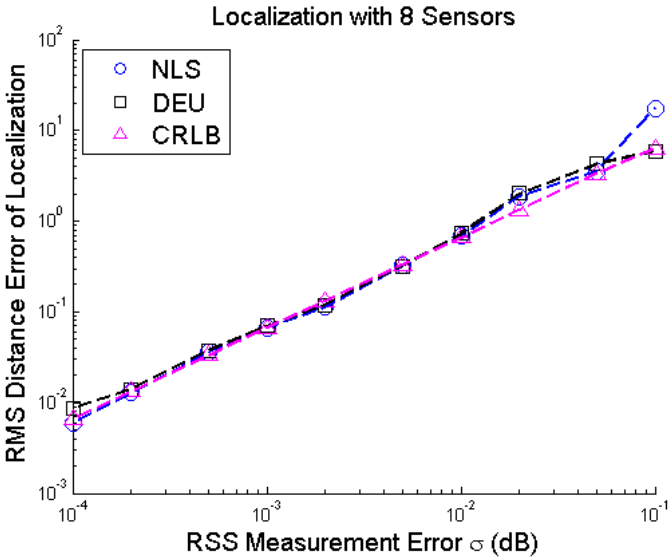

Figure 4.15. *Comparison of the performance of NLS and intersection of DEUs via Monte Carlo Simulation (8 sensors)*

While it is possible to obtain similar accuracy by intersection of DEUs, it can approximately perform 20 times faster than DRSS based NLS algorithm. Same experiments are conducted to compare the speeds of the algorithms. In Figure 4.16, the average execution times of localization algorithms are provided for NLS and intersection of DEUs for different number of sensors when these algorithms are performed on an ordinary desktop computer with Intel Core(TM) i7-3630QM CPU@2.40 GHz Processor and 16 GB RAM by means of MATLAB [77]. As can be seen, intersection of DEUs always performs significantly faster than NLS regardless of the number of sensors involved in localization. The struggle to simplify the localization process via geometrical observations, discovering the linear nature of DEU and finally skillfully exploiting this discovery in RSS based localization lead to a very effective solution compared to NLS. As discussed in Section 4.3.2, NLS must conduct a search within a three dimensional space namely (x, y, n) to come up with the solution. NLS also requires an initial point to start the search for the minimum point and its performance is highly sensitive to the location of this initial point. Unlike NLS, intersection of DEUs requires no initial point.

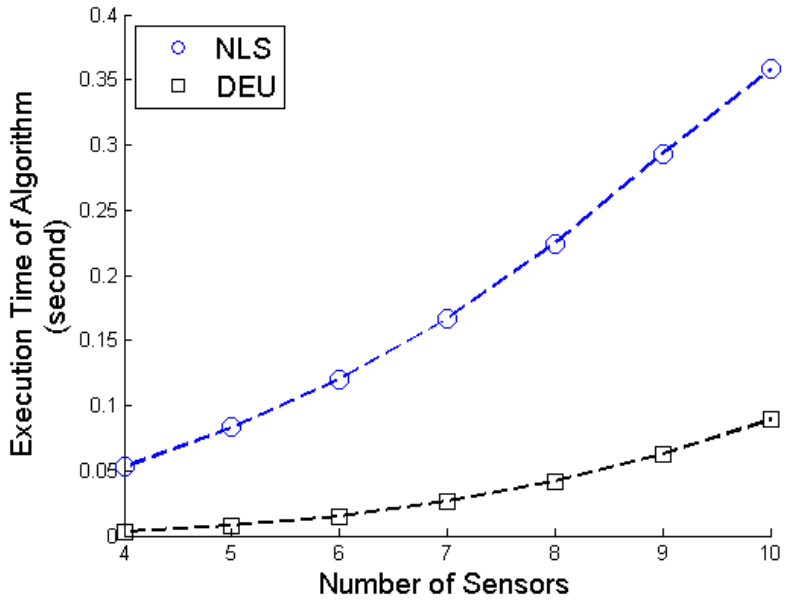

Figure 4.16. *The average time of execution of NLS and intersection of DEUs for different number of sensors*

4.5.2. Moving Towards Emitter: DEU is a Route Planning Tool

In this section, an illustrative simulation for tracking scenario is presented to be able to briefly discuss the benefit of DEU as a dynamic route planning tool. A simple tracking rule is established for a moving sensors based on the concept of DEU: firstly derive DEU by using the last three measurements and, secondly move along DEU until the next measurement. A rival tracking method is established as the following: firstly estimate the location of the emitter by using the last four measurements, and secondly move towards this point until the next measurement. This rival method has to engage the last four measurements because at least four measurements are necessary to make a localization as explained in Section 4.5.1. The flowchart of the tracking algorithms can be found in Figure 4.17.

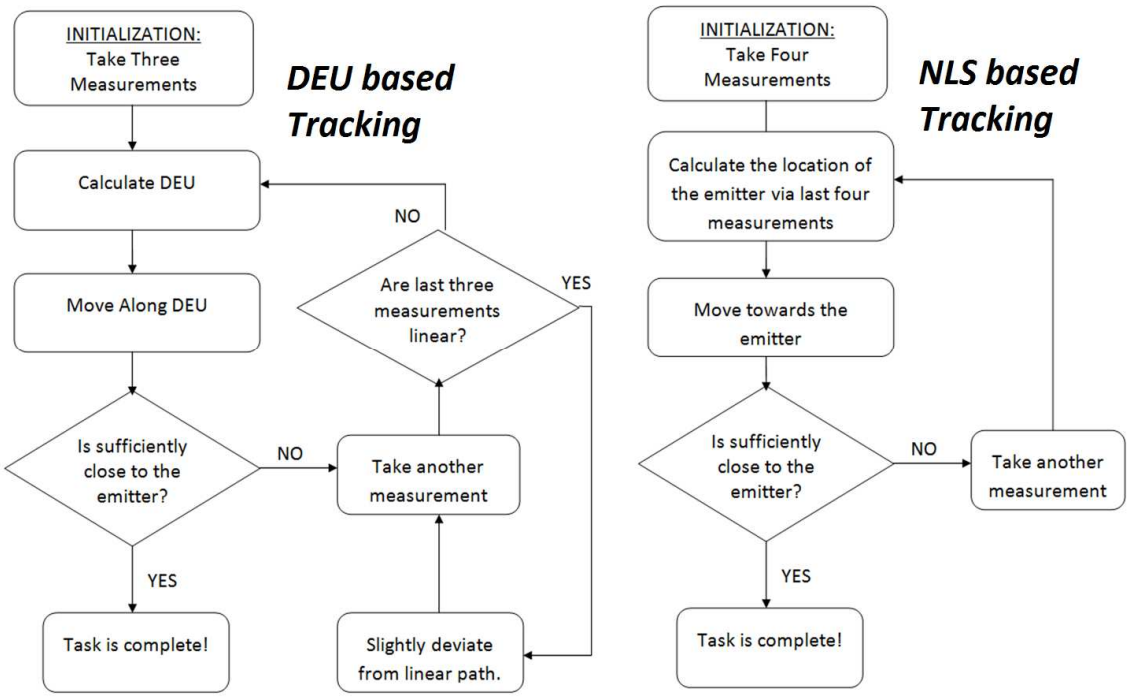

Figure 4.17. *Tracking Algorithms' Flowcharts*

The speed of the moving sensor is assigned as 3 unit/sec and the emitter starts a random motion 100 units apart from the moving sensor. In Table 4.1, the total length that the moving sensor travels on average until it reaches to emitter is presented for different RSS measurement error levels and different speed levels of emitter. Both high level of RSS measurement error and high level of speed of emitter are tricking the tracking method. Therefore, the average length travelled by the moving sensor increases from upper left corner to lower right corner in Table 4.1.

Table 4.1. *Comparison of average travel lengths and failure rates of emitter tracking methods.*

Emitter speed (unit/sec)	RSS error (dB)	σ = 0		σ = 10^{-3}		σ = 10^{-1}	
		Average Travel Length	Failure Rate	Average Travel Length	Failure Rate	Average Travel Length	Failure Rate
0.1	NLS	106.20	%0	106.53	%0	129.36	%0
	DEU	106.14	%0	106.23	%0	120.84	%0
0.5	NLS	113.37	%0	112.08	%0	131.76	%0
	DEU	112.05	%0	110.13	%0	121.71	%0
1	NLS	133.15	%1	131.00	%5	153.32	%5
	DEU	121.14	%0	120.83	%2	131.54	%2

By taking shorter paths before reaching the emitter, the tracking algorithm based on DEU performs better compared to DRSS based NLS. Moreover, in this simulation, not being able to catch the emitter even after taking 200 units is defined as "failure of the task". As seen in Table 4.1, DEU displays a lower rate of failure compared to NLS. A descriptive video about DEU based tracking is presented in the permanent link https://youtu.be/nGyzCvXR8SM whose screen captures are shown in Figure 4.18. Moreover, an illustrative sample video about the tracking simulations can be found in the permanent link https://youtu.be/NF26-Y6C_q4 whose screen captures are shown in Figure 4.19.

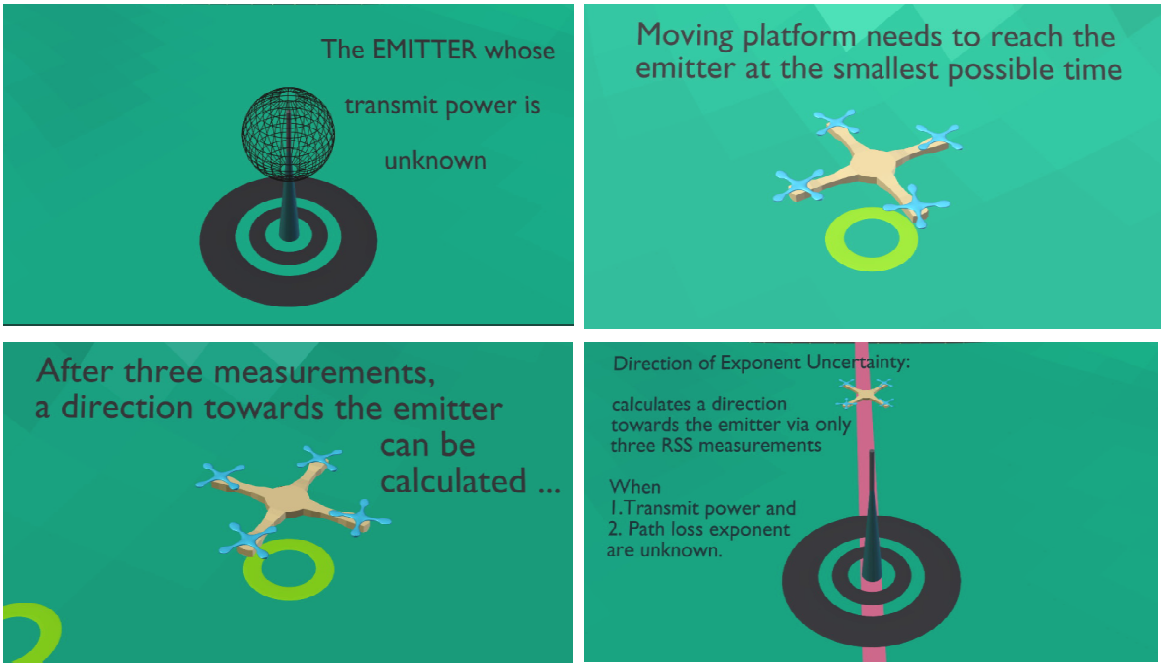

Figure 4.18. *Screen captures of the descriptive video about DEU based tracking*

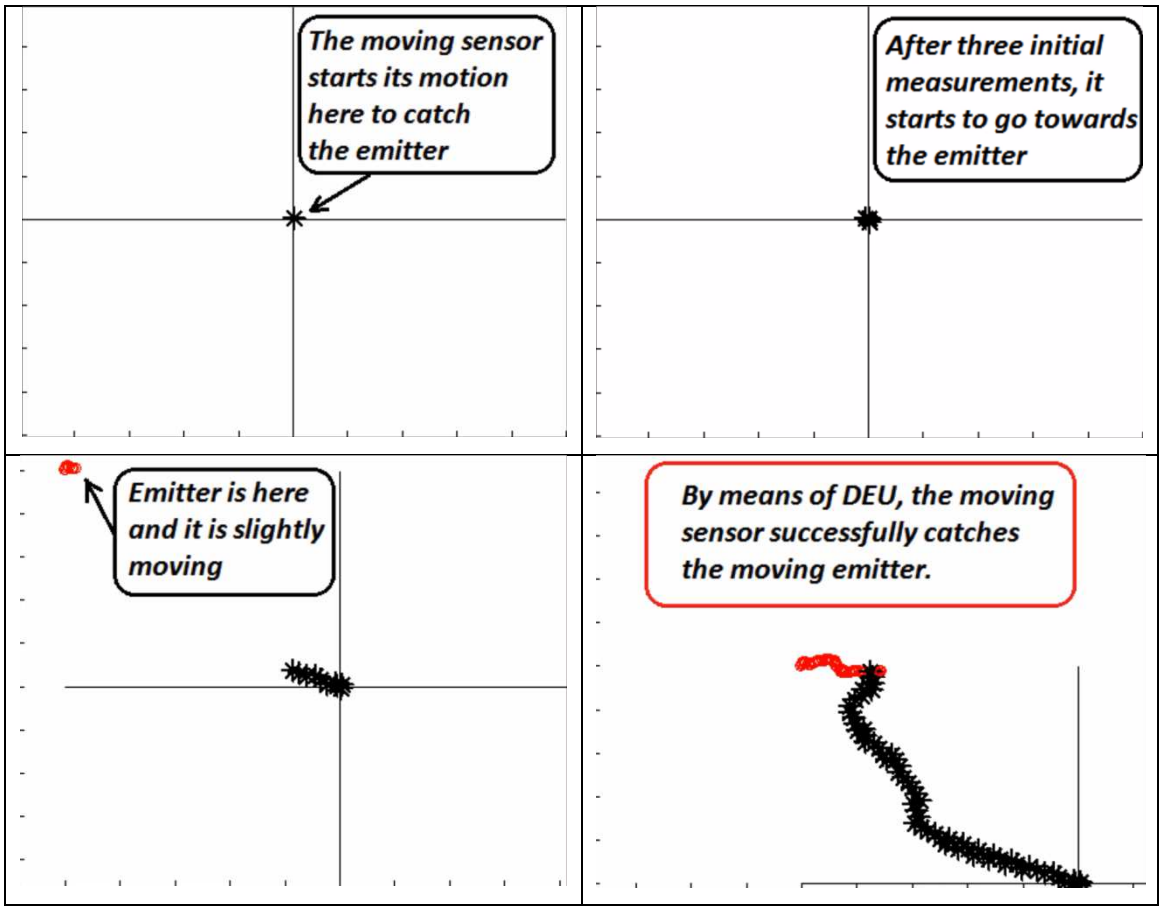

Figure 4.19. *Screen captures of the illustrative sample video about the emitter tracking simulations*

4.5.3. Limitation about DEU

In this section, it will be mentioned that the guess points with respect to different n_{guess} values lose their ability to align linearly for linear measurement patterns. Linear measurement patterns which are not preferable because of bringing the issue of mirror effect in localization are also problematic in yielding linear DEU structures as shown in Figure 4.20.a. However, the DEUs can quickly recover their linear patterns for even very small angular deviation from linear measurement. Figure 4.20.b illustrates how DEUs are perfectly reconstructed for only 30 degrees deviation from linear measurement. Therefore, a sensor moving along a linear path can make a small deviation from the line of motion, if it wants to check its direction by means of DEU.

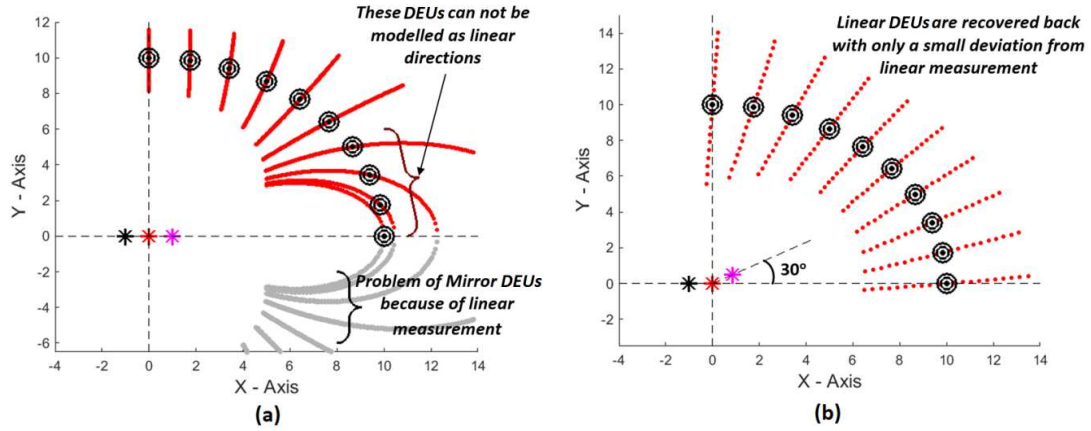

Figure 4.20. *(a) Linear measurement patterns brings the problem of non-linear DEUs as well as mirror DEUs (b) A small deviation from linear measurement is enough to recover linear DEUs back*

5. CIRCULAR UNCERTAINTY METHOD FOR RANGE-ONLY LOCALIZATION WITH IMPRECISE SENSOR POSITIONS

Emitter or source localization is a field of sensor array processing, which attempts to find the location of different of type of sources through the information from various sensors especially in noisy environments. There can be several types of error within the information utilized in source localization such as the error at measurements or the error at measurement positions etc. In the literature, it is mentioned that if the sensors are moving, then it is very likely that the measurement positions are imprecise. Moreover, the uncertainties in the measurement positions can dominate the localization error of the systems. Therefore, the uncertainties in the measurement positions must be carefully handled when dealing with the moving sensors. This chapter is dedicated to build a robust localization scheme when the sensor positions are imprecise.

5.1. Introduction to Circular Uncertainty

This chapter provides an effective new method called Circular Uncertainty to solve the range-only localization in the presence of sensor position errors. In practice, the sensors can stay only within a limited region whereas the target can be far from there. To increase the estimation capability, some peripheral measurements with moving sensors can be obtained which results in the issue of imprecise sensor positions. In these situations, sensor positions also become unknown parameters which need to be jointly estimated together with the target location. Because of the large number of unknown parameters, reaching the global minimum becomes a significant challenge. This chapter is dedicated to build a robust localization scheme for these scenarios. A new search strategy namely Circular Uncertainty is proposed which allows the localization system to safely find the global minimum of Maximum Likelihood cost function in case of imprecise sensor positions. Circular uncertainty not only makes it possible to reach Maximum Likelihood estimation, but also significantly simplifies this task.

In the rest of this chapter, firstly CRLB for localization error is explicitly obtained for the case of imprecise sensor positions. Next, the basis of the new proposed method namely Circular Uncertainty is presented by visually displaying the cost surfaces of localization of targets. Then, a formal proof for Circular Uncertainty is provided. Circular Uncertainty significantly reduces the size of the search spaces of the minimization processes. It conveniently finds the global minimum of the MLE surface

which gets quite complicated together with the uncertainties in the sensor positions. The performance of the new proposed method is tested by simulations for different scenarios, and also compared with the WLS solution of [63] which is specifically designed to attain CRLB in the presence of sensor position uncertainties. The proposed solution, which takes the advantage of obtaining MLE in a robust way, attains CRLB regardless of the noise level whereas other solutions partly fail to achieve this performance.

5.2. The Basis for The Research

In this part, CRLB for the range-only localization with imprecise sensor positions is obtained, and then, MLE solution for this localization scheme is described.

5.2.1. CRLB for Localization with Imprecise Sensor Locations

This part will formulate CRLB for localization with imprecise sensor positions. When there are N independent distance observations from N different sensor locations, the Fisher information matrix is as the following [67],

$$I(x,y) = \frac{1}{\sigma_D^2}\begin{bmatrix} \sum_{i=1}^{N}\frac{(x-x_i)^2}{(x-x_i)^2+(y-y_i)^2} & \sum_{i=1}^{N}\frac{(x-x_i).(y-y_i)}{(x-x_i)^2+(y-y_i)^2} \\ \sum_{i=1}^{N}\frac{(x-x_i).(y-y_i)}{(x-x_i)^2+(y-y_i)^2} & \sum_{i=1}^{N}\frac{(y-y_i)^2}{(x-x_i)^2+(y-y_i)^2} \end{bmatrix} \quad (74)$$

where $(x,\ y)$ is the target location and $(x_i,\ y_i)$'s are the sensor positions where distance-to-target measurements are taken for $i = 1,..,N$. Distance measurements are obtained with the standard deviation σ_D. This Fisher Information Matrix is only for localization with precise information for sensor positions. Therefore, the Fisher information has to be obtained for the case of imprecise sensor positions. Now, let us define the whole measurement model when sensor positions are imprecise,

$$D_i = \sqrt{(x-x_i)^2+(y-y_i)^2} + W_i \sim N(0,\sigma_D) \quad (75)$$

$$X_i = x_i + Z_i \sim N(0,\sigma_X) \quad (76)$$

$$Y_i = y_i + T_i \sim N(0,\sigma_Y) \quad (77)$$

where D_i is distance measurement at the sensor position (x_i, y_i). The sensors are physically in their exact positions (x_i,y_i). But, the localization system does not have the precise information for the sensor positions. However, this does not affect D_i measurements. Therefore, the position of sensors must be modeled as imprecise information. Consequently, in addition to D_i namely distance to target measurement, (X_i, Y_i) is also included within model as the observation of ith sensor position i.e. (x_i, y_i). In this model, W_i, Z_i and T_i represent the zero-mean normal distributed error terms within D_i, X_i and Y_i respectively. The standard deviations of D_i, X_i and Y_i are σ_D, σ_X and σ_Y respectively.

Now, based on the addition rule of Fisher Matrix, the Fisher information for the measurement model that has been just defined above can be written as the following,

$$I(\vec{q}) = \sum_{i=1}^{N} I_{D_i}(\vec{q}) + \sum_{i=1}^{N} I_{X_i}(\vec{q}) + \sum_{i=1}^{N} I_{Y_i}(\vec{q}) = I_D(\vec{q}) + I_X(\vec{q}) + I_Y(\vec{q}) \tag{78}$$

where $\vec{q}$ is parameter set, which defines the location of the target and all sensors,

$$\vec{q} = [x, y, x_1, y_1, \dots, x_N, y_N] \tag{79}$$

If a 2x2 matrix is defined such that,

$$A_i = \begin{bmatrix} \dfrac{(x-x_i)^2}{(x-x_i)^2+(y-y_i)^2} & \dfrac{(x-x_i).(y-y_i)}{(x-x_i)^2+(y-y_i)^2} \\ \dfrac{(x-x_i).(y-y_i)}{(x-x_i)^2+(y-y_i)^2} & \dfrac{(y-y_i)^2}{(x-x_i)^2+(y-y_i)^2} \end{bmatrix} \tag{80}$$

The information matrix for a single distance-to-target measurement D_i becomes,

$$I_{D_i}(\vec{q}) = \frac{1}{{\sigma_D}^2} \begin{bmatrix} A_i & \underline{0} & \cdots & A_i & & \\ \underline{0} & \underline{0} & & & & \\ \vdots & & \ddots & & & \\ A_i & & & A_i & & \\ & & & & \underline{0} & \\ & & & & & \underline{0} \end{bmatrix} \tag{81}$$

where $\underline{0}$ is the 2x2 zero matrix. Therefore, FIM for all distance measurements is,

$$I_D(\vec{q}) = \frac{1}{{\sigma_D}^2}\begin{bmatrix} \sum_{i=1}^{N} A_i & A_1 & \cdots & A_i & \cdots & A_N \\ A_1 & A_1 & & & & \\ \vdots & & \ddots & & & \\ A_i & \underline{0} & & A_i & & \\ \vdots & & & & \ddots & \underline{0} \\ A_N & & & & \underline{0} & A_N \end{bmatrix} \tag{82}$$

FIM for measurements of x positions of all sensor is,

$$I_X(Q) = \frac{1}{{\sigma_X}^2}\begin{bmatrix} 0 & & & & & & \\ & 0 & & & & & \\ & & 1 & & & & \\ & & & 0 & & & \\ & & & & 1 & & \\ & & & & & 0 & \\ & & & & & & \ddots \\ & & & & & & & \ddots \end{bmatrix} \tag{83}$$

and FIM for measurements of y positions of all sensors is,

$$I_Y(Q) = \frac{1}{{\sigma_Y}^2}\begin{bmatrix} 0 & & & & & & \\ & 0 & & & & & \\ & & 0 & & & & \\ & & & 1 & & & \\ & & & & 0 & & \\ & & & & & 1 & \\ & & & & & & \ddots \\ & & & & & & & \ddots \end{bmatrix} \tag{84}$$

If the standard deviations of sensor position errors are equal in x and y-axis namely,

$$\sigma_S = \sigma_X = \sigma_Y \tag{85}$$

then, FIM of measurements of positions of all sensors can be written as,

$$I_S(\vec{q}) = \frac{1}{{\sigma_S}^2}\begin{bmatrix} 0 & & & & & & \\ & 0 & & & & & \\ & & 1 & & & & \\ & & & 1 & & & \\ & & & & 1 & & \\ & & & & & 1 & \\ & & & & & & \ddots \\ & & & & & & & \ddots \end{bmatrix} \tag{86}$$

Finally, the total FIM is as the following:

$$I(\vec{q}) = I_D(\vec{q}) + I_S(\vec{q}) \tag{87}$$

The lower bound for the mean squared distance error of any localization scheme can be calculated by summing the first two diagonal elements of the inverse of the total FIM, i.e. $I^{-1}(\vec{q})$. The overall effect of having some level of uncertainty in the sensor positions is to levitate the CRLB for all levels of distance error.

5.2.2. Maximum Likelihood Solution for Target Localization with Imprecise Sensor Positions

The ordinary NLS solution for range-only target localization can be written as the following [3]:

$$(\hat{x}, \hat{y}) = \underset{(x,y)}{\operatorname{argmin}} \sum_{i=1}^{N} \left(\sqrt{(x - X_i)^2 + (y - Y_i)^2} - D_i \right)^2 \tag{88}$$

where $(X_i,\ Y_i)$ is the observed position of ith sensor and D_i is the distance measurement at this sensor. Dedicated to minimize only the overall error in distance measurements, this solution neglects if the sensor positions are imprecise, however still it can be a convenient way to solve the localization problem with imprecise sensor positions. Therefore, ordinary distance NLS will be always included during the simulations as a baseline solution. The ordinary distance NLS can be MLE solution when sensor positions are precise. However, for imprecise sensor positions, the cost of estimation must be a complete equation which includes two different parts for both distance-to-target measurement errors and sensor position errors. Therefore, to obtain MLE cost function, let us write the log likelihood of all parameters in $\vec{q}$ as the following:

$$\begin{aligned} \ln p\left(\vec{D}, \vec{X}, \vec{Y}; \vec{q}\right) = & - \frac{1}{2(\sigma_D)^2} \sum_{i=1}^{N} \left(\sqrt{(x - x_i)^2 + (y - y_i)^2} - D_i \right)^2 \\ & - \frac{1}{2\ (\sigma_S)^2} \sum_{i=1}^{N} [(X_i - x_i)^2 + (Y_i - y_i)^2] + K \end{aligned} \tag{89}$$

where is K is a constant such that,

$$K = - N\ \ln\left(\sqrt{2\ \pi\ (\sigma_D)^2}\right) - 2\ N\ \ln\left(\sqrt{2\ \pi\ (\sigma_S)^2}\right) \tag{90}$$

From this point of view, a maximum likelihood estimation (MLE) for all parameters of the parameter set $\vec{q}$ can be proposed as the following:

$$(\hat{x}, \hat{y}, \hat{x}_1, \hat{y}_1 \dots \hat{x}_N, \hat{y}_N) = \underset{(x,y,x_1,y_1 \dots x_N,y_N)}{\operatorname{argmin}} \left(\begin{array}{c} \frac{1}{(\sigma_D)^2} \sum_{i=1}^{N} \left(\sqrt{(x - x_i)^2 + (y - y_i)^2} - D_i \right)^2 \\ + \frac{1}{(\sigma_S)^2} \sum_{i=1}^{N} (X_i - x_i)^2 + (Y_i - y_i)^2 \end{array} \right) \quad (91)$$

This MLE function allows us to take into account the error in sensor positions to better estimate the target positions. To obtain the MLE solution, the global minimum of the MLE cost has to be found in a $(2N + 2)$ dimensional space of the parameters included within $\vec{q}$. Estimating jointly all these parameters, i.e. the location of target and all of the sensor positions at the same time, is a quite difficult joint estimation problem. Therefore, this study has built a new concept, namely Circular Uncertainty, in order to conveniently search for the global minimum of the MLE function.

5.3. Methodology

In this part, first the new method i.e. Circular Uncertainty is introduced via some illustrative examples of cost surfaces, and then Circular Uncertainty is formally proved. Next, NLS and MLE solutions by means of Circular Uncertainty are described.

5.3.1. A New Concept in Range-Only Localization: Circular Uncertainty

With the motivation to solve maximum likelihood localization problem when sensor positions are imprecise, this study proposes a new search strategy, which is called as Circular Uncertainty. Circular uncertainty roughly means that once "a base cost surface" is established by means of a couple of central measurements which are confined to a limited area, in case of some new measurements are received which disturb the initial estimation, the disturbed new estimation has a tendency to move along a particular circle or arc. This study calls this special circle as Circular Uncertainty of the base central measurements. Let us start to introduce this concept by demonstrating examples of NLS cost surfaces obtained via some central measurements with precise positions.

In Figure 5.1.a, the sensors are circularly located around the origin, and noisy distance measurements are obtained in accordance with the distance measurement

model in (75). Based on these distance measurements, the value of distance NLS cost function shown in (88) is obtained for all the (x, y) points, so the distance NLS cost surface is obtained. In Figure 5.1.a, this NLS cost surface is depicted as a contour plot. As seen, the global minimum of NLS cost surface naturally occurs around the target. However, the interesting point is that this NLS cost function have a tendency to stretch along a special circle, so it has a croissant-like shape surrounding the origin.

The croissant-like shape of contour of NLS surface is due to the fact that there exist a few central distance-to-target measurements and the target is located far from the measurement points. As a result, the angular position error of the target dominates the overall error of the NLS solution. In other words, NLS solution for this scenario has a limited capability for estimating the angular position of the target compared to its radial position. When the NLS surface with respect to polar coordinates is plotted as shown in Figure 5.1.b, it can be seen that NLS surface has a neat appearance which resembles a bivariate normal distribution with a diagonal covariance matrix. Of course, while the distribution can be an ordinary normal distribution along radial coordinate, it must be a circular normal distribution (i.e. von Mises distribution) along angular coordinate because of the periodicity of the angular coordinate. It can be observed that the variance along the angular coordinate is quite larger than the variance along the radial coordinate. In this sense, because this distribution is a bivariate normal distribution in polar coordinates as seen Figure 5.1.b, then its Cartesian counterpart shown in Figure 5.1.a can be viewed as a circularly wrapped bivariate normal distribution around the origin of Cartesian plane. Consequently, this explains the croissant-like shape of NLS surface in Figure 5.1.a.

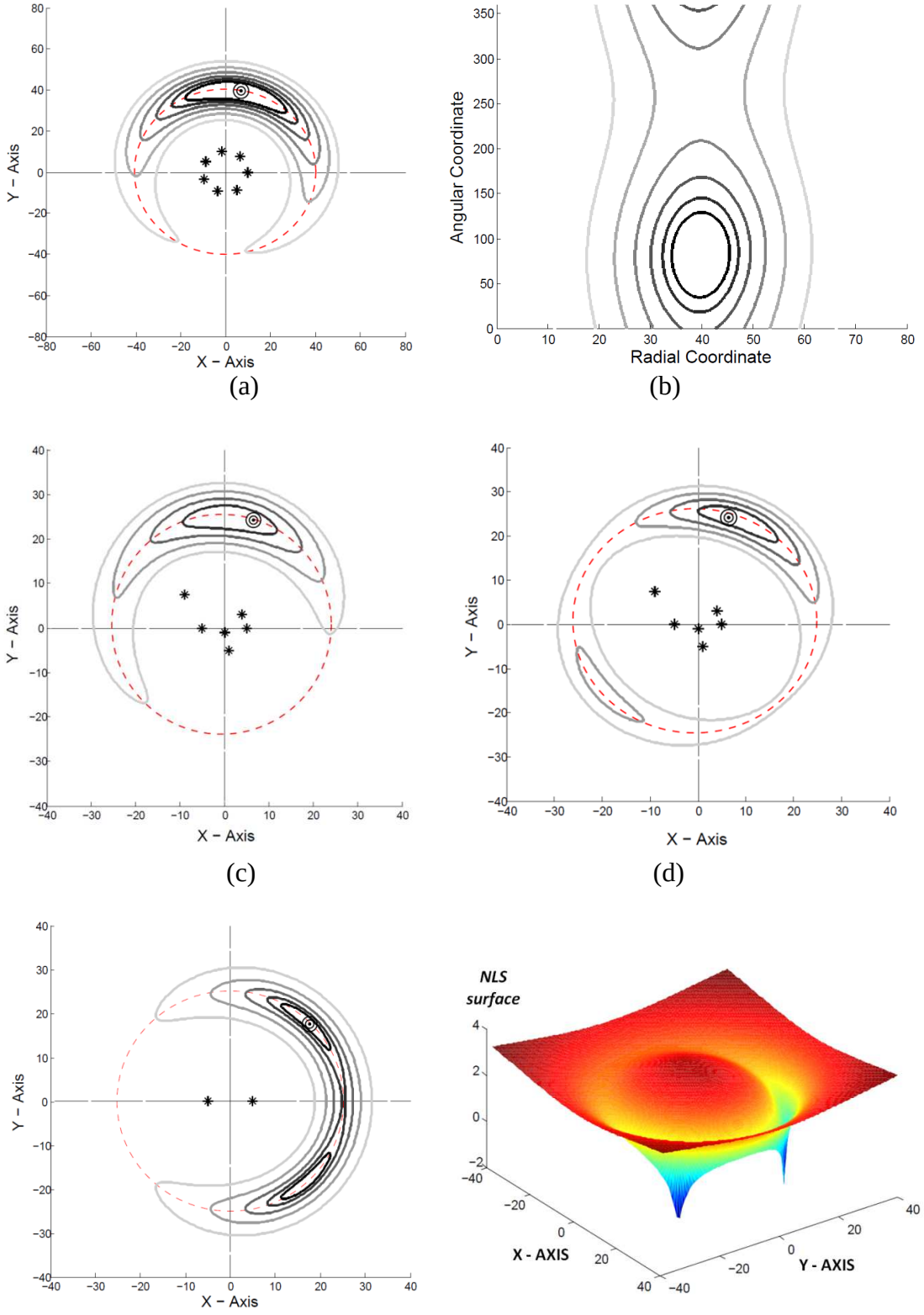

Figure 5.1. *Circular Uncertainty demonstration by means of examples of NLS cost surfaces*

The sensor geometry in Figure 5.1.a is a special one, so it may be wondered if this type of behavior exists for random sensor geometries. In Figure 5.1.c for a random measurement geometry located roughly around the origin, it can be again observed that NLS surface stretches along a special circle i.e. not along some other type of closed curve. For this case, the croissant shape is not symmetric around the global minimum, but it still perfectly stretches along a circle. Consequently, this study will name this circle as "the Circular Uncertainty" of the particular cost surface. Intuitively, the parameters of the circular uncertainty are defined as:

$$(x_{CU}\,, y_{CU}) = \left(\frac{1}{N}\sum_{i=1}^{N} x_i \;\,, \frac{1}{N}\sum_{i=1}^{N} y_i \;\right) \tag{92}$$

$$r_{CU} = \frac{1}{N}\sum_{i=1}^{N} D_i \tag{93}$$

where $(x_{CU}\,, y_{CU})$ is the center and r_{CU} is the radius of the Circular Uncertainty. The center of Circular Uncertainty is defined as the centroid of measurement points, and the radius of the Circular Uncertainty is defined as the average distance measurements. The important property of Circular Uncertainty is that global minimum of cost surface occurs along the Circular Uncertainty. In Figure 5.1.a and Figure 5.1.c, it can be observed that the global minimum is located along the Circular Uncertainty. In Figure 5.1.d, another interesting point can be observed that when NLS cost surface has a local minimum, this local minimum also occurs along the Circular Uncertainty.

Next, it may be wondered if Circular Uncertainty starts to occur only after some specific number of measurements. In Figure 5.1.e, the NLS cost surface of only two measurements are shown where there must be two global minima. Surprisingly, in spite of the existence of only two measurements (and consequently two global minima), NLS surface still tends to stretch along the Circular Uncertainty. The Circular Uncertainty of this surface is quite visible in 3D plot of the NLS surface shown in Figure 5.1.f. If it is considered that a single distance measurement is also basically a circular uncertainty, then it can be argued that the defined Circular Uncertainty always occurs regardless of the number of measurements.

At the beginning of this section, it is mentioned that once "a base cost surface" is established by means of a couple of central measurements, in case of receiving some

new measurements which disturb the initial estimation, the disturbed new estimation has a tendency to move along the Circular Uncertainty trajectory. This situation occurs because of the croissant shape of the NLS surface along the Circular Uncertainty. Circular Uncertainty is basically "a circular valley" within the surface of NLS cost function as demonstrated in Figure 5.1.f. When new measurements are received which disturbs the initial estimation, the new disturbed estimation will move along this "circular valley" instead of climbing the hillsides.

This phenomenon is depicted in Figure 5.2 where there are two base measurements creating a circular uncertainty. In addition to these base measurements, a third measurement with a sensor position error is obtained. Finally, based on these three measurements, the location of the target is estimated and then plotted as a small circular point in Figure 5.2. When a random error is repeatedly added to the position of third measurement, and then NLS localization is forced to locate the target as a Monte Carlo simulation, a set of disturbed NLS solutions can be obtained. Due to the above explanations, the disturbed solutions are accumulated along the Circular Uncertainty. A similar picture can be observed in literature (see Fig.9 in [78]), yet the authors did not pay attention to the above defined Circular Uncertainty phenomenon.

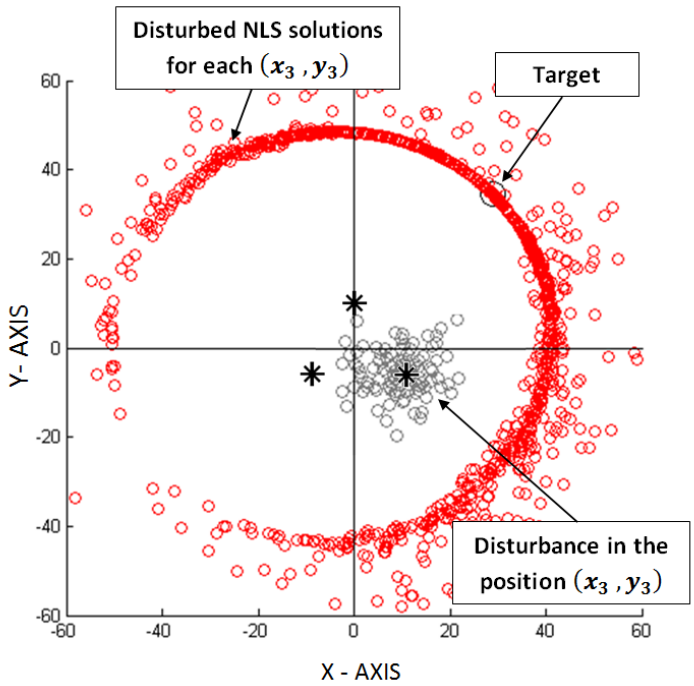

Figure 5.2. *The distribution of disturbed NLS solutions along the Circular Uncertainty*

Eventually, this study lists "the properties of Circular Uncertainty" which helps to create a new understanding in range-only localization of targets:

1) Global minimum occurs along the Circular Uncertainty trajectory (possibly with a small deviation).
2) Local minima (if any) have a tendency to occur along the Circular Uncertainty.
3) When the initial estimation is disturbed with new measurements, the disturbed estimation moves along the Circular Uncertainty trajectory, which is the circular valley of the cost surface.

Property 1 will allow us to conveniently find the global minimum of the cost surface of localization when sensor positions are precise. Property 3 will further allow us to handle the issue of imprecise sensor positions via Circular Uncertainty. The overall idea of Circular Uncertainty is visually demonstrated in a movie to give more tangible understanding of this concept (https://youtu.be/sj5CUsZs8W8).

5.3.2. Proof of Circular Uncertainty

In this section, the new proposed concept i.e., circular uncertainty which has just introduced in the previous section will be proved by formulating the polar equation of the NLS solution. The r value which minimizes the NLS cost for a specific the direction θ can be expressed as the following:

$$\hat{r}(\theta) = \underset{r}{\operatorname{argmin}} \sum_{i=1}^{N} \left(\sqrt{(r\cos(\theta) - X_i)^2 + (r\sin(\theta) - Y_i)^2} - D_i \right)^2 \tag{94}$$

Therefore, the r value minimizing the NLS cost shown in (94) must satisfy the following condition:

$$\frac{\partial}{\partial r} \sum_{i=1}^{N} \left(\sqrt{(r\cos(\theta) - X_i)^2 + (r\sin(\theta) - Y_i)^2} - D_i \right)^2 = 0 \tag{95}$$

When the derivate in (95) is accomplished, the following equation is obtained:

$$\sum_{i=1}^{N} \left[2\left(D_i - \widetilde{D}_i(r)\right) \frac{\cos(\theta)\,(r\cos(\theta) - X_i) + \sin(\theta)\,(r\sin(\theta) - Y_i)}{\widetilde{D}_i(r)} \right] = 0 \tag{96}$$

where $\widetilde{D}_i(r)$ represents the distance between the point $(r\cos(\theta), r\sin(\theta))$ and the position of ith sensor (x_i, y_i) as shown in Figure 5.3. D_i is the distance-to-target

measurement obtained by the ith sensor. As seen in Figure 5.3, the line which passes through the origin with the angle θ with respect to x-axis is labeled as L_θ. It can be observed that the nominator of the division at right in (96) is the projection of the line segment with the length $\widetilde{D}_i$ onto the line L_θ. Therefore, (96) can be rewritten as:

$$\sum_{i=1}^{N}\left[\left(D_i - \widetilde{D}_i\right)\frac{\widetilde{D}_i\cos(\alpha_i)}{\widetilde{D}_i}\right] = 0 \tag{97}$$

where α_i is the angle between L_θ and the line segment connecting the points $(r\cos(\theta), r\sin(\theta))$ and (x_i, y_i). After canceling the common terms, the following expression is obtained:

$$\sum_{i=1}^{N}\left[D_i\cos(\alpha_i) - \widetilde{D}_i\cos(\alpha_i)\right] = 0 \tag{98}$$

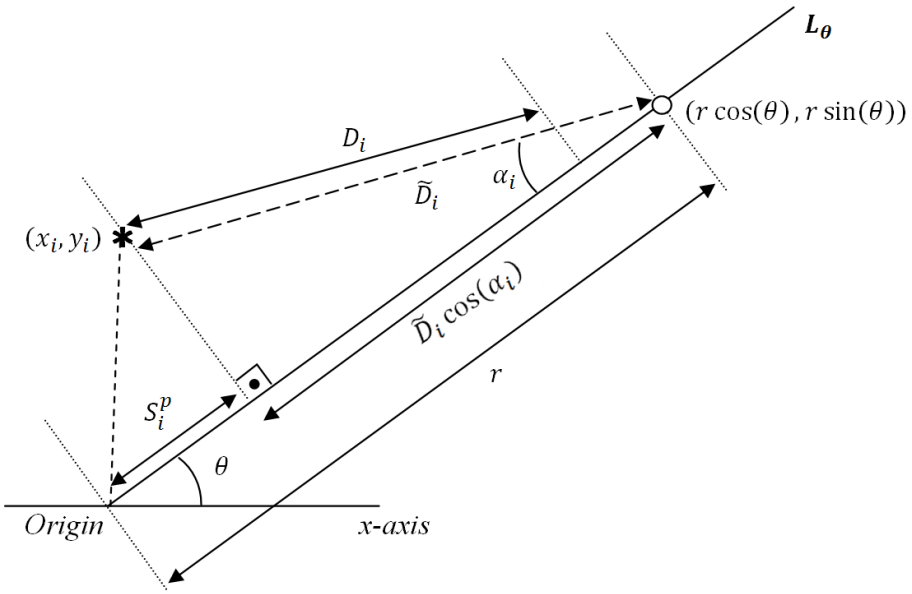

Figure 5.3. *The proof for Circular Uncertainty and its parameters*

Then, $\widetilde{D}_i\cos(\alpha_i)$ can be replaced by $\left(r - S_i^p\right)$, so the following expression appears:

$$\sum_{i=1}^{N}\left[D_i\cos(\alpha_i) - \left(r - S_i^p\right)\right] = 0 \tag{99}$$

where S_i^p is the projection of the line segment connecting the origin to the position of ith sensor (x_i, y_i) onto the line L_θ as shown in Figure 5.3. Obviously, S_i^p is a

function of θ, while α_i is a function of both θ and r, consequently (99) can be rewritten as the following:

$$\sum_{i=1}^{N}\left(S_i^p(\theta) + D_i \cos[\,\alpha_i(\theta, r)\,] - r\right) = 0 \tag{100}$$

The difficult point is that α_i is a function of r, so finding the root of (100) becomes a complex task. To simplify this task, for sufficiently large r values, $\cos[\alpha_i(\theta, r)]$ can be roughly approximated as 1. This approximation is consistent with the case of Circular Uncertainty where the central measurements are scattered just around the origin, and the target is assumed to be located in a point far from the measurements. Finally by means of this approximation, the following equation appears:

$$\sum_{i=1}^{N}\left(S_i^p(\theta) + D_i - r\right) \approx 0 \tag{101}$$

Therefore, the r value which minimizes the NLS cost for a specific the direction θ can be formulated as the following:

$$\hat{r}(\theta) \approx \frac{1}{N}\sum_{i=1}^{N} S_i^p(\theta) + \frac{1}{N}\sum_{i=1}^{N} D_i \tag{102}$$

The first term in (102) is just the projection of the centroid of the sensor positions onto the line L_θ as shown in (103) and (104). And, the second term in (102) is the average of the measured distances by the central measurements. Therefore, (102) is the proof for circular uncertainty and for its parameters which have been intuitively defined in the previous section.

$$\hat{r}(\theta) \approx \frac{1}{N}\sum_{i=1}^{N} [\cos(\theta)\ \sin(\theta)] \begin{bmatrix} x_i \\ y_i \end{bmatrix} + \frac{1}{N}\sum_{i=1}^{N} D_i \tag{103}$$

$$\hat{r}(\theta) \approx [\cos(\theta)\ \sin(\theta)] \left(\frac{1}{N}\sum_{i=1}^{N} \begin{bmatrix} x_i \\ y_i \end{bmatrix}\right) + \frac{1}{N}\sum_{i=1}^{N} D_i \tag{104}$$

5.3.3. Solving NLS Equation via Circular Uncertainty

In this section, it is demonstrated how Circular Uncertainty can be utilized to conveniently solve the NLS equation in (88). By means of Circular Uncertainty, the size of search space will be reduced. As mentioned above, global minimum occurs along the Circular Uncertainty possibly with a small deviation. Therefore, the global minimum must be searched along the Circular Uncertainty whose parameters are defined in (92) and (93). Let us write the equation of Circular Uncertainty as a function of θ as the following:

$$x(\theta) = x_{CU} + r_{CU} \cos(\theta) \tag{105}$$

$$y(\theta) = y_{CU} + r_{CU} \sin(\theta) \tag{106}$$

Therefore, the NLS equation in (88) can be rewritten as the following:

$$(\hat{\theta}) = \underset{(\theta)}{\operatorname{argmin}} \sum_{i=1}^{N} \left(\sqrt{(x_{CU} + r_{CU} \cos(\theta) - X_i)^2 + (y_{CU} + r_{CU} \sin(\theta) - Y_i)^2} - D_i \right)^2 \tag{107}$$

As seen, the size of search space is reduced by means of Circular Uncertainty. Furthermore, because θ is periodic, only the range $(0,2\pi]$ is of interest instead of infinite intervals for x or y in (88). In Figure 5.4.a, the setup of a Monte Carlo simulation which consists of 1000 iterations is shown. In each iteration, the eight sensors are randomly positioned within square area limited by the interval [-10, 10] along x and y axis. The target (emitter or source) is randomly located anywhere within the interval [-80, 80] along x and y axis, yet it is not allowed to stay close to the origin smaller than 30 units i.e. not inside the circle drawn as dashed line. In Figure 5.4.b, the performances of localization by Circular Uncertainty and conventional distance NLS are shown as root mean squared (RMS) distance error. As seen, both distance NLS and Circular Uncertainty can attain CRLB. However, in Section 5.4.3, it will be shown that the execution time of the Circular Uncertainty is quite smaller than NLS. Therefore, Circular Uncertainty is found to be a convenient solution when all sensor positions are precise. However, the real benefit of this solution will be apparent in the next sections in which the issue of imprecise sensor positions is discussed.

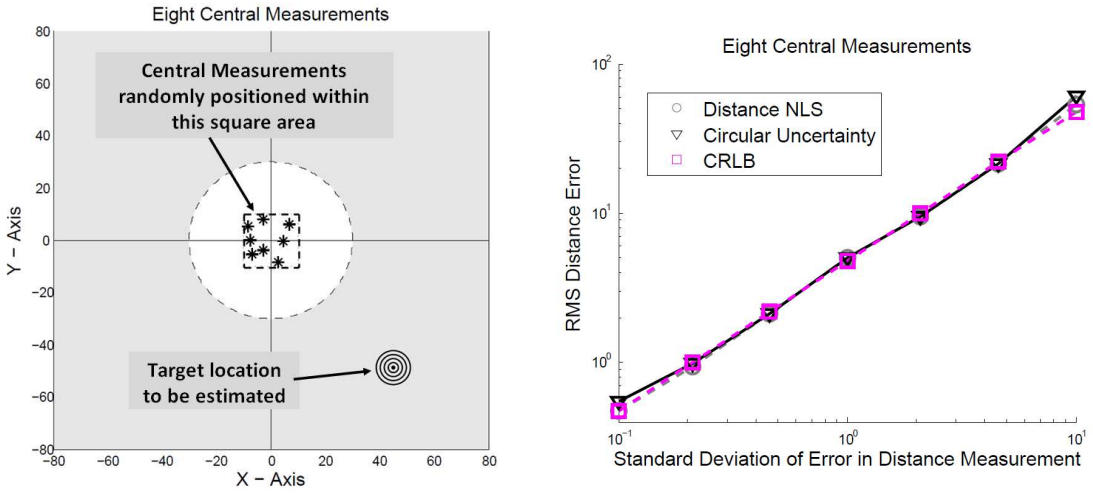

(a) (b)

Figure 5.4. *(a) The simulation setup - a sample measurement scheme and (b) the RMS distance error of localization: Circular Uncertainty and NLS*

5.3.4. MLE Solution by Circular Uncertainty

In practical situations, the sensors can only be allowed to be located within a limited region and the target can be located far from the sensors. In order to increase estimation capability, in addition to the central measurements taken within a limited region, a few number of peripheral measurements can be deployed. However, to scan a broad peripheral area, the peripheral measurements can be designed as moving sensors, which, as a result, brings the issue of uncertainties in the positions of sensors as discussed in the literature [54]. In this section, it is demonstrated how Circular Uncertainty can be utilized to conveniently solve the MLE for this type scenario in which there are uncertainties in sensor positions for peripheral measurements. First, let us rewrite the parameters of the Circular Uncertainty as the following:

$$(x_{CU}, y_{CU}) = \left(\frac{1}{M} \sum_{i \in C} x_i \, , \frac{1}{M} \sum_{i \in C} y_i \right) \tag{108}$$

$$r_{CU} = \frac{1}{M} \sum_{i \in C} D_i \tag{109}$$

where C is the set of central measurements with precise positions and M is the number of elements in this set. In accordance with the Circular Uncertainty equations of (105) and (106), MLE equation in (91) can be rearranged as the following:

$$(\hat{\theta}\,,\{\hat{x}_j,\hat{y}_j \mid j \in P\}) = \underset{(\theta,\ \{x_j,y_j \mid j\in P\})}{\operatorname{argmin}} \left(\begin{array}{c} \frac{1}{(\sigma_D)^2}\sum_{i\,\in\,C}\left(\sqrt{(x(\theta)-x_i)^2+\,(y(\theta)-y_i)^2}-\,D_i\right)^2 \\ +\sum_{j\,\in\,P}\left\{ \begin{array}{c} \frac{1}{(\sigma_D)^2}\left(\sqrt{\left(x(\theta)-x_j\right)^2+\,\left(y(\theta)-y_j\right)^2}-\,D_j\right)^2 \\ +\frac{1}{(\sigma_S)^2}\,\left(\left(X_j-x_j\right)^2+\,\left(Y_j-y_j\right)^2\right) \end{array} \right\} \end{array} \right) \qquad (110)$$

where P is the set of peripheral measurements with imprecise positions. In order to find the global minimum, the number of parameters to be estimated is $2L+2$ where L is the number of measurements with imprecise positions (i.e. the size of the set P). By means of circular uncertainty, this number is reduced to $2L+1$ by representing both x and y-axis of the target as a function of θ. Moreover, if the imprecise sensor positions minimizing the MLE cost are also achieved to be represented as functions of θ, then the total number of parameters to be estimated will be reduced to 1 i.e. only θ. Let us consider the estimation of a single imprecise sensor position which minimizes jointly distance and sensor position error given the location of the target $\left(x(\theta),y(\theta)\right)$:

$$\left(\hat{x}_j,\hat{y}_j\right) = \underset{(x_j,y_j)}{\operatorname{argmin}} \left(\begin{array}{c} \frac{1}{(\sigma_D)^2}\left(\sqrt{\left(x(\theta)-x_j\right)^2+\,\left(y(\theta)-y_j\right)^2}-\,D_j\right)^2 \\ +\,\frac{1}{(\sigma_S)^2}\,\left(\left(X_j-x_j\right)^2+\,\left(Y_j-y_j\right)^2\right) \end{array} \right) \qquad (111)$$

First of all, in order to minimize (111), the estimated position of the sensor $\left(\hat{x}_j\,,\,\hat{y}_j\right)$, the measured position of the sensor $\left(X_j\,,\,Y_j\right)$ and the location of the target (x,y) must linearly align because of triangular inequality. Let us designate the distance error as Δ and the sensor position error as δ. In Figure 5.5.a, an estimation for the sensor position is shown which does not lie on the line which passes through $\left(X_j\,,\,Y_j\right)$ and $\left(x(\theta),y(\theta)\right)$. It is apparent that the projection point of this estimation onto this line would yield smaller Δ and δ so a smaller cost value. Therefore, the solution of (111) must be located on the line which passes through the measured position of the sensor $\left(X_j\,,\,Y_j\right)$ and the location of the target $\left(x(\theta),y(\theta)\right)$ as shown in Figure 5.5.b. For this scheme, only the lengths of Δ and δ are required.

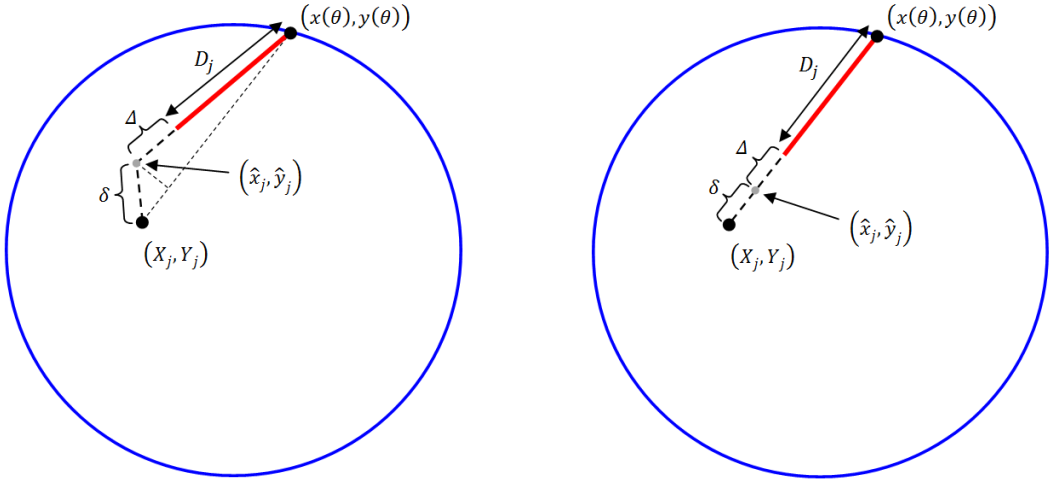

(a) (b)

Figure 5.5. *The estimated position of the sensor* $(\hat{x}_j\ ,\ \hat{y}_j)$*, the measured position of the sensor* $(X_j\ ,\ Y_j)$ *and the location of the target* (x, y) *must linearly align*

Therefore, solving (111) can be equivalently achieved by the solving following equation:

$$(\hat{\Delta},\hat{\delta}) = \underset{(\Delta,\delta)}{\operatorname{argmin}}\left(\frac{1}{(\sigma_D)^2}\,(\Delta)^2 + \frac{1}{(\sigma_S)^2}\,(\delta)^2\right) \tag{112}$$

subjected to the constraint:

$$\Delta + \delta = \zeta = \sqrt{\left(x(\theta) - X_j\right)^2 + \left(y(\theta) - Y_j\right)^2} - D_j \tag{113}$$

where ζ is the difference between the measured distance D_j and the distance between the target and the measured position of the sensor $(X_j\ ,\ Y_j)$. If the following equity is inserted into the cost function shown in (112):

$$\Delta = \zeta - \delta \tag{114}$$

and then if the derivative of this cost function is taken with respect to δ, the following the equation is obtained:

$$2\,(\sigma_D)^2\,\delta - 2\,(\sigma_S)^2\,(\zeta - \delta) = 0 \tag{115}$$

Therefore, the estimated value of δ which minimizes (112) is as the following:

$$\hat{\delta} = \frac{(\sigma_S)^2}{(\sigma_S)^2 + (\sigma_D)^2}\left(\sqrt{\left(x(\theta) - X_j\right)^2 + \left(y(\theta) - Y_j\right)^2} - D_j\right) \tag{116}$$

Based on this value, the estimated sensor position $(\hat{x}_j, \hat{y}_j)$ which minimizes (111) can be written as the following:

$$\hat{x}_j = X_j + \hat{\delta}\frac{(x - X_j)}{\sqrt{(x - X_j)^2 + (y - Y_j)^2}} \tag{117}$$

$$\hat{y}_j = Y_j + \hat{\delta}\frac{(y - Y_j)}{\sqrt{(x - X_j)^2 + (y - Y_j)^2}} \tag{118}$$

Finally, (117) and (118) can be written as the functions of θ:

$$\hat{x}_j(\theta) = X_j + \frac{(\sigma_S)^2}{(\sigma_S)^2 + (\sigma_D)^2}\left(1 - \frac{D_j}{\sqrt{(x(\theta) - X_j)^2 + (y(\theta) - Y_j)^2}}\right)(x(\theta) - X_j) \tag{119}$$

$$\hat{y}_j(\theta) = Y_j + \frac{(\sigma_S)^2}{(\sigma_S)^2 + (\sigma_D)^2}\left(1 - \frac{D_j}{\sqrt{(x(\theta) - X_j)^2 + (y(\theta) - Y_j)^2}}\right)(y(\theta) - Y_j) \tag{120}$$

To sum up, the MLE cost function in (110) can be rewritten as a function of θ:

$$(\hat{\theta}) = \underset{\theta}{\operatorname{argmin}}\left(\begin{array}{c}\frac{1}{(\sigma_D)^2}\sum_{i \in C}\left(\sqrt{(x(\theta) - x_i)^2 + (y(\theta) - y_i)^2} - D_i\right)^2 \\ + \sum_{j \in P}\left\{\begin{array}{c}\frac{1}{(\sigma_D)^2}\left(\sqrt{(x(\theta) - \hat{x}_j(\theta))^2 + (y(\theta) - \hat{y}_j(\theta))^2} - D_j\right)^2 \\ + \frac{1}{(\sigma_S)^2}\left((X_j - \hat{x}_j(\theta))^2 + (Y_j - \hat{y}_j(\theta))^2\right)\end{array}\right\}\end{array}\right) \tag{121}$$

After representing the imprecise sensor positions as a function of θ, the total number of parameters to be estimated within MLE equation in (110) is reduced from $2L + 1$ to 1, in other words, the global minimum will be only searched through the parameter θ.

5.4. Simulations

5.4.1. Imprecise Sensor Positions within Central Measurements

In this section, a Monte Carlo simulation which consists of 1000 iterations is conducted for the scenario where there are eight central measurements with precise position together with three central measurements with imprecise positions. The

standard deviation of the sensor position error σ_S is set to 3. Figure 5.6.a shows the simulation setup by means of a sample measurement scheme. In each iteration, while both the sensors and target are randomly positioned, they are subjected to the same constraints of Figure 5.4.a (concerning the positions of the sensors and the target). In Figure 5.6.b, the performance of various localization techniques are compared to each other by means of RMS distance error of localization.

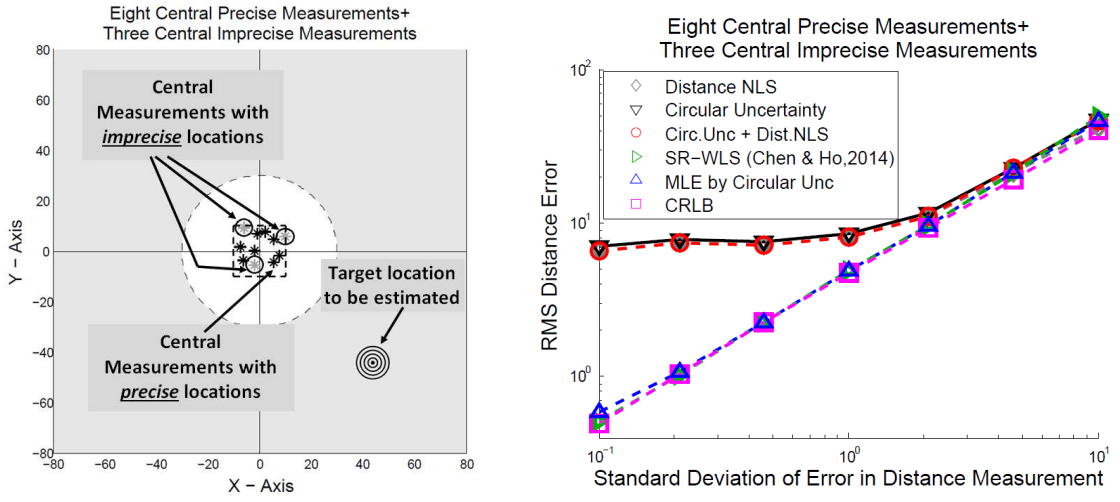

Figure 5.6. *(a) The simulation setup - a sample measurement scheme with eight central precise and three central imprecise measurements and (b) the RMS distance errors for various localization method*

Distance NLS is the localization which simply minimizes the conventional NLS cost function in (88) without taking the uncertainties in certain sensor positions into account. Circular Uncertainty is the localization technique that this study has introduced in (107). Circular Uncertainty in (107) again does not take the uncertainties in certain sensor positions into account. "Circ. Unc. + Dist NLS" is the method where the estimation of the Circular Uncertainty is used as the initial point of Distance NLS. The significance of this type initialization will be apparent in the next sections. For this scenario, these methods i.e. Distance NLS, Circular Uncertainty and "Circ. Unc. + Dist NLS" have the equivalent rate of performance which is significantly above CRLB. SR-WLS is the abbreviation of the squared range weighted least-squares introduced by [63]. They introduce this algorithm in order to conveniently solve the localization problems with imprecise sensor positions. Unlike MLE, SR-WLS avoids jointly estimating the

target and the sensor positions. It solves a least squares equation whose terms are skillfully weighted by also taking the uncertainties in the sensor positions into account.

While implementing SR-WLS, because this study assumes that the standard deviation of sensor position errors along x and y axis are the same i.e. σ_S and the errors are independent, the A matrix (introduced in [63]) is removed during calculation of the weighting matrix W as shown below:

$$W = [B\ (Q_D + Q_S)\ B\ ]^{-1} \tag{122}$$

where Q_D is the diagonal matrix whose diagonal elements are $(\sigma_D)^2$, and Q_S is an 11x11 matrix as the following:

$$Q_S = \begin{bmatrix} 0 & & & & & \\ & \ddots & & & & \\ & & 0 & & & \\ & & & \sigma_S^2 & & \\ & & & & \sigma_S^2 & \\ & & & & & \sigma_S^2 \end{bmatrix}_{11x11} \tag{123}$$

and B is the matrix as defined in [63]. While constructing Q_S, it is assumed that the last three measurements have imprecise positions. By removing the matrix A, the need for an initial estimation for the target position mentioned in [63] is also removed.

As seen in Figure 5.6.b, SR-WLS and MLE by the Circular Uncertainty in (121) introduced in the previous section can attain CRLB while the former methods which do not take the uncertainties in the sensor positions into account fail to achieve this performance. SR-WLS weights the sensor according to their closeness to target, the relative error level in distance measurements and the standard deviation of sensor positions. In this sense, for the simulation setup that this study has defined in Figure 5.6.a, SR-WLS opts to weight the three sensors with imprecise positions by smaller numbers. By doing this, SR-WLS reduces the importance of these sensors because they are not reliable due to their uncertain positions. This is the justification of the success of SR-WLS in attaining CRLB. However, a trade-off will occur when you need to heavily rely on the sensors with imprecise sensors if they are peripheral measurements instead of central ones. Therefore, the true benefit of MLE with Circular Uncertainty will be more apparent in the next sections.

5.4.2. The Benefit of Peripheral Measurements

It has been discussed that when there are only central sensors which take distance-to-target measurements, the localization suffers from a low capability of estimating the angular position of the target. Therefore, in addition to the central measurements, a few number of peripheral measurements can be deployed to increase the estimation capability of localization system. To scan a broad peripheral area, the peripheral measurements can be designed as moving sensors which at the end brings the issue of uncertainties in the positions of peripheral sensors. Nevertheless, in this section, it is shown how peripheral measurements even with imprecise positions can significantly increase the performance of the localization systems. In Figure 5.7, two CRLBs are shown for two different localization scenarios.

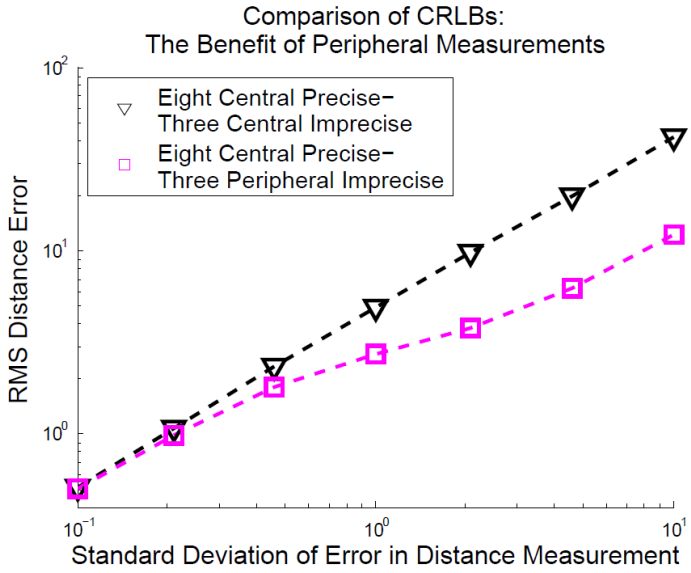

Figure 5.7. *Increase in the performance of localization systems by means of peripheral measurements*

Both of two scenarios in Figure 5.7 employ the same number of measurements i.e. eight measurements with precise positions and three measurements with imprecise positions. However, the distinction is that in the first scenario, three imprecise measurements are the central ones together with other eight measurements, while in the second scenario, they are employed as peripheral measurements. The first scenario is the one which is already shown in Figure 5.6.a and the second scenario is depicted in Figure 5.8.a. In the second scenario, the peripheral measurements are allowed to be randomly distributed within peripheral area just like the target, however they are not

allowed to get close to the target smaller than 5 units. The standard deviation of the sensor position error σ_S is set to 3. As seen in Figure 5.7, the peripheral measurements can significantly increase the performance of the range-only localization system. Please note that RMS distance errors are plotted in log-scale, so the difference between these two CRLBs points to a significant increase in the performance.

5.4.3. Peripheral Measurements with Imprecise Positions

In this section, the simulation including peripheral measurements with imprecise positions is presented. A Monte Carlo simulation which consists of 1000 iterations is conducted to determine the localization performance of the algorithms. The simulation setup is depicted in shown in Figure 5.8.a by means of a sample measurement scheme where there are eight central measurements with precise positions and three peripheral measurements with imprecise positions and the standard deviation of the sensor position error σ_S is set to 3. In each iteration, the sensors and the target are randomly positioned in accordance with the peripheral and central constraints settled in previous simulations. As depicted previously, in order to take the advantage of the peripheral measurements, the localization system must rely on the peripheral measurements even though their positions are imprecise.

The first method shown in Figure 5.8.b is Distance NLS. Because of peripheral measurements, the surface of the conventional distance NLS cost function becomes somewhat complicated, so the conventional distance NLS suffers from local minima. Therefore, Distance NLS presents the worst performance in this scenario because of convergence issues. However, Circular Uncertainty that this study has introduced in (107) presents a better performance compared to distance NLS. It has been mentioned that Circular Uncertainty is a safe and reliable way of obtaining global minimum. When the estimation of Circular Uncertainty is employed as the initial point of Distance NLS, then Distance NLS can be also guided to obtain the global minimum. Therefore, "Circ. Unc. + Dist. NLS" has the same level of RMS error with Circular Uncertainty which is quite smaller than that of only Distance NLS. In this context, the important advantage of Circular Uncertainty which safely obtains the global minimum becomes visible.

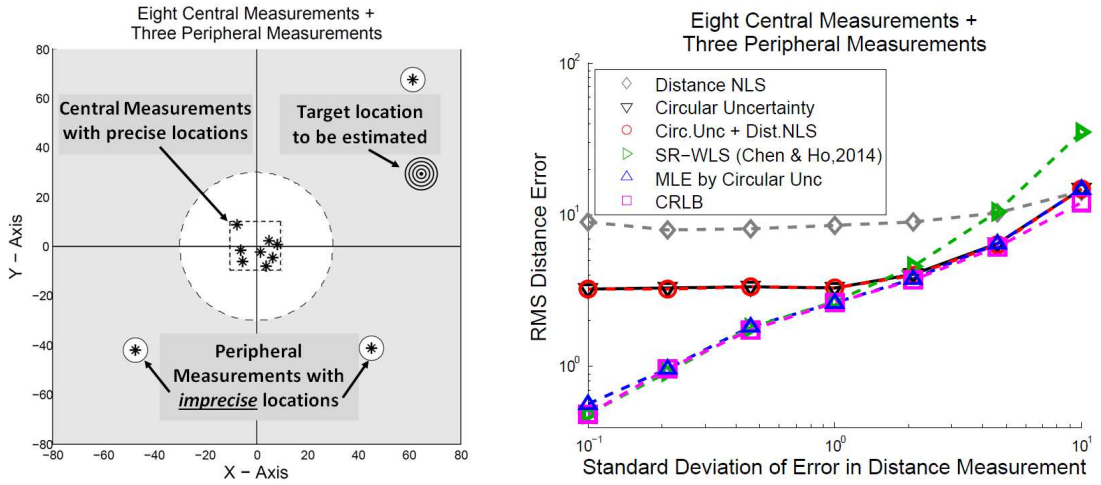

(a) (b)

Figure 5.8. *(a) The simulation setup - a sample measurement scheme with eight central precise and three peripheral imprecise measurements, (b) the RMS distance errors for various localization methods*

The next thing to be discussed about Figure 5.8.b is that SR-WLS fails to attain CLRB for high level of distance-to-target measurements. It has been discussed that the strategy of the SR-WLS is to reduce the weights of the measurements with imprecise positions in order not to rely on these measurements. However, the major aim here is to take the advantage of the peripheral measurements as much as possible despite their positions are imprecise in order to exploit all available information for localization of the target. Therefore, this situation creates a trade-off for SR-WLS. On the other hand, as a complete basis for estimation, the MLE solution can apparently do better than weighted least squares algorithms. MLE solution automatically takes the standard deviations of errors in distance measurements and imprecise sensor positions into account. Not only these, it also takes the geometry or the arrangement of sensors into account, which guarantees a superior performance. Eventually, the proposed method, i.e. MLE by Circular Uncertainty, can demonstrate better performance compared to all other competing methods. Circular Uncertainty or "Circ. Unc. + Dist. NLS" can not attain CRLB for low σ_D levels and oppositely SR-WLS can not attain CRLB for high σ_D levels. However, MLE by Circular Uncertainty can always attain CRLB for all levels of σ_D as seen in Figure 5.8.b.

Finally, average execution times of these algorithms are provided in Table 5.1, when these algorithms are performed on an ordinary desktop computer with Intel Core(TM) i7-3630QM CPU@2.40 GHz Processor and 16 GB RAM via MATLAB

[77]. As can be seen, Circular Uncertainty has the smallest execution time (0.049 seconds) while Distance NLS follows it with an important gap. Circular Uncertainty attains this performance gain because it skillfully reduces the NLS localization problem to a simple task. Circular Uncertainty searches the global minimum in a one-dimensional space while distance NLS makes a two-dimensional search. Circ. Unc. + Dist NLS comes after these methods with 0.071 seconds. After these three methods which do not take the uncertainty in the sensor positions into account, SR-WLS comes with 0.073 seconds of execution time in average. This execution time is quite closer to that of Distance NLS or Circ. Unc. + Dist NLS. The success of SR-WLS in terms of execution time is that it makes use of the squared ranges in order not deal with square roots in the estimation cost function. The last method in terms execution time is MLE by Circular Uncertainty. However, the average execution time of MLE by Circular Uncertainty and SR-WLS are almost same. When it is considered that this method achieves a very complicated task and it outperforms all the other methods in terms of localization error, MLE by Circular Uncertainty appears as the most effective method among others. When, there exist uncertainties in sensor positions, the success of MLE by Circular Uncertainty in terms of both localization accuracy and execution time is due to the fact that it reduces the multi-dimensional search space in into one-dimensional space without decreasing the localization accuracy.

Table 5.1. *Average execution times of the algorithms when these algorithms are performed on an ordinary desktop computer*

Method	Execution Time (sec)
Circular Uncertainty	0.049
Distance NLS	0.069
Circ. Unc. + Dist. NLS	0.071
SR-WLS (Chen & Ho, 2104)	0.073
MLE by Circular Unc.	0.074

Finally, the overall idea of Circular Uncertainty is visually demonstrated in a movie to give more tangible understanding of this concept which has been uploaded to the permanent link https://youtu.be/sj5CUsZs8W8 and its screen captures are provided in Figure 5.9.

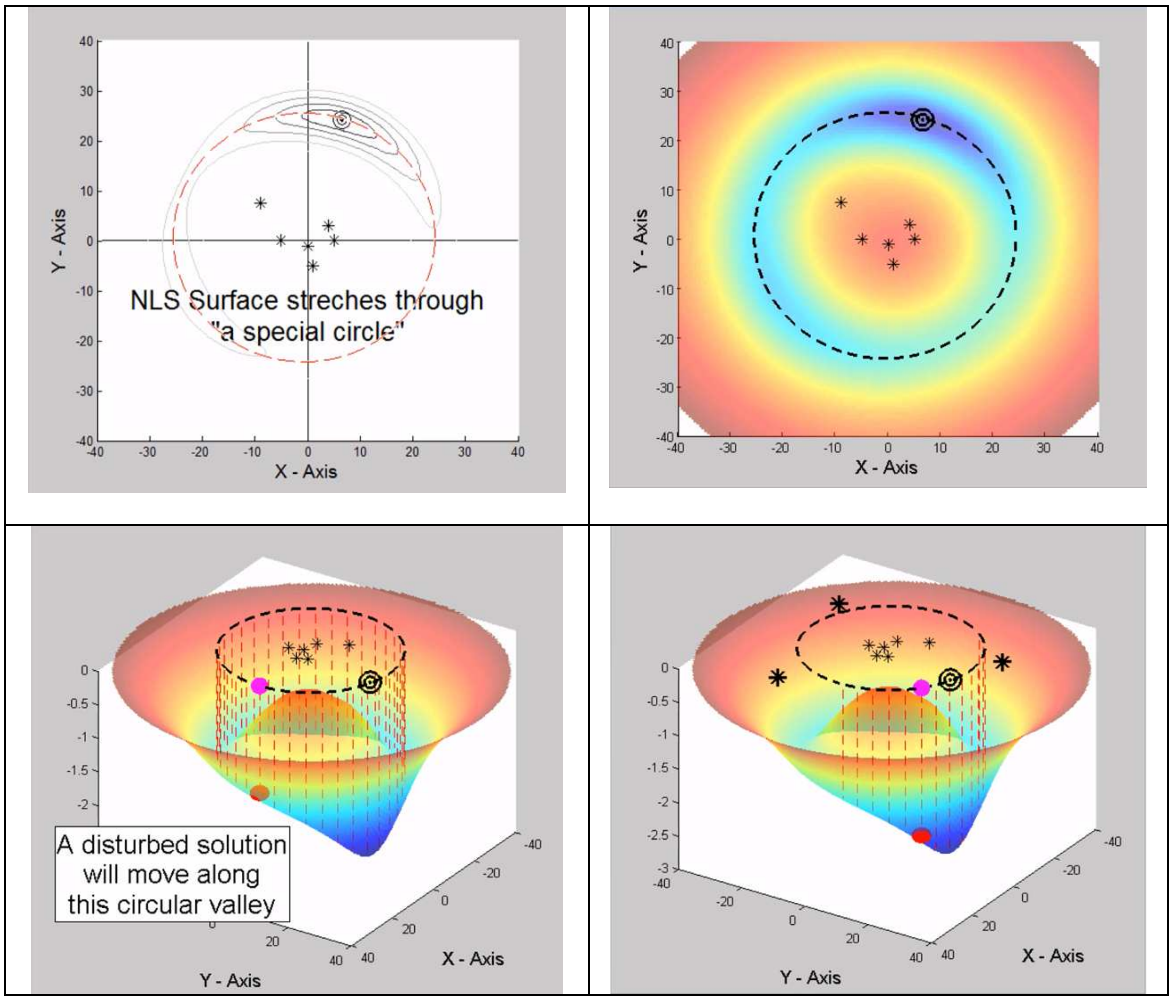

Figure 5.9. *Screen captures of the descriptive video about Circular Uncertainty*

6. DISCUSSION

Wireless localization is a significant research area which addresses many different applications from rescue activities to smart transportation systems etc. Wireless localization with moving sensors is a challenging task which involves several research directions such as trajectory planning and optimization, creating effective localization strategies, building efficient algorithms and so on. Moving platforms have a couples of physical constraints such as a limited useful load and limited time of flight, so the localization systems must include the most efficient hardware and software combinations. While RSS based localization systems are criticized not to able to result in robust solutions, undoubtedly they are the most affordable solutions among other RF localization parameters. Therefore, there exists a growing attention on RSS based localization systems to take the advantage of their affordable and simple structures.

In this study, a thorough literature review has been provided. First, basics of RSS and range-only localization are discussed together with related formulas. The basic idea behind RSS and range-only localization is depicted with illustrative flow diagrams in order to provide a better insight into the localization processes. Second, current research areas in RSS based localization are discussed. Next, a broad literature review on Differential RSS (DRSS) is presented. The literature of RSS based localization is so spread that different expressions are being used for the same concepts by different authors. For this reason, a rigorous literature review is provided which exhaustively includes all related previous studies. Next, the previous studies about joint estimation of path loss exponent and emitter's location, and RSS based Localization via UAVs are provided. Then, trajectory optimization for emitter localization are discussed and finally, a comprehensive literature review on sensor position uncertainty is presented.

When a moving sensor travels with the aim of estimating the location of the emitter, the first goal must be to create an effective route planning strategy which statistically guarantees the best possible estimation capability at the end of the travel of moving sensor. Section 3 deals with trajectories of the moving sensors and describes the essence of trajectory planning through a new perspective. Moving sensors can be carried by many different moving platforms such unmanned aerial vehicles etc. As mentioned above, mini UAVs can have a couple of physical constraints including maximum flight time, maximum weight of useful load etc. All these constraints can lead to a limited range of travel for small UAVs. Moreover, the emergency of the

localization mission may imply time constraints which also result in limited total lengths of travel. Therefore, the best possible estimation capability can be desired given a limited length of travel which is shorter than initial distance to emitter. Consequently, Section 3 explores the best angular direction given a limited length of travel for both RSS and range-only based localization.

The common point of trajectory optimization studies in the literature is to model the motion of the sensor as a set of discrete waypoints together with discrete measurements. However, the motion of moving sensors is in fact a continuous path, therefore when measurements are frequent enough, they can be regarded as continuous time stochastic processes. Therefore, a new perspective which views trajectories of the moving sensors as continuous paths is required. The summation operators within FIM can be appropriately converted to line integrals [69]. Consequently, to provide a detailed insight into trajectory optimization for range-only and RSS-based localization, this study shifts the scope of Fisher Information Matrix (FIM) from discrete measurement geometries to continuous measurement curves. In order to differentiate continuous curve FIMs from usual discrete FIMs, the FIMs associated with continuous trajectories has been called as Fisher Continuous Information Matrices (FCIM) in this study.

By means of FCIM, Section 3 has demonstrated that the best direction is only function of the ratio to $|L|/\Delta$ i.e. the ratio of the total length of travel and the initial distance to emitter. Then, Section 3 presents the plots of the best angular orientation for range only and RSS based localization with respect to $|L|/\Delta$. For range only localization, the best angular orientation mostly matches the arccosine function for small values of $|L|/\Delta$. However, for large values $|L|/\Delta$, the best angular orientation deviates from the arccosine function because of the need for uniform distribution of projected measurements along unit circle. For RSS based localization, the best angular orientation always stays well below arccosine because the measurement points which are close to the target are more valuable due to log-normal shadowing. The important point regarding to RSS based localization is that the best angular direction is 0 degree when $|L|/\Delta$ is 1. In other words, if the moving sensor is able to reach to emitter, then it must be directed towards the emitter for best possible estimation capability. This result justifies the main idea of Direction of Exponent Uncertainty which aims to create a direction towards the emitter for any time of the travel.

In Section 4, DRSS based emitter localization is analyzed from a geometrical point of view. The new proposed method, Direction of Exponent Uncertainty (DEU), is a powerful geometrical solution which brings significant computational efficiency and robustness in emitter localization. It has been described that in case of three measurements, the uncertainty in the location of the emitter can be modeled as a special line when path loss exponent is unknown. When there are multiple number of measurements from different locations, multiple DEUs can be obtained corresponding to different triple combinations of measurements. Finally, it has been shown that finding the intersection point of these DEUs is an effective way of estimating the location of the emitter, which attains CRLB.

The initial motivation behind DEU is to create a building block for an RSS-based tracking system whose objective is to move the sensor towards the location of the emitter at the smallest possible time. DEU based tracking is valuable because the sensor moves towards the emitter without calculating the location of the emitter. By this way, the sensor can more quickly initialize its motion and it can more flexibly update its route because only three measurements are engaged to derive a DEU. DEU based systems will be useful in a lot of important applications such as rescue activities, detecting unlicensed radio broadcasting etc. where the task is to reach to the target as soon as possible.

The new method, DEU, emerges as a critically important tool when some of the parameters of path loss model are changing during localization process, such as the emitter is slightly moving (i.e. (x, y) is changing), noise level is changing or finally path loss exponent is varying over time. With these changes in the parameters of path loss model, the measurement history can lose its validity after a period of time, therefore the localization system may need to start over by taking new measurements. In this kind of scenarios, DEU based tracking systems can effectively continue to function because it is based on very small number of measurements. DEU can calculate a direction towards emitter before the consistency between measurements is degraded.

The power of DEU is to be a geometrical solution. DEU is a powerful geometrical tool which removes a lot of computational waste such as iterations or grid searches. It converts minimization of non-convex cost function to a very simple task which is to find the intersection points of lines. Therefore, this study is an important research which

brings a significant emphasis on the benefits of innovative geometrical solutions to localization problems.

In Section 5, a new method, i.e. Circular Uncertainty, is introduced to deal with the issue of imprecise sensor positions in emitter localization. Emitter or source localization is a field of sensor array processing, which attempts to find the location of different of type of sources through the information from various sensors especially in noisy environments. There can be several types of error within the information utilized in source localization such as the error at measurements or the error at measurement positions etc. In the literature, it is mentioned that if the sensors are moving, then it is very likely that the measurement positions are imprecise. Therefore, Section 5 provides an effective new method to solve the localization problem by means of distance-to-target measurements in the presence of sensor position errors.

Distance-to-target measurements are nonlinear observations with respect to the unknown parameters namely the coordinates of the target location [63]. This situation makes target localization based on distance-to-target measurements a challenging task. Therefore, the estimators seeking the best possible estimation such as maximum likelihood estimation (MLE) require iterative searches along nonlinear cost surfaces. Iterative solutions are computationally expensive and their accuracy significantly depends on the initial points of the iterations. In various localization scenarios, MLE cost surface can be complicated with a couple of local minima and saddles points. Therefore, depending on the initial point, the minimization process can end up with a local minimum, so this can lead the performance of estimator to diverge from the ideal case. However, Section 5 proposes a completely safe localization scheme without any convergence issue.

When the sensor positions have uncertainties in addition to the uncertainties in distance measurements, it brings an additional difficulty for localization system. In these cases, the positions of sensors also become unknown parameters which need to be jointly estimated together with the target location. The number of parameters to be estimated becomes very large, so reaching the global minimum becomes a significant challenge for iterative solutions [63]. Taking this fact into account, this study removes this issue by conveniently reducing the multi-dimensional search space to a single dimensional space by means of the proposed method called Circular Uncertainty. The method of Circular Uncertainty allows the localization system to safely find the global

minimum even for complicated cost functions in the existence of imprecise sensor locations.

Distance based localization can be solved by nonlinear least squares (NLS) of errors of distance-to-target measurements. However, NLS solutions are not suitable to deal with the uncertainties in sensor positions. Weighted least squares (WLS) can be regarded as a special case of NLS where each term is skillfully weighted by taking the uncertainties in sensor positions into account. Weighting the squared distance errors can be quite useful to manage the uncertainties in sensor positions. However, to obtain a better scheme of localization, the cost of estimation must be a complete equation which includes two different parts for both distance-to-target measurement errors and sensor position errors. Therefore, in this study, the complete maximum likelihood cost function is established and solved in a smart and convenient way which guarantees to obtain the Cramer Rao Lower Bound (CLRB) in any condition.

In practical situations, the sensors can only be allowed to be located within a limited region whereas it is very likely that the target can be located far from this region. The important observation is that while it is very common to encounter this type of localization scenario, it provides a very limited capability for estimating the angular position of the target via distance-to-target observations. Therefore, in addition to the central measurements taken within a limited region, a few number of peripheral measurements can be deployed to dramatically increase the estimation capability of localization system. However, to scan a broad peripheral area, the peripheral measurements can be designed as moving sensors, which, as a result, brings the issue of uncertainty in the position of sensors. Moreover, both the error in the sensor positions and the error of distance measurements can be significantly high in practical situations. Therefore, the localization systems must be so robust that they keep functioning even under high level of noise and they must try to localize the target as accurate as possible in every case. Section 5 is dedicated to build this type of robust localization system.

For the scenario mentioned in the above paragraph, it is demonstrated that NLS cost surface of range-only localization has the croissant shape which results in the new concept Circular Uncertainty. Circular Uncertainty is basically "a circular valley" within the surface of NLS cost function. When new measurements are received which disturbs the initial estimation, the new disturbed estimation will move along this "circular valley" instead of climbing the hillsides. Once "a base cost surface" is established by

means of a couple of central measurements, in case of receiving some new measurements which disturb the initial estimation, the disturbed new estimation has a tendency to move along the Circular Uncertainty trajectory. Using this observation, a new robust localization scheme which finds the global minimum of the MLE solution has been created. The new solution, which takes the advantage of obtaining MLE in a robust way, attains CRLB regardless of the noise level whereas other solutions partly fail to achieve this performance.

In localization systems, the biggest problem with the MLE solution is that it is said to be computationally inefficient. Moreover, because of local minima or irregular cost functions, attempting to reach MLE solution can be sometimes problematic or even impossible. In this study, a new method, Circular Uncertainty, is established to effectively and reliably solve a very complicated MLE problem. Circular certainty not only makes it possible to reach MLE solutions, but also significantly simplifies this task. A high dimensional joint estimation problem is reduced to the estimation of only a single parameter i.e. θ. The success of Circular Uncertainty is to innovatively handle the range-only localization problem with solid observations.

7. CONCLUSION

Recent advancements in wireless technology has dramatically increased the use of wireless devices in every field of the life. Therefore, localization of wireless devices has become an important requirement for many different contemporary and prospective applications. In rescue activities, the nature travelers, the climbers or the people who are lost in some regions due to accidents, natural disasters or any other reasons can be searched via the wireless devices that they carry. Moreover, the workers or the people who are subjected to this type of risks can be requested to carry special wireless devices which can broadcast some special high level emergency signals to allow the rescue teams find their location. Another subject of wireless localization is to localize the unlicensed broadcasts. Unlicensed broadcasts can be delivered from a changing position via moving platforms such as cars or trucks, so detecting these broadcasts can be a quite challenging task. Wireless localization also includes detection or localization of vehicles to build smart transportation or smart traffic systems. Localizing the trespassing people, vehicles or drones within a specific area through the wireless devices that they have is also another topic of wireless localization. Finally, tracking some special animals or endangered species can be also achieved by means of wireless localization.

Commercialization of UAVs (especially mini drones or quadcopters) in the recent years has allowed a very large of bulk of people to access this technology. The increased popularity of UAVs in civil applications takes the attention of both academic and industrial environments. Therefore, researchers throughout the world are trying to expand the scope of the applications that can be achieved by means of commercial UAVs. Wireless localization is among the applications that is desired to be achieved via mini commercial UAVs. Several issues such as the signals of target RF emitters are weak, the duration of the broadcast is short, the signal is distorted due to rural or urban terrain and weather conditions, the target RF emitter are moving and so on make it necessary to mount the localization systems on moving platforms namely UAVs. However, commercial UAVs are small, inexpensive, and easily accessible aerial vehicles which are mostly used for civilian purposes, and they have significant restrictions on the amount of useful load they may carry and the flight time. Therefore, use of these commercial UAVs in wireless localization requires the localization algorithms to be made feasible under very important constraints and lower components, so it requires new research.

RSS based and range only localization of wireless emitters with moving sensors is a multidimensional problem which requires us to consider many different aspects. Optimization of trajectories of the moving sensors to obtain the best possible localization capability, a robust estimation structure which has no convergence issue while finding the location of the emitter, a fast localization algorithm with several unknown parameters for real-time systems, a framework to handle the uncertainties in sensor positions are all among the requirements of creating a successful localization system with moving sensors. This study provides a complete localization structure which covers all of the issues mentioned above. All the proposed methods include innovative and smart solutions to the research problems. The proposed solutions in this study are based on remarkable new observations obtained after careful investigation of the problems. All the new concepts are depicted not only with clear formulation but also with visual materials such as figures, flow diagrams and illustrative movies in order to give better insight into the subject. The proposed solutions namely Direction of Exponent Uncertainty for unknown path loss exponent and Circular Uncertainty for imprecise sensor positions are attaining CRLB while they are also computationally efficient. Consequently, creating effective yet efficient solutions at the same time has been the major goal of the study. At the end, from trajectory planning to localization with several unknown parameters, from efficient strategies for emitter tracking to skillfully managing the uncertainties in sensor positions, this study provide a complete structure for RF emitter localization with moving sensors.

In the future research, the new proposed methods which are designed for limited number of moving platforms in this study can be expanded for multi-platform systems. As an example, two moving sensors starting their motions far from each other can be engaged to obtain DEUs from two different locations. Therefore, the location of emitter can be effectively estimated by means of intersection of DEUs at the very beginning. Moreover, the proposed methods can be combined with different parameters such TDOA or AOA in order to create more robust systems. Finally, this study provided new methods which have great potentials to be developed in order to obtain more robust wireless localization systems in the future.

8. REFERENCES

[1] Uluskan, S., & Filik, T. (2017). A geometrical closed form solution for RSS based far-field localization: Direction of Exponent Uncertainty, *Wireless Networks*, https://doi.org/10.1007/s11276-017-1553-7.

[2] Uluskan, S., Filik, T., & Gerek, Ö. N. (2017). Circular Uncertainty method for range-only localization with imprecise sensor positions, *Multidimensional Systems and Signal Processing*, https://doi.org/10.1007/s11045-017-0527-3.

[3] Zekavat, R., & Buehrer, R. M. (2011). *Handbook of position location: Theory, practice and advances*. Hoboken, NJ: John Wiley & Sons, Inc.

[4] Liu, C., Wu, K., & He, T. (2004). Sensor localization with ring overlapping based on comparison of received signal strength indicator, in *International Conference on Mobile Ad-hoc and Sensor Systems*, pp. 516-518.

[5] Patwari, N., Ash, J. N., Kyperountas, S., Hero III, A. O., Moses, R. L., & Correal, N. S. (2005). Locating the nodes: cooperative localization in wireless sensor networks, *Signal Processing Magazine, IEEE*, 22(4), 54-69.

[6] Wang, G., & Yang, K. (2009). Efficient semidefinite relaxation for energy-based source localization in sensor networks., in *International Conference on Acoustics, Speech and Signal Processing, ICASSP*, pp. 2257-2260.

[7] Lee, J. H., & Buehrer, R. M. (2009). Location estimation using differential RSS with spatially correlated shadowing, in *Global Telecommunications Conference (GLOBECOM)*, pp. 1-6.

[8] Gezici, S. (2008). A survey on wireless position estimation, *Wireless personal communications*, 44(3), 263-282.

[9] Wang, S., & Inkol, R. (2011). A near-optimal least squares solution to received signal strength difference based geolocation., in *International Conference on Acoustics, Speech and Signal Processing (ICASSP)*, pp. 2600-2603.

[10] Jackson, B. R., Wang, S., & Inkol, R. (2011). Received signal strength difference emitter geolocation least squares algorithm comparison, in *Canadian Conference on Electrical and Computer Engineering (CCECE)*, pp. 1113-1118.

[11] Lee, J. H. (2011). *Physical layer security for wireless position location in the*

presence of location spoofing. PhD Dissertation: Virginia Polytechnic Institute and State University.

[12] Lee J. H. and Buehrer, R. M. (2012). Fundamentals Of Received Signal Strength - Based Position Location, in *Handbook of Position Location: Theory, Practice, and Advances*, S. A. Zekavat & R. M. Buehrer, Ed. Hoboken, NJ: John Wiley & Sons, Inc., 175-212.

[13] Lin, L., So, H. C., & Chan, Y. T. (2013). Accurate and simple source localization using differential received signal strength, *Digital Signal Processing*, 23(3), 736-743.

[14] Wang, S., Inkol, R., & Jackson, B. R. (2012). Relationship between the maximum likelihood emitter location estimators based on received signal strength (RSS) and received signal strength difference (RSSD), in *Biennial Symposium on Communications (QBSC)*, pp. 64-69.

[15] Taylor, R. C. (2013). *Received Signal Strength-Based Localization of Non-Collaborative Emitters in the Presence of Correlated Shadowing*. MS Thesis: Virginia Polytechnic Institute and State University.

[16] Tsui, A. W., Chuang, Y. H., & Chu, H. H. (2009). Unsupervised learning for solving RSS hardware variance problem in WiFi localization, *Mobile Networks and Applications*, 14(5), 677-691.

[17] Cheng, W., Tan, K., Omwando, V., Zhu, J., & Mohapatra, P. (2013). RSS-Ratio for enhancing performance of RSS-based applications, in *Proceedings IEEE INFOCOM*, pp. 3075-3083.

[18] Cai, L., Zeng, K., Chen, H., & Mohapatra, P. (2011). Good Neighbor: Secure Pairing of Nearby Wireless Devices by Multiple Antennas., in *Proceedings of the 18th Annual Network and Distributed System Security Symposium.*

[19] Lohrasbipeydeh, H., Gulliver, T. A., & Amindavar, H. (2014). Blind Received Signal Strength Difference Based Source Localization With System Parameter Errors, *IEEE Transactions on Signal Processing*, 62(17), 4516-4531.

[20] Sternowski, R. (2016). Power difference of arrival geolocation, *U.S. Patent No. 9316719*.

[21] Li, X. (2006). RSS-based location estimation with unknown pathloss model, *IEEE*

Transactions on Wireless Communications, 5(12), 3626-3633.

[22] Shirahama, J., & Ohtsuki, T. (2008). RSS-based localization in environments with different path loss exponent for each link, in *Vehicular technology conference, VTC spring*, pp. 1509-1513.

[23] Mao, G., Anderson, B. D., & Fidan, B. (2007). Path loss exponent estimation for wireless sensor network localization, *Computer Networks*, 51(10), 2467-2483.

[24] Chan, Y. T., Lee, B. H., Inkol, R., & Chan, F. (2011). Received signal strength localization with an unknown path loss exponent, in *24th Canadian Conference on Electrical and Computer Engineering (CCECE)*, pp. 456-459.

[25] Wang, G., Chen, H., Li, Y., & Jin, M. (2012). On received-signal-strength based localization with unknown transmit power and path loss exponent, *Wireless Communications Letters*, 1(5), 536-539.

[26] Salman, N., Ghogho, M., & Kemp, A. H. (2012). On the joint estimation of the RSS-based location and path-loss exponent, *Wireless Communications Letters, IEEE*, 1(1), 34-37.

[27] Chan, Y. T., Lee, B. H., Inkol, R. J., & Chan, F. (2012). Estimation of emitter power, location, and path loss exponent, in *IEEE Canadian Conference on Electrical & Computer Engineering CCECE*, Montreal, pp. 1-5.

[28] Gholami, M. R., Vaghefi, R. M., & Ström, E. G. (2013). RSS-based sensor localization in the presence of unknown channel parameters, *IEEE Transactions on Signal Processing*, 61(15), 3752-3759.

[29] Scerri, P., Glinton, R., Owens, S., Scerri, D., & Sycara, K. (2007). Geolocation of RF emitters by many UAVs, in *AIAA Infotech@ AerospaceConference and Exhibit*, pp. 2858-2871.

[30] Dehghan, S. M. M., Moradi, H., & Shahidian, S. A. A. (2014). Optimal path planning for DRSSI based localization of an RF source by multiple UAVs., in *International Conference on Robotics and Mechatronics (ICRoM)*, pp. 558-563.

[31] Shahidian, S. A. A., & Soltanizadeh, H. (2016). Optimal trajectories for two UAVs in localization of multiple RF sources, *Transactions of the Institute of Measurement and Control*, 38(8), 908-916.

[32] Shin, H. S., de Corlieu, T., & Tsourdos, A. (2014). Civil GPS Jammer Geolocation

from a UAV Equipped with a Received Signal Strength Indicator Sensor, in *International Conference on Intelligent Unmanned Systems*.

[33] Uluskan, S., Gökçe, M., & Filik, T. (2017). RSS based localization of an emitter using a single mini UAV, in *IEEE Signal Processing and Communications Applications Conference, DOI: 10.1109/SIU.2017.7960239*.

[34] Wagle, N., & Frew, E. W. (2010). A particle filter approach to wifi target localization, in *AIAA Guidance, Navigation, and Control Conference*, pp. 2287-2298.

[35] Carvalho, G. G. C. (2014). *Unmanned Air Vehicle Based Localization and Range Estimation of Wi-Fi Nodes*. MS Thesis: Universidade Do Porto.

[36] Ibrahim, M. A., & Sharawi, M. S. (2014). *Real Time RSS Based Adaptive Beam Steering Algorithm for Autonomous Vehicles*. Progress In Electromagnetics Research: (52) 13-25.

[37] Ullah, K., Custodio, I. V., Shah, N., & dos Santos Moreira, E. (2013). An Experimental Study on the Behavior of Received Signal Strength in Indoor Environment, in *International Conference on Frontiers of Information Technology (FIT) IEEE*, pp. 259-264.

[38] Cheng, L., Wu, C. D., Zhang, Y. Z., & Wang, Y. (2012). An indoor localization strategy for a mini-UAV in the presence of obstacles, *International Journal of Advanced Robotic Systems*, 9(4), 1-8.

[39] Walter, D. J., Bryan, K., Stephens, J., Bullmaster, C., & Chakravarthy, V. (2012). Localization of RF Emitters using Compressed Sensing with Multiple Cooperative Sensors, in *National Aerospace and Electronics Conference (NAECON)*, pp. 236-240.

[40] Dogancay, K. (2007). Online optimization of receiver trajectories for scan-based emitter localization, *IEEE Transactions on Aerospace and Electronic Systems*, 43(3), 1117-1125.

[41] Dogancay, K., Hmam, H., Drake, S. P., & Finn, A. (2009). Centralized path planning for unmanned aerial vehicles with a heterogeneous mix of sensors, in *Intelligent Sensors, Sensor Networks and Information Processing (ISSNIP)*, pp. 91-96.

[42] Dogancay, K. (2012). UAV path planning for passive emitter localization, *IEEE Transactions on Aerospace and Electronic systems*, 48(2), 1150-1166.

[43] Frew, E., Dixon, C., Argrow, B., and Brown, T. (2005). Radio Source Localization by a Cooperating UAV Team, in *AIAA Infotech@Aero-space*, Reston, VA, pp. 10–20.

[44] Dehghan, S. M. M., Tavakkoli, M. S., and Moradi, H. (2013). Path planning for localization of an RF source by multiple UAVs on the Crammer-Rao Lower Bound, in *International Conference on Robotics and Mechatronics (ICRoM)*, pp. 68-73.

[45] Yılmaz, A. (2015). *On localization and tracking using received signal strength measurements*. Master of Science Thesis: Middle East Technical University.

[46] Choi, H. L., and How, J. P. (2010). Continuous trajectory planning of mobile sensors for informative forecasting, *Automatica*, 46(8), 1266-1275.

[47] Hinich, M. J., & Rule, W. (1975). Bearing estimation using a large towed array, *The Journal of the Acoustical Society of America*, 58(5), 1023-1029.

[48] Bucker, Homer P. (1978). Beamforming a towed line array of unknown shape, *The Journal of the Acoustical Society of America*, 63(5), 1451-1454.

[49] Carter, G. C. (1979). Passive ranging errors due to receiving hydrophone position uncertainty, *The Journal of the Acoustical Society of America*, 65(2), 528-530.

[50] Schultheiss, P. M., & Ianniello, J. P. (1980). Optimum range and bearing estimation with randomly perturbed arrays, *The Journal of the Acoustical Society of America*, 68(1), 167-173.

[51] Rockah, Y., & Schultheiss, P. (1987). Array shape calibration using sources in unknown locations--Part I: Far-field source, *IEEE Transactions on Acoustics, Speech, and Signal Processing*, 35(3), 286-299.

[52] Krim, H., & Viberg, M. (1996). Two decades of array signal processing research: the parametric approach, *IEEE Signal processing magazine*, 13(4), 67-94.

[53] Chen, J. C., Hudson, R. E., & Yao, K. (2002). Maximum-likelihood source localization and unknown sensor location estimation for wideband signals in the near-field, *IEEE Transactions on Signal Processing*, 50(8), 1843-1854.

[54] Ho, K. C., Lu, X., & Kovavisaruch, L. O. (2007). Source localization using TDOA

and FDOA measurements in the presence of receiver location errors: analysis and solution, *IEEE Transactions on Signal Processing*, 55(2), 684-696.

[55] Ho, K. C., & Yang, L. (2008). On the use of a calibration emitter for source localization in the presence of sensor position uncertainty, *IEEE Transactions on Signal Processing*, 56(12), 5758-5772.

[56] Qu, X., & Xie, L. (2012). Source localization by TDOA with random sensor position errors—part I: static sensors, in *15th International Conference on Information Fusion (FUSION)*, pp. 48-53.

[57] Qu, X., & Xie, L. (2012). Source localization by TDOA with random sensor position errors—part II: mobile sensors, in *15th International Conference on Information Fusion (FUSION)*, pp. 54-59.

[58] Li, J., Pang, H., Guo, F., Yang, L., & Jiang, W. (2015). Localization of multiple disjoint sources with prior knowledge on source locations in the presence of sensor location errors, *Digital Signal Processing*, 40, 181-197.

[59] Li, S., & Ho, K. C. (2016). Accurate and Effective Localization of an Object in Large Equal Radius Scenario, *IEEE Transactions on Wireless Communications*, 15(12), 8273-8285.

[60] Srirangarajan, S., Tewfik, A. H., & Luo, Z. Q. (2007). Distributed sensor network localization with inaccurate anchor positions and noisy distance information, in *IEEE International Conference on Acoustics, Speech and Signal Processing (ICASSP)*, pp. (3) 521-524.

[61] Lui, K. W. K., Ma, W. K., So, H. C., & Chan, F. K. W. (2009). Semi-definite programming algorithms for sensor network node localization with uncertainties in anchor positions and/or propagation speed, *IEEE Transactions on Signal Processing*, 57(2), 752-763.

[62] Ma, Z., & Ho, K. C. (2011). TOA localization in the presence of random sensor position errors, in *IEEE International Conference on Acoustics, Speech and Signal Processing (ICASSP)*, pp. 2468-2471.

[63] Chen, S., & Ho, K. C. (2014). Reaching asymptotic efficient performance for squared processing of range and range difference localizations in the presence of sensor position errors, in *IEEE International Conference on Acoustics, Speech and*

Signal Processing (ICASSP), pp. 1419-1423.

[64] Li, J., Ho, K. C., Guo, F., & Jiang, W. (2014). Improving the projection method for TOA source localization in the presence of sensor position errors, in *Sensor Array and Multichannel Signal Processing Workshop (SAM)*, pp. 45-48.

[65] Moreno-Salinas, D., Pascoal, A. M., & Aranda, J. (2013). Optimal sensor placement for multiple target positioning with range-only measurements in two-dimensional scenarios, *Sensors*, 13(8), 10674-10710.

[66] Bishop, A. N., & Jensfelt, P. (2009). An optimality analysis of sensor-target geometries for signal strength based localization, in *Intelligent Sensors, Sensor Networks and Information Processing (ISSNIP)*, pp. 127-132.

[67] Bishop, A. N., Fidan, B., Anderson, B. D., Doğançay, K., & Pathirana (2010). Optimality analysis of sensor-target localization geometries, *Automatica*, 46(3), 479-492.

[68] A. Montanari (2014). Principal component analysis, *University of Bologna*, http://www2.stat.unibo.it/montanari/Didattica/Multivariate/PCA1.pdf.

[69] Wilson, A. D., Schultz, J. A., & Murphey, T. D. (2014). Trajectory synthesis for Fisher information maximization, *IEEE Transactions on Robotics*, 30(6), 1358-1370.

[70] Alexander, R. Lines and tangents in polar coordinates, *Iowa State University*, http://orion.math.iastate. edu/alex/166H/polar_lines_tangents.pdf.

[71] Uluskan, S., & Filik, T. (2016). A survey on the fundamentals of RSS based localization, in *IEEE Signal Processing and Communication Application Conference (SIU)*, pp. 1633-1636.

[72] Ren, L., Chen, X., Xie, B., Tang, Z., Xing, T., Liu, C., Nie, W. & Fang, D. (2016). DE2: Localization based on the rotating RSS using a single beacon, *Wireless Networks*, 22(2), 703-721.

[73] Sono, H., Ohno, A., Kojima, T., & Yamane, Y. (2007). Retrospective estimation of the spatial dose distribution and the number of fissions in criticality accident using area dosimeters, *Journal of nuclear science and technology*, 44(1), 43-53.

[74] Traa, J. (2013). Least Squares Intersection of Lines, http://cal.cs.illinois.edu /~johannes/research/LS_line_intersect.pdf (Accessed on: 01/02/2015).

[75] Kay, S. M. (1993). *Fundamentals of statistical signal processing, Volume I: Estimation theory*. Upper Saddle River, NJ: Prentice Hall.

[76] Patwari, N., Hero, A. O., Perkins, M., Correal, N. S., & O'dea, R. J. (2003). Relative location estimation in wireless sensor networks, *IEEE Transactions on signal processing*, 51(8), 2137-2148.

[77] MATLAB 2014b, The MathWorks, Inc., Natick, Massachusetts, United States, License Number: 991708.

[78] Olson, E., Leonard, J., & Teller, S. (2006). Robust range-only beacon localization, *IEEE Journal Of Oceanic Engineering*, 31(4), 949-958.